REMOTE SENSING ANALYSIS OF COVID-19 LOCKDOWN EFFECTS ON URBAN HEAT ISLAND (UHI), LAND SURFACE TEMPERATURE (LST) AND GREENHOUSE GASES IN ABUJA.

BY

UHUNMWANGHO OSAGIE OSAYOMWANBOR

LSC2006966

DEPARTMENT OF ENVIRONMENTAL MANAGEMENT AND TOXICOLOGY

FACULTY OF LIFE SCIENCES

UNIVERSITY OF BENIN

BENIN CITY

NOVEMBER, 2025

REMOTE SENSING ANALYSIS OF COVID-19 LOCKDOWN EFFECTS ON URBAN HEAT ISLAND (UHI), LAND SURFACE TEMPERATURE (LST) AND GREENHOUSE GASES IN ABUJA.

BY

UHUNMWANGHO OSAGIE OSAYOMWANBOR

LSC2006966

AN UNDERGRADUATE PROJECT SUBMITTED TO THE DEPARTMENT OF ENVIRONMENTAL MANAGEMENT AND TOXICOLOGY, FACULTY OF LIFE SCIENCES, UNIVERSITY OF BENIN, BENIN CITY, EDO STATE, NIGERIA; IN PARTIAL FULFILLMENT OF THE REQUIREMENTS FOR AWARD OF BACHELOR OF SCIENCE (B.SC) DEGREE IN ENVIRONMENTAL MANAGEMENT AND TOXICOLOGY

NOVEMBER, 2025

CERTIFICATION

This is to certify that this research titled **"Remote Sensing Analysis Of COVID-19 Lockdown Effects On Urban Heat Island (UHI), Land Surface Temperature (LST) And Greenhouse Gases In Abuja."** was carried out by **Uhunmwangho Osagie Osayomwanbor** and presented to the Department of Environmental Management and Toxicology, Faculty of Life Sciences, University of Benin, Benin City; in partial fulfilment of the requirements for the award of Bachelor of Science (B.Sc) in Environmental Management and Toxicology. It was conducted under suitable conditions, was carefully supervised and subsequently approved as having met the requirements for the award of a Bachelor of Science degree in Environmental Management and Toxicology.

_____ _____

PROF. A. A. ENUNEKU **DATE**

(PROJECT SUPERVISOR)

_____ _____

Dr A. F. EGHOMWANRE **DATE**

(PROJECT COORDINATOR)

_____ _____

PROF. (Mrs) AISIEN E. T. **DATE**

(HEAD OF DEPARTMENT)

DECLARATION

I, Uhunmwangho Osagie Osayomwanbor declare that Remote Sensing Analysis Of COVID-19 Lockdown Effects On Urban Heat Island (UHI), Land Surface Temperature (LST) And Greenhouse Gases In Abuja. With Landsat 8 and Sentinel-5P Satellite Technology is my own work and that all sources that I have used or quoted have been acknowledged by means of complete references and that this work has not been submitted before for any other degree at any other University.

_____ _____

UHUNMWANGHO OSAGIE OSAYOMWANBOR **DATE**

DEDICATION

I dedicate this project work to God Almighty, my creator, who made it possible for me to successfully complete my coursework and thesis.

ACKNOWLEDGEMENT

I wish to express my profound gratitude to my project supervisor, Professor Alex Enuneku, for his continuous guidance, mentorship, and unwavering support throughout the course of this research. His insightful suggestions and encouragement have been instrumental in shaping the success of this work.

My sincere appreciation also goes to Dr. Ehinlaiye Ayamezimi Oziofu, whose proficient tutelage, readiness to assist, and commitment to academic excellence greatly contributed to my learning experience. I am equally grateful to the Head of Department and all the lecturers in the Department of Environmental Management and Toxicology for their dedication, patience, and professionalism in imparting knowledge to my colleagues and me.

I owe my deepest gratitude to my beloved parents, Dr. Augustine Uhunmwangho and Dr. (Mrs.) Iyobosa Uhunmwangho, whose love, prayers, understanding, and unwavering support have been my greatest source of strength throughout my B.Sc. programme.

A special word of appreciation goes to my Auntie's, Aunty Joy Edoghogho Omoruyi, Dr. (Mrs.) Nosa Betty Agbonkpolor, Dr. Osaretin Chukwumah, and Uncle Dr. Victor Agbonkpolor, my Grandma Osiowanri .C.Omoruyi, my cousins and siblings, for their constant encouragement, kindness, and belief in my dreams.

I also wish to acknowledge my amazing friends, members of The Christian Fellowship International, Jeshua Family, My Amigo's, The Hex Hive, and my course mates, whose companionship, shared ideas, and moral support have contributed immensely to both my academic and spiritual growth. To everyone who supported me in one way or another on this journey, I say thank you. Your encouragement has been a constant reminder that success is best achieved through the love and support of others.

TABLE OF CONTENTS

LIST OF TABLES

LIST OF FIGURES

LIST OF PLATES

ABSTRACT

The rapid urbanization of the 21st century significantly alters local climates, manifesting in phenomena like the Urban Heat Island (UHI) effect and elevated concentrations of greenhouse gases (GHGs). The COVID-19 lockdown offered a rare natural experiment to evaluate the extent to which human activities influence urban thermal environments and atmospheric conditions. This study employed remote sensing and Geographic Information System (GIS) techniques to analyse the effects of the COVID-19 lockdown on Urban Heat Islands (UHIs), Land Surface Temperatures (LST), and Greenhouse Gases (GHGs) in Abuja, Nigeria. Landsat 8 satellite imagery was used to derive UHI and LST data, while Sentinel-5P provided atmospheric measurements for key GHGs including sulphur dioxide (SO_2), aerosols, and ozone (O_3). The analysis covered three temporal phases which are the pre-lockdown (2017–2018), lockdown (2019–2020), and post-lockdown (2021–2024) and data were processed using Google Earth Engine and ArcGIS environments to classify spatial variations and identify thermal patterns across the study area. The results revealed a significant decline in both UHI and LST intensity during the lockdown period, with mean UHI values dropping from 6.00°C in 2017–2018 to 4.93°C in 2019–2020, before rising again to 6.72°C post-lockdown. LST followed a similar trend, decreasing from 6.96°C to 5.14°C during lockdown and increasing thereafter. A corresponding reduction was also observed in atmospheric pollutants, with sulphur dioxide, aerosols, and ozone concentrations all declining during the lockdown. Pearson correlation analysis showed a strong positive relationship between UHI and LST ($r = 0.786–0.877$), confirming their interdependence and direct link to anthropogenic activity. These findings underscore the dominant role of human activities in shaping urban climatic and atmospheric conditions. The temporary cooling and emission reduction during the lockdown illustrate the potential environmental benefits of reduced fossil fuel consumption and improved urban planning. The study highlights the critical importance of integrating green infrastructure, energy-efficient systems, and climate-responsive policies into Abuja's urban development framework. It further demonstrates the value of remote sensing and GIS as essential tools for continuous environmental monitoring and policy formulation toward achieving Sustainable Development Goals 11 (Sustainable Cities and Communities) and 13 (Climate Action)

CHAPTER ONE

1.0 INTRODUCTION

The 21st century is defined by rapid and widespread urbanization, a global phenomenon that acts as a powerful driver of environmental change (Uju *et al.*, 2025). While cities are celebrated as engines of economic growth and innovation, their concentrated populations and intensive activities fundamentally alter the natural environment, leading to significant and often adverse local and global climatic impacts. A primary manifestation of this anthropogenic forcing is the Urban Heat Island (UHI) effect, a well-documented phenomenon where "urban areas exhibit higher temperatures than their surrounding rural areas" (Oke, 1982; Oke *et al.,* 2017; Abimbola *et al.,* 2025). This thermal discrepancy is not trivial; studies have recorded UHI intensities where city temperatures can be several degrees Celsius warmer than their rural peripheries, with profound implications for energy consumption, public health and overall ecosystem viability (Piracha and Chaudhary, 2022).

The genesis of the UHI effect lies in the radical physical and metabolic transformation of the landscape during urbanization. This process involves the "replacement of natural landscape with artificial heat absorbing, non-reflecting, water resistant and impermeable surface materials that absorb the sun radiation during the day" (Anyakora *et al.,* 2025). Common urban materials like asphalt and concrete possess low albedo (reflectivity) and high thermal capacity, leading to greater absorption and storage of solar energy, which is then slowly released as heat throughout the night (Abimbola *et al.,* 2025). This phenomenon is compounded by the urban canyon effect, where the geometry of tall buildings traps solar radiation and reduces natural airflow and a critical anthropogenic component: "the heat released due to urban activities" (Dong *et al.,* 2017). This anthropogenic heat emission (AHE) originates from diverse sources, including "vehicle exhaust, appliances, building operations (heating, cooling, lighting, etc.), transportation activities, power plants, etc." (Piracha and Chaudhary,

2022). The complex interplay of these factors, modified surface properties, altered urban geometry and direct heat release from human activities creates a characteristic urban thermal climate that is consistently warmer, particularly during the night.

Concurrently, urban areas are dominant sources of greenhouse gases (GHGs) and air pollutants, creating a dangerous feedback loop with the UHI effect. "The higher temperatures due to heat island in cities increase energy consumption for cooling," with electricity demand rising by "1.5 to 2.0% for every 0.6°C increase in air temperatures," leading to an overall energy demand increase of "5 to 10%" (Bhargava, *et al.,* 2017). This surge in energy demand, often met through the combustion of fossil fuels, results in "elevated emissions of air pollutants and greenhouse gases" such as carbon dioxide (CO_2), nitrogen oxides (NO_x) and carbon monoxide (CO) (Bhargava, *et al.,* 2017). These emissions not only contribute to long-term global climate change but also interact with the UHI to worsen local air quality, forming a complex and self-reinforcing cycle of urban climatic degradation.

The COVID-19 pandemic, while a profound global health and socio-economic crisis, inadvertently created an unprecedented global "natural experiment" for studying the intricate relationships between human activity, UHIs and GHG emissions (Liu *et al.,* 2022). The imposition of large-scale lockdowns led to an "unprecedented reduction in human activities, including closure of road transportation, shutdown of nonessential business and industrial activities and restrictions of outdoor activities" (Liu *et al.,* 2022). This sudden halt resulted in a dramatic, albeit temporary, plunge in energy consumption and associated anthropogenic emissions. Global studies documented this stark change; for example, "the COVID-19 lockdown reduced $PM_{2.5}$ and NO_2 by more than 14%" and was associated with a "sharp decrease (over 25%) in UHI night" in several major urban agglomerations (Feng *et al.,* 2023). A synthesis of 29 studies confirmed that a majority of the 46 cities examined showed a decrease in UHI during the lockdown period (Dogan *et al.,* 2024). This unique period provides a critical lens through which to observe urban climatic systems with significantly reduced anthropogenic forcing, offering

invaluable empirical evidence for informing long-term climate mitigation and urban planning strategies.

Within this global context, Abuja, Nigeria, presents a critical and compelling case study. As a purpose-built capital city, Abuja has experienced rapid spatial expansion and population growth, characteristics of intense urban sprawl. Empirical data illustrates this dramatic transformation: "The results show that there is significant increase of built up from 341.97 km² to 1310.35 km² between 2002 and 2023. There is also sharp decrement in vegetation from 510.26 km² to 53.98 km²" (Uju *et al.,* 2025). This pattern of land consumption, where natural and vegetated surfaces are relentlessly replaced by impervious built up areas, is a textbook driver of UHI intensification. The resulting increase in land surface temperature (LST) poses a direct threat to the city's inhabitants, as "heat stress could cause rash, cramps, heat exhaustion and heat stroke and may exacerbate underlying medical conditions" (Pantavou *et al.,* 2011). Therefore, a spatiotemporal assessment of UHI and GHG dynamics in Abuja, specifically analysing the transient changes induced by the COVID-19 lockdowns against the backdrop of persistent urban sprawl, is not merely an academic inquiry. It is an essential undertaking for generating evidence-based insights to guide the city's future climate resilience, public health policy and sustainable urban development trajectory.

1.1 Aim and Objectives

The aim of the study is to access and analyse the spatiotemporal variations of UHIs, LSTs and GHG reductions in Abuja before, during and after COVID-19 lockdown.

The Objectives are to;

1. Map UHI intensity across the three COVID-19 periods.
2. Quantify variations in GHG proxies (SO_2, O_3, Aerosol) and human activity indicators.
3. Map LST across the three COVID-19 periods.

4. Model statistical relationships between UHI and GHG proxies.

5. Provide evidence-based policy recommendations for urban climate resilience in Abuja.

1.2 Problem Statement

Abuja demonstrates the environmental costs of rapid urban sprawl: low-density development consumes natural land, while impervious surfaces intensify UHIs (Oyeniyi *et al.,* 2025; Abimbola *et al.,* 2025). Rising urban heat has escalated public health risks and energy demand, creating a feedback loop of greater GHG emissions from cooling needs (Jamei *et al.,* 2022; Almeida *et al.,* 2021).

COVID-19 lockdowns globally reduced emissions and UHI intensity (Liu *et al.,* 2022; Dogan *et al.,* 2024). Yet, there is little understanding of whether similar reductions occurred in Abuja and whether sprawl muted these effects. A major gap exists in integrated spatiotemporal studies that jointly analyse UHIs, GHG proxies (NO_2, CO) and sprawl across pre, during and post-COVID periods in sub-Saharan cities. Addressing this gap is crucial for sustainable urban planning and climate adaptation in Abuja.

1.3 Justification of the Study

The justification for this research lies in the urgent need to understand and manage the growing environmental pressures associated with urbanization in rapidly developing cities such as Abuja. As Nigeria's capital and one of the fastest growing urban centres in Africa, Abuja exemplifies the complex interplay between urban expansion, climate alteration and environmental degradation. Over the past two decades, the city's built up area has expanded nearly fourfold, largely at the expense of vegetated and permeable surfaces (Uju *et al.*, 2025). This rapid transformation has intensified Urban Heat Island (UHI) effects, deteriorated air quality and increased the vulnerability of residents to heat stress and other climate-related hazards.

Understanding these dynamics is especially critical given the climate feedback loop linking urban heat and greenhouse gas (GHG) emissions. As cities warm, energy demand for cooling rises, driving up fossil fuel consumption and GHG emissions, which in turn amplify warming (Abimbola *et al.,* 2025). This cycle not only threatens environmental sustainability but also undermines public health, urban livability and energy security. In Abuja, where dependence on fossil fuels remains high and urban planning struggles to keep pace with population growth, this feedback loop represents a serious environmental governance challenge.

The COVID-19 pandemic created an unprecedented opportunity to study this relationship. Global lockdowns in 2020 led to sudden reductions in industrial operations, transportation and energy demand, resulting in significant, though temporary, declines in air pollutants and GHG concentrations (Le Quéré *et al.,* 2020; Liu *et al.,* 2022). In many cities, UHI intensity also decreased during this period (Dogan *et al.,* 2024; Feng *et al.,* 2023). Yet, in the African context and particularly in Abuja, there remains a critical knowledge gap on how such abrupt reductions in human activity affected local climatic conditions and emissions. Addressing this gap is vital for evidence-based policy and sustainable urban development.

From a scientific standpoint, this study is justified by its integrated approach combining remote sensing, GIS and spatiotemporal modelling to explore the interconnections between UHI, GHG variations and urban sprawl. Most existing research on UHIs in Africa has focused on surface temperature mapping alone, neglecting the atmospheric components that influence air quality and climate feedbacks (Bassett *et al.,* 2020; Odunsi and Rienow, 2024). By incorporating multiple datasets (Landsat and Sentinel-5P), this work provides a more comprehensive understanding of how urban growth and anthropogenic activity shape local and regional climate patterns.

From a policy perspective, this research provides crucial insights for urban planners, environmental regulators and policymakers in Nigeria. Abuja's urban sprawl threatens to erode the city's

environmental resilience and without targeted interventions such as expanding urban green spaces, improving land use efficiency and promoting renewable energy, the UHI effect and related emissions will continue to worsen. The findings from this study can inform revisions of Abuja's Master Plan, guide sustainable zoning practices and support national commitments under Sustainable Development Goals 11 (Sustainable Cities) and 13 (Climate Action).

Ultimately, the justification for this study lies in its potential to bridge the gap between scientific evidence and urban policy, offering actionable knowledge to mitigate the adverse climatic effects of urban growth. By focusing on Abuja, a city at the nexus of rapid development, environmental vulnerability and climate risk, the study contributes to both global and local efforts toward building resilient, low-carbon and climate-smart cities.

CHAPTER TWO

LITERATURE REVIEW

2.1 Conceptual Overview

The 21st century is characterized by rapid and widespread urbanization, a global trend that profoundly reshapes landscapes and atmospheric environments. A dominant feature of this growth, particularly in developing nations, is urban sprawl which is defined as the physical pattern of low-density, often unplanned, expansion of urban areas into the surrounding countryside (UN-HABITAT, 2018). This expansive growth consumes natural and agricultural lands, replacing permeable, vegetated surfaces with impervious materials like asphalt for roads and concrete for buildings and infrastructure (Chinedu *et al.,* 2024; Uju *et al.,* 2025). This fundamental transformation of the land surface is the primary catalyst for a suite of interconnected environmental challenges, most notably the Urban Heat Island (UHI) effect and elevated Greenhouse Gas (GHG) emissions, which together form a critical nexus in the study of urban climate change (Oyeniyi *et al.,* 2025; Piracha and Chaudhary, 2022).

The Urban Heat Island (UHI) effect is a well-established phenomenon in urban climatology, describing the characteristic warmth of a city compared to its surrounding rural environments (Oke, 1982). It is fundamentally defined as a metropolitan area that is significantly warmer than its neighboring rural areas (Oke *et al.,* 2017). This thermal disparity is not a single phenomenon but can be categorized based on the layer of the urban atmosphere in which it is observed (Aruya *et al.,* 2021). The Surface Urban Heat Island (SUHI) refers to the higher temperature of urban surfaces relative to rural surfaces. This is most effectively measured using Land Surface Temperature (LST) retrieved from satellite thermal infrared sensors, making it ideal for spatial analysis over large areas (Voogt and Oke, 2003; Feng *et al.,* 2023). In contrast, the Urban Canopy Heat Island (UCHI) describes the warmer air temperatures found within the layer of the atmosphere where people live, from the ground level to the tops of buildings and trees (Aruya *et al.,* 2021). A third type, the Urban Boundary Layer

Heat Island (UBLHI), occurs in the atmosphere above the urban canopy and is influenced by the heat and roughness of the city below (Aruya *et al.,* 2021).

The development of the UHI is driven by specific modifications to the urban environment that alter the local energy balance. Research synthesizes four key drivers: (1) the loss of natural vegetation, which reduces shading and cooling via evapotranspiration; (2) the introduction of urban construction materials like asphalt and concrete that are more efficient at absorbing and storing thermal energy; (3) the creation of 'urban canyons' formed by buildings, which trap solar radiation and reduce airflow; and (4) the emission of waste heat from buildings, vehicles and industries, known as anthropogenic heat flux (AHF) (Vargo *et al.,* 2016; Arnfield, 2003). These factors collectively reduce surface albedo (reflectivity), increase the heat capacity of the urban fabric and directly inject heat into the environment, leading to elevated temperatures (Rizwan *et al.,* 2008; Salata *et al.,* 2017).

Concurrently, urban areas are major sources of Greenhouse Gases (GHGs), such as carbon dioxide (CO_2), methane (CH_4) and nitrous oxide (N_2O) (Piracha and Chaudhary, 2022). These emissions are primarily generated from the combustion of fossil fuels to power transportation, industrial activities and the energy demands of buildings (Le Quéré *et al.,* 2020; Jamei *et al.,* 2022). The relationship between the UHI and GHG emissions is not merely concurrent but synergistic, creating a positive feedback loop that exacerbates both local and global climate challenges. The UHI effect significantly increases energy demand, particularly for space cooling during hot periods (Jamei *et al.,* 2022). This elevated demand, often met by fossil-fuel-reliant power grids, leads to higher emissions of GHGs and other air pollutants (Rizwan *et al.,* 2008). These increased GHG concentrations contribute to global warming, which can in turn intensify the frequency and severity of heat events, thereby reinforcing the UHI effect (Dong *et al.,* 2017). This creates a vicious cycle where urban heat drives energy consumption, which fuels further warming.

The COVID-19 pandemic created a unique, unplanned global experiment, often termed an "anthropause," which provided compelling empirical evidence of the link between human activity, UHI and GHG emissions. The implementation of strict lockdowns in 2020 led to an unprecedented reduction in transportation and industrial activity globally (Liu *et al.,* 2022). This resulted in a dramatic, though temporary, decline in global CO_2 emissions, with one study estimating a peak reduction of 17% in early April 2020 compared to 2019 levels (Le Quéré *et al.,* 2020). This reduction in anthropogenic heat and air pollutants had a measurable impact on urban climates. Multiple studies using remote sensing data documented a noticeable weakening of the UHI effect in cities across the world during lockdown periods. For instance, research showed significant reductions in the intensity of both surface and canopy UHIs in cities across China, while studies of European cities like Prague and Milan also reported lower UHI magnitudes coinciding with improved air quality (Liu *et al.,* 2022; Dogan *et al.,* 2024; Mijania *et al.,* 2022). This period provides a critical spatiotemporal benchmark, highlighting the sensitivity of urban climate systems to changes in human behaviour and offering a real-world validation of the conceptual links within the UHI-GHG nexus.

To effectively assess these complex and dynamic interrelationships, Geographic Information Systems (GIS) and Remote Sensing are indispensable methodological tools. Remote sensing provides consistent, synoptic data on key environmental variables. Satellites such as Landsat and MODIS are used to derive Land Surface Temperature (LST), which is the primary metric for quantifying the SUHI (Uju *et al.,* 2025; Feng *et al.,* 2023). These platforms also provide data for calculating the Normalized Difference Vegetation Index (NDVI), a measure of greenness that is consistently shown to be negatively correlated with LST, confirming the cooling role of vegetation (Oyeniyi *et al.,* 2025; Chinedu *et al.,* 2024). Furthermore, satellites like Sentinel-5P can monitor atmospheric pollutants like nitrogen dioxide (NO_2), which serve as proxies for certain combustion-related GHG emissions (Jamei *et al.,* 2022; Feng *et al.,* 2023). GIS platforms, particularly cloud-based systems like Google Earth Engine, enable the integration, processing and spatial analysis of these multi-temporal datasets

(Oyeniyi *et al.,* 2025; Odunsi and Rienow, 2024). This allows researchers to quantify changes in urban sprawl, UHI intensity and emission-related indicators across the distinct periods of before, during and after the COVID-19 pandemic, facilitating a robust spatiotemporal assessment.

In conclusion, the conceptual framework for this study is built upon the interconnected dynamics of urban sprawl, the Urban Heat Island effect (quantified through Land Surface Temperature) and greenhouse gas emissions. These components form a feedback loop that is both a cause and a consequence of climate change. The application of GIS and remote sensing provides the essential toolkit for analyzing these phenomena across space and time. The unique circumstances of the COVID-19 pandemic offer a valuable natural experiment to isolate and examine the anthropogenic influence on this system, providing critical insights for developing sustainable urban planning and climate mitigation strategies (Anyakora *et al.,* 2025; Ramakreshnan *et al.,* 2018).

2.2 Importance of Urban Heat and Greenhouse Gases

The phenomena of Urban Heat Islands (UHI) and elevated concentrations of Greenhouse Gases (GHGs) represent two of the most critical environmental challenges confronting contemporary urban areas. Their significance extends far beyond localized temperature increases or atmospheric chemistry, profoundly impacting energy systems, public health, economic stability and the global climate. A thorough understanding of their importance is therefore foundational for developing sustainable, resilient and equitable urban futures.

2.2.1 Importance of Urban Heat

The Urban Heat Island effect is a significant anthropogenic modification of the local climate, with extensive and serious implications for cities. Its importance is rooted in its multifaceted impacts, which affect nearly every aspect of urban life.

First, the UHI effect directly exacerbates urban energy consumption, particularly for space cooling. As cities become warmer than their rural surroundings, the demand for air conditioning rises substantially.

This creates a positive and unsustainable feedback loop: higher temperatures increase the demand for cooling, which in turn releases more waste heat from buildings and power plants, further intensifying the urban heat island (Oke *et al.,* 2017). This elevated demand places a significant strain on electrical grids, increases utility costs for residents and businesses and contributes to higher emissions of greenhouse gases from energy generation.

Second, the public health implications of elevated urban temperatures are severe and well documented. The UHI effect significantly increases thermal discomfort and the risk of heat related morbidity and mortality. As noted, "Heat stress could cause rash, cramps, heat exhaustion and heat stroke and may exacerbate underlying medical conditions, such as heart or lung disease" (Pantavou *et al.,* 2011). The convergence of UHIs and natural heat waves is particularly dangerous, as evidenced by the 2003 European heat wave which resulted in tens of thousands of excess deaths (Pantavou *et al.,* 2011). Vulnerable populations, including the elderly, children and those with pre-existing health conditions, are at the greatest risk during such extreme heat events.

Third, UHIs have demonstrable consequences for environmental quality and urban ecosystems. They contribute to the degradation of air quality by facilitating the chemical reactions that form harmful secondary pollutants like ground-level ozone (Piracha and Chaudhary 2022). Furthermore, the effect can alter local microclimates and hydrological cycles. The replacement of natural vegetation with impervious surfaces not only reduces evaporative cooling but also leads to heated stormwater runoff, which can raise the temperature of rivers and streams, causing stress or mortality to aquatic life (Anyakora, *et al.,* 2025).

Finally, from a socio-economic and planning perspective, the UHI effect is a major barrier to urban sustainability and equity. The effect often disproportionately impacts lower-income neighborhoods, which may have less vegetation and older housing stocks with inadequate ventilation, thereby exacerbating social inequalities (Piracha and Chaudhary 2022). The increased costs associated with

healthcare, energy and infrastructure maintenance place a significant financial burden on municipalities and individuals. Consequently, addressing the UHI effect is not merely an environmental or technical issue but a crucial aspect of responsible urban governance, public health policy and social justice.

2.2.2 Importance of Greenhouse Gases

Greenhouse Gases are of paramount importance due to their central role in driving global climate change, with urban areas being the dominant source of anthropogenic emissions. The significance of GHGs lies in their capacity to alter the Earth's fundamental energy balance, with cascading effects on every component of the planetary system and human society.

The primary importance of GHGs, particularly carbon dioxide (CO_2), is their function in causing global warming. The "rapid expansion of urban areas, combined with the increasing concentration of greenhouse gases in the atmosphere, has significantly influenced global temperature trends and altered climate patterns" (Anyakora *et al.,* 2025). The combustion of fossil fuels for urban energy, industry and transportation releases vast quantities of CO_2 and other GHGs, which enhance the natural greenhouse effect by trapping outgoing longwave radiation. This process leads to a rise in global average temperatures, which in turn drives "a further rise in global mean surface temperature, global mean sea level and changes in the frequency and the intensity of extreme weather events and precipitation" (Pantavou *et al.,* 2011).

The intrinsic link between urban activities, UHIs and GHG emissions creates a dangerous feedback cycle. As previously established, the "increase in urban temperature will lead to more energy demands required for operating cooling devices, consequently leading to more greenhouse gas productions" (Abimbola *et al.,* 2025). This direct coupling means that the drivers of UHI are also significant sources of GHG emissions. Therefore, strategies aimed at mitigating urban heat, such as improving energy

efficiency and increasing vegetation, can deliver co-benefits by simultaneously reducing a city's carbon footprint.

The critical importance of anthropogenic GHG emissions was starkly illustrated during the COVID-19 pandemic, which served as an unplanned global experiment. The drastic reduction in human activity provided clear evidence of the direct impact of urban economic and transportation systems on atmospheric composition. Studies documented "reductions in $PM_{2.5,}$ PM_{10} and NO_2 concentrations, respectively, in cities across the globe due to restrictions on anthropogenic emission sources during the lockdown," as well as a global reduction in CO_2 emissions of 8.8% (Dogan *et al.,* 2024). This period unequivocally demonstrated that changes in urban human behavior can lead to immediate and measurable improvements in air quality and GHG levels.

Furthermore, GHG emissions are a central focus of international policy and governance frameworks, underscoring their global political importance. For instance, the European Union's Climate and Energy package has set binding targets for member states, including a "20% reduction in their greenhouse gas emissions (measured in CO_2 equivalent) by 2020 compared to 1990 levels," with a trajectory aiming for an 80% reduction by 2050 (Salata *et al.,* 2017). This high-level political recognition confirms that controlling GHG emissions is universally acknowledged as essential for mitigating the most severe and irreversible impacts of climate change on a planetary scale.

In conclusion, the importance of urban heat and greenhouse gases is both profound and interconnected. The UHI effect imposes immediate, local-scale stresses on human health, energy systems and ecological function within cities. In contrast, GHG emissions, largely originating from urban areas, drive long-term, global-scale climate disruption that threatens the stability of natural and human systems worldwide. Addressing these twin challenges in an integrated manner is not just an academic or environmental imperative, but a fundamental prerequisite for achieving sustainable development and safeguarding a viable future for urban populations.

2.3 Relationship Between Urban Heat, Land Surface Temperatures and Greenhouse Gases

The relationship between urban heat, Land Surface Temperatures (LST) and greenhouse gas (GHG) emissions forms a tightly coupled, cyclical system that is central to understanding urban climate change. This section delineates the fundamental connections between the Urban Heat Island (UHI) effect, its primary proxy LST and the concentration of atmospheric GHGs, outlining the core mechanisms that bind them together.

2.3.1 Relationship Between Urban Heat and Land Surface Temperatures (LST)

The Urban Heat Island phenomenon is most directly observed and quantified through Land Surface Temperature. LST, as measured by satellite thermal infrared sensors, provides a spatially continuous measure of the radiative skin temperature of the Earth's surface. This makes it an ideal metric for assessing the spatial pattern and intensity of the surface urban heat island, or SUHI (Zhou *et al.,* 2019). The UHI develops due to profound alterations in the urban energy balance, primarily driven by the replacement of natural landscapes with built surfaces. As cities expand, soils and vegetation are replaced by impervious materials like concrete, asphalt and buildings. These materials significantly alter the surface albedo and runoff characteristics, which in turn impacts local and regional land-atmosphere energy exchange processes (Aruya *et al.,* 2021).

The physical properties of urban areas directly elevate LST. The combination of radiative geometry and the thermal characteristics of the urban fabric accounts for a large portion of the urban heat island magnitude (Oke, 1982). For instance, urban canyons trap longwave radiation and reduce the sky view factor, substantially slowing nocturnal cooling. The spatial distribution of UHI often evolves from a mixed pattern to an extensive, contiguous heat island as urbanized blocks grow larger (Odunsi and Rienow 2024). This relationship is so robust that studies consistently find a strong negative correlation between LST and vegetation indices like the NDVI and a strong positive correlation with impervious

surface indices like the NDBI (Oyeniyi *et al.,* 2025; Anyakora *et al.,* 2025). In essence, LST serves as the direct thermal expression of the urban heat island effect at the surface level, providing a clear and measurable indicator of urban thermal pollution.

2.3.2 Relationship Between Urban Heat and Greenhouse Gases

The relationship between urban heat and greenhouse gases is synergistic and self-reinforcing, creating a positive feedback loop that is primarily mediated through urban energy consumption. Higher temperatures resulting from the heat island effect significantly increase energy demand for cooling. This elevated demand is predominantly met by burning fossil fuels, which emits pollutants including carbon dioxide (CO_2), a primary greenhouse gas (Piracha and Chaudhary 2022; Jamei *et al.,* 2022). Consequently, the UHI effect acts as a catalyst for increased GHG emissions through its direct impact on urban energy use.

This dynamic creates a dangerous feedback cycle. As urban air temperatures rise, more energy is used for air conditioning. This consumption causes greater anthropogenic heat emission and releases more GHGs from power plants, which further intensifies the urban heat island (Dong *et al.,* 2017; Rizwan *et al.,* 2008). This cycle of heat leading to more energy use, which releases more GHGs and waste heat, which in turn intensifies the original heating, encapsulates the critical relationship between urban heat and atmospheric pollution.

2.3.2.1 Mechanisms Linking Urban Heat and Greenhouse Gases

The primary mechanism linking UHI and GHGs is the anthropogenic heat flux from buildings and vehicles. Urban air temperatures are affected by processes that counteract nocturnal cooling, such as the turbulence and heat released by vehicles and building operations (Oke *et al.,* 2017). This anthropogenic heat is a direct byproduct of energy consumption, which is itself amplified by the UHI. Furthermore, the alteration of surface properties through urban sprawl reduces the natural carbon sequestration capacity. The conversion of vegetated areas, which act as carbon sinks, into impervious

surfaces not only increases LST but also eliminates a key natural mechanism for removing CO_2 from the atmosphere (Olorunfemi *et al.,* 2018).

2.3.2.2 Urbanization, Energy Demand and Emission Dynamics

Rapid urbanization and sprawl are the principal drivers of this relationship. The physical transformation of natural land surfaces to modern land use and land cover is the catalyst for both UHI formation and increased GHG emissions (Oyeniyi *et al.,* 2025). Sprawling cities increase dependence on private vehicles and extend energy infrastructure, leading to higher cumulative emissions. Studies show a direct correlation between the expansion of built-up area, the rise in LST and the increase in energy demand (Uju *et al.,* 2025; Bassett *et al.,* 2020). This expansion, often characterized by a dramatic increase in paved surfaces, is directly linked to rising local temperatures and a corresponding surge in energy consumption for cooling and its associated GHG emissions.

2.3.2.3 Atmospheric Feedback and Climate Implications

The interplay between UHI and GHGs has significant broader climate implications. Higher surface temperatures and heat liberated by anthropogenic activities provide a positive feedback to climate warming by strengthening the greenhouse effect, which can ultimately result in increased global warming (Rizwan *et al.,* 2008). Furthermore, higher urban temperatures can exacerbate the formation of secondary pollutants like ground-level ozone, which is itself a potent greenhouse gas. The higher temperatures in cities brought about by UHI adversely affect air quality because ground-level ozone is produced from precursors in the presence of nitrogen oxides and sunlight (Piracha and Chaudhary 2022). This demonstrates a direct atmospheric feedback where the UHI intensifies the chemical processes that create other climate-warming pollutants.

2.3.2.4 The COVID-19 Anthropause as Evidence of the Relationship

The COVID-19 pandemic and associated lockdowns served as an unprecedented global experiment, providing compelling empirical evidence for the relationship between anthropogenic activity, UHI and

GHG emissions. The sudden reduction in anthropogenic heat from vehicles and industrial activity offered a unique condition to test established theories (Dogan *et al.,* 2024). This period demonstrated a significant, albeit temporary, weakening of the UHI effect in many cities, alongside a sharp decline in atmospheric pollutants (Liu *et al.,* 2022; Feng *et al.,* 2023). Concurrently, satellite and ground-based measurements reported significant reductions in NO_2 and CO_2 in urban centres where vehicular traffic and industrial activities were most restricted (Le Quéré *et al.,* 2020). This period demonstrated a tangible decoupling of intense economic activity from emission levels, validating that the reduction in the mechanisms that cause GHG emissions leads to a direct drop in atmospheric concentrations. The post-lockdown rebound in both economic activity and emissions further cemented this causal link, highlighting how standard urban operations are a primary driver of the interconnected UHI and GHG problem.

2.4 Factors Affecting Urban Heat and Greenhouse Gases

The development and intensity of Urban Heat Islands (UHIs) and the concentration of greenhouse gases (GHGs) in urban areas are driven by a complex interplay of natural and human induced factors. A thorough understanding of these drivers is essential for accurate spatiotemporal assessment and for designing effective mitigation and adaptation strategies, particularly in the context of rapid urbanization and climate change.

2.4.1 Land Use and Land Cover Changes

Land Use and Land Cover Change (LULCC) is a primary driver of both UHI intensification and increased GHG emissions. The process of urbanization involves the conversion of natural landscapes such as forests, grasslands and water bodies into impervious urban surfaces like roads, buildings and pavements. This transformation fundamentally alters the local energy balance. As observed in Lafia, Nigeria, "Natural surfaces like rivers, water bodies and vegetation are typically destroyed during the urbanization process to make way for roads and buildings made of concrete, metal, asphalt and other

highly thermally active materials" (Abimbola *et al.,* 2025). These materials typically possess low albedo and high heat capacity, resulting in significant absorption and retention of solar radiation during the day and slow release at night (Abimbola *et al.,* 2025; Mohammad and Goswami, 2021).

Empirical studies consistently demonstrate a strong correlation between the expansion of built-up areas and rising land surface temperatures. In Abuja, an analysis from 2002 to 2023 revealed a dramatic increase in built-up area from 341.97 km² to 1310.35 km², while vegetation cover plummeted from 510.26 km² to just 53.98 km² (Uju *et al.,* 2025). Similarly, in Lagos, the land surface covered by urban regions expanded from 720 km² in 1984 to 2053 km² in 2016, with a corresponding intensification of the nocturnal spatial UHI from 0.83°C to 1.27°C over the same period (Bassett *et al.,* 2020). This replacement of vegetated, carbon sequestering land with artificial surfaces not only increases heat storage but also reduces the ecosystem's capacity to absorb atmospheric CO_2, thereby contributing to higher GHG concentrations.

2.4.2 Population Growth and Urbanisation

Rapid population growth and the associated rural to urban migration are the underlying catalysts for the LULCC described above. This demographic pressure fuels urban sprawl, which is defined as "the unrestricted growth of housing, commercial development and roads" and is "associated with longer commutes and contributes to traffic congestion and air pollution" (UN-HABITAT, 2018). It is projected that by 2050, Nigeria alone will be home to an additional 189 million urban dwellers, a trend mirrored across the developing world (UN-HABITAT, 2018).

The link between population density and UHI is well established. A higher population concentrates anthropogenic activities such as energy consumption, transportation and industrial processes, which are direct sources of GHG emissions and waste heat. As noted by Rizwan *et al.* (2008), anthropogenic heat release is closely related to "population and its per capita energy use." This creates a positive feedback loop: the UHI effect increases the demand for cooling, which in turn leads to more energy

consumption and associated waste heat and GHG emissions, further intensifying the UHI (Dong *et al.,* 2017).

2.4.3 Surface Characteristics and Building Materials

The physical and thermal properties of urban surfaces are critical determinants of UHI magnitude. Materials commonly used in cities, such as asphalt and concrete, have low solar reflectance (albedo), high thermal capacity and high thermal conductivity. "Roofs and pavements constitute about 60–70% of surface area in a typical city," and these surfaces become strong sources of heat radiation (Rizwan *et al.,* 2008). On a hot summer day, "roofs and pavements in a nearby urban area can reach up to 50°C more than the ambient temperature" (Carpio *et al.,* 2020).

The geometry of urban canyons also plays a crucial role. The introduction of buildings creates 'urban canyons' which trap solar radiation and reduce airflow, hindering convective heat loss (Vargo *et al.,* 2016; Arnfield, 2003). This configuration reduces the sky view factor, meaning the canyon floor is surrounded by warm vertical walls that radiate heat downwards, thereby reducing net radiative loss and significantly slowing nighttime cooling compared to rural areas.

2.4.4 Meteorological Conditions

Local meteorological conditions can either amplify or suppress UHI intensity. The phenomenon is most pronounced during "calm, cloudless conditions at night" (Oke, 1982). Under such conditions, turbulent transfer is minimal and radiative cooling in rural areas is rapid, maximizing the temperature differential between urban and rural zones.

Wind speed and cloud cover are particularly important moderating factors. Higher wind speeds enhance the advective removal of heat from urban areas, while cloud cover reduces incoming solar radiation, limiting the heat stored in urban materials during the day. As noted in a study on future climate interactions, "changes in the magnitude of the UHI effect over the current century will depend at least in part on how cloud cover and wind speed change" (Mika *et al.,* 2018). Furthermore,

phenomena like heat waves can interact synergistically with UHIs, leading to more severe and prolonged thermal stress in cities.

2.4.5 Energy Consumption and Transportation

Anthropogenic heat flux from energy consumption and transportation is a major contributor to both UHIs and GHG emissions. The UHI effect itself drives a positive feedback loop by increasing the demand for space cooling. This elevated energy demand is often met by burning fossil fuels, which releases GHGs like CO_2 and air pollutants such as nitrogen oxides (NO_x) (Piracha and Chaudhary2022). This creates a cycle where "Rising temperatures, resulting from Anthropogenic Heat Emission (AHE), could potentially trigger increasing energy demands for cooling, which in turn, leads to more AHE" (Dong *et al.*, 2017; Crutzen, 2004).

The transportation sector is a key source of this anthropogenic heat and these emissions. The COVID-19 pandemic served as a global experiment that underscored this link; lockdowns led to a drastic reduction in traffic, which in turn was a primary reason for observed reductions in UHI intensity and improved air quality in many cities. For example, in Prague, the lockdown was associated with a 15% reduction in SUHI and a 29% decline in nitrogen dioxide (Dogan *et al.*, 2024).

2.4.6 Vegetation and Green Space Distribution

The presence and distribution of vegetation are among the most significant mitigating factors for UHIs. Vegetation cools the environment through two primary processes: shading and evapotranspiration, which increases latent heat flux and reduces sensible heat. "Vegetation cover is a primary component for moderating land surface temperature through shading and evapotranspiration, hence the reduction in vegetation cover, as observed, is a key driver of urban heat island" (Abimbola *et al.,* 2025).

The cooling effect of vegetation is quantifiable through indices like the Normalized Difference Vegetation Index (NDVI). Studies consistently find a strong negative correlation between NDVI and

Land Surface Temperature (LST). The strategic introduction of vegetation is a proven mitigation strategy; for instance, "tree planting alone reduced summer afternoon temperatures by as much as 1.5 °C" in studied cities (Vargo *et al.,* 2016; Rosenfeld *et al.,* 1998). The loss of urban forests and green spaces not only diminishes this cooling service but also reduces the urban ecosystem's capacity to act as a carbon sink.

2.4.7 Topography and Geographic Location

The topographic and geographic setting of a city imposes a baseline influence on its local climate and can amplify or mitigate UHI effects. Factors such as elevation, proximity to large water bodies and latitude can modulate temperature patterns and pollution dispersion. For instance, a city located in a basin or valley may experience stronger and more persistent UHIs due to the trapping of stable, stagnant air, which also concentrates airborne pollutants and GHGs. Furthermore, a dominant wind direction can advect a city's warmth, a process known as urban heat advection, extending the UHI's influence several kilometers downwind into rural areas (Bassett *et al.,* 2020). Understanding these geographic constraints is vital for contextualizing spatiotemporal UHI assessments and for developing location-specific mitigation and adaptation plans.

In conclusion, the factors affecting urban heat and greenhouse gases are multifaceted and deeply interconnected. Land use changes, propelled by population growth, alter surface properties that interact with local meteorological conditions to dictate UHI intensity. These thermal changes, combined with concentrated energy consumption and transportation patterns, then drive urban GHG emissions, creating a complex, self-reinforcing urban climate system that must be holistically addressed.

2.5 Measurement Methods of Urban Heat and Greenhouse Gases

The accurate quantification of Urban Heat Islands (UHIs) and Greenhouse Gas (GHG) emissions is fundamental to diagnosing urban environmental challenges and formulating effective mitigation

strategies. The spatiotemporal nature of these phenomena necessitates methodologies that can capture data across extensive areas and over time. The integration of Geographic Information Systems (GIS) and remote sensing has revolutionized this field, providing powerful tools for large scale, repetitive and cost effective assessment (Jamei *et al.,* 2022).

2.5.1 Remote Sensing of Urban Heat

Remote sensing technology is an ideal tool for capturing and monitoring urban thermal environments at a fine spatial scale, allowing researchers to characterize the spatial variation of UHIs effectively (Jamei *et al.,* 2022). The primary parameter derived from satellite data for UHI studies is Land Surface Temperature (LST). LST is a fundamental aspect of climate and biology, serving as a critical indicator of energy partitioning at the land atmosphere boundary and is highly sensitive to changing surface conditions (Uju *et al.,* 2025).

Data Sources and Platforms

A variety of satellite sensors are employed for UHI analysis. The Landsat series of satellites, including Landsat 4, 5, 7 and 8, have been extensively used, providing a long-term archive ideal for studying changes over decades (Abimbola *et al.,* 2025; Oyeniyi *et al.,* 2025). For instance, Landsat 8 Operational Land Imager (OLI) and Thermal Infrared Sensor (TIRS) are commonly used for recent analyses. Sensors like the Moderate Resolution Imaging Spectroradiometer (MODIS) on Terra and Aqua satellites offer higher temporal resolution, with daily observations, which are valuable for analyzing diurnal and seasonal variations, though at a coarser spatial resolution of 1 km (Liu *et al.,* 2022; Feng *et al.,* 2023). Sentinel-2 data are also increasingly utilized for high-resolution land cover classification (Jamei *et al.,* 2022).

Land Surface Temperature (LST) Retrieval

The methodology for deriving LST from satellite imagery is a multi-step process. First, the digital numbers (DN) of the thermal infrared bands are converted to Top of Atmosphere (TOA) spectral

radiance. This radiance is then converted to at-satellite brightness temperature (TB) using the Planck equation (Chinedu *et al.,* 2024; Oyeniyi *et al.,* 2025). The formula is typically expressed as:

$$\mathbf{T = K_2 / \ln(K_1 / L_\lambda (+1)}$$

where K_1 and K_2 are calibration constants specific to the satellite sensor and L_λ is the spectral radiance.

To obtain the true LST, a critical correction for land surface emissivity (ε) is applied. Emissivity accounts for how efficiently a surface emits thermal radiation compared to a perfect blackbody. It is often estimated using vegetation indices, with the Normalized Difference Vegetation Index (NDVI) being the most common. The NDVI is calculated as:

NDVI = (NIR - RED) / (NIR + RED)

This index helps estimate the proportion of vegetation (Pv), which is then used in models to calculate emissivity, as surfaces with vegetation have different emissivity properties than impervious surfaces like concrete or asphalt (Oyeniyi *et al.,* 2025; Anyakora *et al.,* 2025). A common formula for the final LST correction is:

$$\mathbf{LST = TB / [1 + (\lambda * TB / \rho) \ln(\varepsilon)]}$$

where λ is the wavelength of emitted radiance and ρ is a constant (Oyeniyi *et al.,* 2025).

Quantifying the Urban Heat Island

The derived LST is used to quantify the Surface Urban Heat Island (SUHI). A standard approach is the simplified urban-extent algorithm, where SUHI intensity (SUHII) is calculated as the difference between the mean LST of urban pixels and the mean LST of rural pixels:

SUHII = LSTUrban - LSTRural (Feng *et al.,* 2023; Liu *et al.,* 2022)

For a more nuanced analysis of ecological impact and human thermal comfort, the Urban Thermal Field Variance Index (UTFVI) is often calculated. This index quantitatively measures the thermal stress level of an urban area and is derived as:

UTFVI = (LST − LSTmean) / LST (Odunsi and Rienow 2024; Oyeniyi *et al.,* 2025)

GIS Integration and Advanced Platforms

Geographic Information Systems (GIS) are indispensable for processing, analyzing and visualizing the spatial data derived from remote sensing. GIS platforms like ArcGIS are used for tasks such as supervised image classification to map Land Use/Land Cover (LULC), zonal statistics to correlate LST with different land cover types and creating thematic maps of UHI intensity (Oyeniyi *et al.,* 2025). The advent of cloud computing platforms like Google Earth Engine (GEE) has further revolutionized the field by enabling the rapid processing of massive satellite datasets and facilitating long-term time-series analysis, which was crucial for assessing the rapid environmental changes associated with the COVID-19 lockdowns (Rahaman *et al.,* 2022; Oyeniyi *et al.,* 2025; Dogan *et al.,* 2024).

2.5.2 Measurement of Greenhouse Gases

The measurement of greenhouse gases employs a combination of ground-based in-situ monitoring, satellite-based remote sensing and inventory-based modeling approaches. The COVID-19 pandemic served as a significant natural experiment, highlighting the value of these methods in capturing changes in anthropogenic emissions (Le Quéré *et al.,* 2020).

Ground-Based and In-Situ Monitoring

Traditional methods rely on a network of ground-based stations that provide high-precision, continuous measurements of atmospheric concentrations of CO_2, CH_4, N_2O and other pollutants like nitrogen dioxide (NO_2) and carbon monoxide (CO). These stations are considered the gold standard

for calibration and validation but are limited by their sparse spatial distribution, making it difficult to capture city-wide heterogeneity (Le Quéré *et al.,* 2020). During the COVID-19 lockdowns, these in-situ measurements were critical in documenting "significant reductions in NO_2, $PM_{2.5}$, CO_2 and other pollutants" due to decreased vehicular and industrial activity (Dogan *et al.,* 2024).

Satellite Remote Sensing of GHGs

Satellite remote sensing provides a broader spatial perspective on GHG emissions and their precursors. Sensors like the TROPOspheric Monitoring Instrument (TROPOMI) on board the Sentinel-5P satellite provide high-resolution data on atmospheric pollutants such as nitrogen dioxide (NO_2) and aerosols (Jamei *et al.,* 2022; Feng *et al.,* 2023). The dramatic, visually evident reduction in NO_2 concentrations observed by Sentinel-5P over urban areas during the lockdowns served as a clear indicator of reduced fossil fuel combustion from transportation and industry (Dogan *et al.,* 2024). MODIS data on Aerosol Optical Depth (AOD) is also used as a proxy for particulate pollution, which often correlates with combustion-related GHG emissions (Feng *et al.,* 2023).

Proxies for Anthropogenic Activity and Emission Inventories

Given the challenge of directly measuring all GHG fluxes, proxies are widely used in spatial analyses. Nighttime light (NTL) data, obtained from satellites like the Visible Infrared Imaging Radiometer Suite (VIIRS), are strongly correlated with human settlements, economic activity and energy use (Dong *et al.,* 2017; Jamei *et al.,* 2022). This makes NTL an invaluable spatial proxy for downscaling national or regional energy consumption data to estimate the spatial distribution of anthropogenic heat flux (AHF) and, by extension, associated CO_2 emissions (Dong *et al.,* 2017). As noted by Dong *et al.* (2017), "nighttime lights are closely correlated with the local economic activities," and a strong linear relationship exists between the digital number of nighttime lights and anthropogenic heat flux density.

Emission inventories compile data from various sectors, such as transportation, industry, power generation and residential energy use to estimate total GHG outputs. These inventories can be spatially

distributed using GIS and proxies like population density and nighttime lights to create high-resolution emission maps. For a top-down estimation, studies often combine data on primary energy consumption with these spatial proxies. For instance, anthropogenic heat emission (AHE) can be derived from human metabolic heating and primary energy consumption, which is divided into sectors and distributed using global population datasets adjusted with radiance-calibrated nighttime lights (Dong *et al.,* 2017). This method allows for the construction of global AHE databases with high spatial and temporal resolution, elucidating the direct link between urban energy use and local climate forcing.

In conclusion, the synergistic use of multi-sensor remote sensing data, GIS-based spatial analysis and ground-based measurements provides a comprehensive toolkit for the spatiotemporal assessment of urban heat islands and greenhouse gas emissions. These methods were critically applied during the COVID-19 pandemic, offering unprecedented empirical evidence of the direct link between human activity and urban environmental conditions and they remain essential for informing climate-responsive urban planning and policy.

2.6 Application of Urban Heat and Greenhouse Gases Data

The data derived from the study of Urban Heat Islands (UHI), Land Surface Temperatures (LST) and Greenhouse Gas (GHG) emissions, primarily acquired through Geographic Information Systems (GIS) and remote sensing, provides a critical evidence base for practical decision-making. These datasets are not merely academic; they are instrumental in guiding sustainable urban development, protecting public health, managing energy resources and building climate-resilient cities. The spatiotemporal data collected before, during and after the COVID-19 pandemic has further illuminated the direct relationship between human activity and urban environmental quality, refining these applications with real-world evidence.

2.6.1 Urban Planning and Sustainable Development

Data on UHIs and GHGs are fundamental for evidence-based urban planning, directly supporting the goals of sustainable development. The identification of thermal hotspots and areas of high emissions allows planners to prioritize interventions and steer urban growth away from environmentally detrimental patterns. For instance, spatiotemporal analysis of Land Surface Temperature (LST) and land use/land cover (LULC) reveals the consequences of urban sprawl, showing how the replacement of natural landscapes with impervious surfaces intensifies the UHI effect (Oyeniyi *et al.,* 2025). This scientific evidence is crucial for enforcing urban growth boundaries and promoting compact city designs.

Furthermore, this data enables the strategic implementation of nature-based solutions. Studies in cities like Abuja have demonstrated that "vegetation and water bodies effectively lower surface temperatures through shading and evapotranspiration, highlighting their importance in urban climate regulation" (Anyakora *et al.,* 2025). By using tools like the Local Climate Zones (LCZ) classification system, planners can standardize urban site descriptions, which aids in creating zoning regulations that discourage heat-absorbing materials and encourage reflective surfaces and vegetative cover (Stewart and Oke, 2012). This approach ensures that urban development is aligned with the objectives of creating sustainable and livable cities.

2.6.2 Climate Change Assessment and Modelling

UHI and GHG data are indispensable for assessing and projecting the impacts of climate change at both local and global scales. Urban areas are significant contributors to global warming and understanding their specific thermal and emissions profile is crucial for accurate climate modeling. The COVID-19 lockdown period served as an unprecedented natural experiment, providing "an improved understanding of the urban climate variations during the global pandemic" (Liu *et al.,* 2022).

The observed, quantifiable reduction in UHI intensity and GHG emissions during this period offered robust empirical evidence of the urban climate's sensitivity to anthropogenic activities.

This data is vital for calibrating and validating climate models. As noted by Ooka (2007), "the inclusion of detailed anthropogenic heating data in atmospheric simulations of the urban environment will elucidate how UHI effects develop spatially and temporally." Long-term data, such as the steady increase in LST observed in many urban areas, provides ground-truthed evidence of regional warming, complementing global climate models and helping to predict future scenarios under continued urbanization (Abimbola *et al.,* 2025).

2.6.3 Air Quality and Public Health Monitoring

The synergistic relationship between UHIs, air pollution and public health makes the integrated application of this data vital for safeguarding urban populations. Higher urban temperatures can accelerate the photochemical reactions that form harmful ground-level ozone, while also increasing energy demand and consequent emissions from power plants. By overlaying spatial data on UHI intensity with air quality measurements from satellites like Sentinel-5P, health officials can identify areas of co-occurring thermal stress and poor air quality.

Epidemiological studies consistently use this data to quantify health burdens. For example, research has linked extreme heat to significant increases in mortality from cardiovascular, respiratory and cerebrovascular diseases (Salata *et al.,* 2017). Mapping thermal vulnerability using indices like the Urban Thermal Field Variance Index (UTFVI) allows for targeted public health interventions, such as heat early warning systems and the strategic placement of cooling centers and green spaces to protect the most at-risk communities during heatwaves.

2.6.4 Energy Management and Urban Cooling Strategies

Quantifying the UHI effect is directly applicable to urban energy management. The increased temperatures in urban cores lead to a higher demand for air conditioning, which in turn elevates energy

consumption and associated GHG emissions. This creates a positive feedback loop that further intensifies the UHI. Data on LST and urban morphology is therefore used to design and evaluate urban cooling strategies.

Mitigation strategies informed by this data, such as cool roofs, green roofs and high-albedo pavements, are proven to reduce heat absorption and lower cooling loads for buildings. Studies have shown that these strategies can lead to substantial reductions in peak energy demand and significant cost savings, simultaneously reducing carbon emissions (Rizwan *et al.,* 2008). The strategic placement of vegetation, which can lead to a dramatic reduction in LST, is another data-driven strategy to reduce the urban energy footprint.

2.6.5 Disaster Risk Reduction and Urban Resilience

In an era of climate change, UHI and GHG data are critical for enhancing urban resilience to disasters, particularly extreme heat events. The combination of UHIs and heatwaves creates health risks that are greater than the sum of their parts. Spatiotemporal assessments help in identifying populations and neighborhoods most vulnerable to heat stress, which is essential for developing Heat Action Plans.

Furthermore, understanding the relationship between urban sprawl, soil sealing and surface runoff informs strategies for "pervious pavements" that not only mitigate UHIs but also aid in "storm water management and then for the prevention from floods" (Salata *et al.,* 2017). By integrating UHI data with other geospatial layers, city managers can develop holistic resilience plans that address multiple climate-related hazards, making urban systems more adaptable and safer for their inhabitants.

2.6.6 Research and Policy Applications

Finally, UHI and GHG data form the foundation of evidence-based research and policymaking. This data helps identify critical research gaps and drives methodological advancements in environmental monitoring. For policy, it provides the metrics needed to set baselines, track progress against environmental targets and evaluate the effectiveness of interventions.

The temporary environmental improvements witnessed during the COVID-19 lockdowns provide a powerful illustration for policymakers of what is achievable through reduced anthropogenic activity, motivating policies that promote sustainable transportation and green infrastructure (Jamei *et al.,* 2022). As emphasized in the context of sustainable urban governance, the aspiration of creating resilient cities is only achievable "when related legislative policies are mainstreamed into planning and the development control system" (Ramakreshnan *et al.,* 2018). Decision Support Systems (DSS) that integrate this geospatial data are increasingly vital tools for helping policymakers visualize scenarios and craft effective, location-specific climate action plans.

2.7 Case Study: Urban Heat Islands and Greenhouse Gas Assessment in Abuja

This section synthesizes global, regional and local studies on Urban Heat Islands (UHI) and greenhouse gas (GHG) dynamics, culminating in a focused assessment of Abuja, Nigeria. This case is particularly instructive for understanding the spatiotemporal interplay between rapid urban sprawl, local climate change and the potential impacts of anomalous events like the COVID-19 pandemic.

2.7.1 Global Studies on Urban Heat and Greenhouse Gas Dynamics

Research across the globe has firmly established that urbanization is a primary driver of local climate modification. The Urban Heat Island (UHI) effect, whereby urban areas experience significantly higher temperatures than their rural surroundings, is a well-documented phenomenon (Oke, 1982; Santamouris, 2015). Its intensity is governed by alterations to the urban energy balance, caused by the urban fabric and anthropogenic activities that simultaneously alter surface properties, the balance between sensible and latent heat fluxes and add excess heat to the environment (Oke *et al.,* 2017).

The link between UHI and GHG emissions is often indirect but significant, operating through increased energy demand. As cities become warmer, the demand for mechanical cooling escalates. This elevated energy consumption, often met by fossil fuel combustion, results in higher emissions of air pollutants and greenhouse gases such as carbon dioxide (CO_2) (Piracha and Chaudhary, 2022). This

creates a feedback loop where UHI intensifies GHG emissions, which in turn contribute to broader climate change that can exacerbate urban heating. The COVID-19 pandemic provided a unique global experiment, with studies showing that lockdown-induced reductions in human activity led to a significant, though temporary, decrease in GHG emissions and a weakening of the UHI effect in many cities, underscoring the direct link between anthropogenic factors and urban climate (Le Quéré *et al.,* 2020; Liu *et al.,* 2022; Dogan *et al.,* 2024).

2.7.2 African and Regional Perspectives

In the African context, the challenges of urbanization are acute. The continent is experiencing rapid urban expansion, which often manifests as urban sprawl which is the unrestricted, low-density growth of urban areas into the countryside (Salata *et al.,* 2017). This pattern is "associated with longer commutes and contributes to traffic congestion and air pollution" (UN-HABITAT, 2018). A significant research gap exists, however, as noted by Bassett *et al.* (2020), who found that of thousands of global UHI studies, only a tiny fraction focused on Nigeria. Despite this, the impacts are severe. Studies across the continent consistently link the conversion of vegetated land to impervious surfaces with rising Land Surface Temperatures (LST) and intensified UHI effects, as seen in cities like Lagos and Akure (Bassett *et al.,* 2020; Oyeniyi *et al.,* 2025).

2.7.3 Urban Heat Island and Greenhouse Gas Assessment in Nigeria

In Nigeria, the narrative of rapid urbanization and its environmental consequences is pronounced. Studies in cities like Lagos, Benin City and Kaduna have consistently documented intense UHI phenomena driven by urban sprawl and land cover change. In Lagos, for instance, intense urbanization between 1984 and 2016 saw the city's spatial extent grow from 720 km² to 2053 km², with a corresponding intensification of the nocturnal UHI (Bassett *et al.,* 2020). Research in Benin City confirmed the existence of a strong UHI, with the highest diurnal Urban Canopy Heat Island (UCHI) reaching 6.34°C, closely attributed to impervious surfaces and anthropogenic activities (Aruya *et al.,*

2021). The established methodological approach for these assessments relies heavily on GIS and remote sensing, using satellite imagery from Landsat and MODIS to analyze the spatiotemporal dynamics of LST and its correlation with indices like the Normalized Difference Vegetation Index (NDVI) and the Normalized Difference Built-up Index (NDBI) (Oyeniyi *et al.,* 2025).

2.7.4 Implications for Abuja

As the federal capital territory, Abuja represents a critical case study of planned urban development experiencing the pressures of rapid sprawl and its climatic consequences. Recent studies provide a detailed spatiotemporal assessment of UHI and its drivers in the city.

Spatiotemporal Patterns of Land Use and Land Cover (LULC): Analysis of LULC changes in Abuja reveals a dramatic transformation. Between 2002 and 2023, built-up areas increased significantly from 341.97 km² to 1310.35 km², a surge of 968.39 km². This expansion occurred primarily at the expense of vegetation, which decreased sharply from 510.26 km² to just 53.98 km² (Uju *et al.,* 2025). This rapid conversion of pervious, vegetated land to impervious surfaces is a fundamental driver of the UHI effect.

Land Surface Temperature (LST) and UHI Intensity: The change in LULC has had a direct and substantial impact on LST. Research shows that the mean LST in Abuja increased by 6.89°C, from 32.31°C in 2002 to 39.2°C in 2023 (Uju *et al.,* 2025). Built-up areas were consistently associated with the highest temperatures. Furthermore, analysis using the Urban Thermal Field Variance Index (UTFVI) indicated that areas such as GUI, Kabusa, Orozo and Jiwa experience the worst thermal comfort levels, classifying them as the city's strongest UHI zones (Anyakora *et al.,* 2025).

The Role of Blue-Green Infrastructure and Mitigation: A critical finding for Abuja's planning is the quantifiable cooling effect of blue-green spaces. An assessment of Jabi Lake demonstrated a clear thermal gradient, with the lake itself at 29.73°C, rising to 40.74°C at a 300-meter buffer (Anyakora *et al.,* 2025). This confirms that vegetation and water bodies play a critical role in cooling urban areas,

emphasizing the importance of preserving and strategically integrating such spaces into the urban fabric to mitigate UHI effects. Mitigation strategies such as increasing vegetation cover, implementing cool roofs and promoting reflective pavements are therefore highly relevant for Abuja's sustainable development (Salata *et al.,* 2017).

Link to Greenhouse Gases and Anthropogenic Activities: The growth of Abuja is inextricably linked to GHG emissions. The expansion of built-up areas, industries and infrastructure leads to the replacement of natural carbon sinks with surfaces that contribute to heating. In industrial areas like Gwagwalada, "increased greenhouse gas emissions can lead to higher temperatures and altered weather patterns," releasing gases such as CO_2, methane (CH_4) and nitrous oxide (N_2O) (Uju *et al.*, 2025). This creates a feedback loop where higher urban temperatures increase demand for cooling, thereby consuming more energy and releasing more GHGs and waste heat (Jamei *et al.,* 2022).

In conclusion, the case of Abuja powerfully illustrates the central themes of this research. It demonstrates a clear spatiotemporal pattern where urban sprawl drives land cover change, which in turn intensifies the UHI effect and contributes to regional GHG emissions. The lessons from Abuja, supported by global and regional evidence, underscore the critical need for integrated urban planning that leverages GIS and remote sensing to implement climate-sensitive strategies, such as protecting blue-green infrastructure and promoting energy-efficient materials, to build a more sustainable and resilient urban future.

2.8 Impacts, Mitigation Strategies and Challenges of Urban Heat and Greenhouse Gases

This section synthesizes the multifaceted consequences of Urban Heat Islands (UHIs) and greenhouse gas (GHG) emissions, explores the spectrum of available mitigation strategies and outlines the persistent challenges in accurately assessing and combating these interconnected urban climate issues.

2.8.1 Impacts of Urban Heat and Greenhouse Gases on Human Health and the Environment

The synergistic effects of UHIs and elevated GHG concentrations pose severe and interconnected risks to human health, ecological systems and urban infrastructure. The UHI phenomenon, where "urban areas exhibit higher temperatures compared to their rural surroundings" (Odunsi and Rienow 2024), acts as a powerful localized amplifier of global climate change, exacerbating its negative outcomes.

The impacts on human health are direct and severe. Exposure to extreme urban heat, particularly during heatwaves intensified by the UHI effect, can overwhelm the human body's capacity to regulate its temperature. This can lead to a range of heat-related illnesses, from heat cramps and exhaustion to fatal heat strokes (Pantavou *et al.,* 2011). The interaction is particularly deadly; "UHI and SUHI combined with natural phenomena, such as Heat Waves (HWs), can potentiate the impacts on human health, culminating in increased mortality" (Almeida *et al.,* 2021). The 2003 European heatwave, for instance, resulted in tens of thousands of excess deaths, with research suggesting "that the UHI was responsible for half the excess mortality in some regions" (Bassett *et al.,* 2020). Furthermore, UHIs and air pollution form a dangerous combination. Higher temperatures can accelerate the chemical reactions that form ground-level ozone, a harmful pollutant. Studies have shown that this leads to increased "hospital respiratory admissions" (Piracha and Chaudhary 2022), disproportionately affecting vulnerable populations such as the elderly, children and those with pre-existing respiratory or cardiovascular conditions.

The environmental and economic impacts are equally profound and create a damaging feedback loop. UHIs lead to a substantial "increase in energy demands required for operating cooling devices, consequently leading to more greenhouse gas productions and financial burden on individuals" (Abimbola *et al.,* 2025). For example, "electricity demand for cooling increases 1.5-2.0% for every 0.6°C increase in air temperatures" (Mohajerani *et al.,* 2017). This heightened demand for energy,

often met by burning fossil fuels, releases more GHGs and waste heat, which in turn further intensifies the UHI. This cycle results in "deteriorated air quality [and] higher CO2 emissions" (Piracha and Chaudhary2022). Ecologically, the replacement of natural landscapes with impervious surfaces and the resulting temperature increase have a "negative impact on urban biodiversity, as species that are less heat-tolerant struggle to adapt to higher temperatures in urban contexts" (Abimbola *et al.,* 2025). Additionally, heated stormwater runoff from warm pavements and roofs can harm aquatic ecosystems by abruptly raising water temperatures in streams and rivers, which can be "particularly stressful and even fatal to aquatic life" (Mohajerani *et al.,* 2017).

2.8.2 Mitigation Strategies for Urban Heat and Greenhouse Gases

Addressing the dual challenges of UHIs and GHG emissions requires a multi-pronged approach that targets urban form, materials and vegetation. These strategies are often most effective when implemented in combination.

A cornerstone of mitigation is the implementation of greening strategies. Increasing urban vegetation through tree planting, parks and green roofs is one of the most effective measures. "The benefits of increased urban vegetation... has been demonstrated in a large number of modeling studies" (Vargo *et al*., 2016). Vegetation cools the environment through shading and evapotranspiration. For instance, "tree planting alone reduced summer afternoon temperatures by as much as 1.5 °C, diminishing the region's average summer heat island by more than half" (Vargo *et al.,* 2016). The strategic introduction of trees has been found to produce "the largest impact," with a mitigation effect "estimated in around 2 °C in the peak hours" (Salata *et al.,* 2017).

Another critical strategy involves the use of high-albedo and cool materials. Replacing dark, heat-absorbing surfaces with reflective materials for roofs and pavements directly reduces heat absorption. "UHI reduction strategies commonly take two forms: (i) increase the solar reflectance (albedo) of roofs and pavements and (ii) increase green areas" (Piracha and Chaudhary 2022). Studies focusing on

the Los Angeles basin found that "extensive albedo enhancement of building rooftops and paved surfaces could result in a reduction in afternoon summer temperatures of between 1.5 °C and 2 °C" (Vargo *et al.,* 2016). Cool roofs and façades, which utilize materials with high solar reflectance, reduce cooling loads and the associated waste heat from air conditioning systems (Salata *et al.,* 2017).

Effective mitigation also depends on sustainable urban planning and policy. Instruments like the 'green area ratio' (GAR), a "longstanding zoning tool in Germany," specify "minimum vegetative cover requirements for privately owned property" and provide flexibility in how these standards are met (Vargo *et al.,* 2016). Combating unstructured urban sprawl is critical, as it leads to the loss of natural vegetation and increases dependence on private vehicles. Recommendations include the "optimization of vertical to horizontal expansion of city" and "decentralization of urban areas" to manage growth (Yaro *et al.,* 2017). Furthermore, promoting sustainable transportation, including "electric vehicles" and "safe shared mobility," can directly reduce GHG emissions from the transport sector, a major contributor to both GHGs and anthropogenic heat (Jamei *et al.,* 2022).

The COVID-19 lockdowns served as a large-scale, unintended experiment that validated the effectiveness of reducing anthropogenic activities. The "unprecedented reduction in human activities... led to a significant reduction in SUHI" (Mijania *et al.,* 2022) and a "weakened UHI effect" (Dogan *et al.,* 2024), demonstrating that policies aimed at reducing transportation and industrial emissions can have immediate and measurable co-benefits for the urban thermal environment.

2.8.3 Challenges in Urban Heat and Greenhouse Gas Estimation

Despite significant advancements in technology and methodology, accurately estimating and mitigating UHIs and GHGs remains fraught with challenges that span methodological, technical and governance domains.

A primary challenge is methodological inconsistency and data limitations. A critical review of UHI studies highlighted "an insufficiency and paucity of field measurements," "a vague set of site

classification," and the use of "uncontrolled and old set of data" (Ramakreshnan *et al.,* 2018). This lack of standardization makes cross-comparison between studies difficult. Remote sensing, while excellent for spatial coverage, can be hampered by factors like cloud cover and has inherent limitations; for instance, satellite-based Surface Urban Heat Island (SUHI) studies have "low temporal resolution," while ground-based Atmospheric UHI (AUHI) measurements suffer from "poor spatial resolution" (Odunsi and Rienow 2024). Quantifying a key UHI driver, anthropogenic heat flux (AHF), is particularly difficult, with researchers noting that "the attempt of looking for an effective and reliable method of estimating the amount of anthropogenic heat release is tough but necessary" (Manoli *et al.,* 2020).

Furthermore, there is a significant implementation and policy gap. A persistent "deep gap between researchers, or specialists, in urban climates and urban planners, or policy makers" means that a "vast wealth of urban climate knowledge has not been sufficiently applied to urban design or planning" (Ooka 2007). This is evident in contexts like Malaysia, where "there are no policies... that specifically address the UHI phenomenon, even in the National Policy on Climate Change" (Ramakreshnan *et al.,* 2018). The challenge is compounded by the transboundary nature of urban sprawl, where "urban expansion is frequently not constrained within municipal limits" (UN-HABITAT 2018), making coordinated governance and the implementation of unified, large-scale mitigation strategies exceedingly difficult.

Finally, the rapid pace of urbanization itself presents a constant challenge. Urban sprawl, described as an "unrestricted growth of housing, commercial development and roads," leads to the continuous "conversion of other types of land use" (Kuddus *et al.,* 2020), which perpetually alters the urban fabric and makes long-term, stable planning and monitoring a moving target.

2.9 Research Gap Identification

A thorough review of existing scholarly work reveals substantial progress in understanding Urban Heat Islands (UHIs), Land Surface Temperatures (LST) and their connections with greenhouse gas (GHG) emissions. Despite this progress, several crucial research deficiencies remain, particularly concerning rapidly growing urban areas in developing nations and the unique circumstances created by the COVID 19 pandemic. This section details the specific gaps in the literature that the present study aims to fill.

A fundamental methodological shortcoming is the lack of integrated spatiotemporal studies. Existing research frequently treats UHI phenomena and GHG emissions as separate subjects. There is a notable absence of analyses that concurrently examine their dynamic interactions across both space and time (Feng *et al.,* 2023; Jamei *et al.,* 2022). This issue is exacerbated in studies of African cities, where Ramakreshnan *et al.* (2018) note an "insufficiency and paucity of field measurements," and a reliance on "uncontrolled and old set of data." Bassett *et al.* (2020) further confirm that a "lack of observations and technology barriers... mean there are comparably fewer UHI studies" in Africa. The consistent application of integrated GIS and remote sensing techniques to explore the UHI-GHG relationship over long time series, especially those including significant events like a global pandemic, is a gap this research will address.

Closely related is a significant geographical and contextual bias in the existing literature. While cities in Europe, North America and Asia are well-studied, there is a critical shortage of detailed research focusing on mid-sized, sprawling cities in developing nations, particularly in Sub-Saharan Africa (Oyeniyi *et al.,* 2025; Bassett *et al.,* 2020). The urban growth patterns, climatic conditions and socio-economic factors in these regions are distinct. Oyeniyi *et al.* (2025) wisely caution that "evidence from a mid-sized city might not be extended to other cities of similar size and socioeconomic characteristics without caution." The specific dynamics of how urban sprawl in a city like Abuja influences LST and GHG emissions and how effective common mitigation strategies might be in this context, are not yet

fully understood. This study will provide a focused analysis of Abuja, contributing to a more geographically balanced body of knowledge.

The COVID 19 pandemic provided an unprecedented natural experiment for urban climate science. The global lockdowns led to a sudden and dramatic reduction in human activities, such as transportation and industry, which are primary sources of anthropogenic heat and GHG emissions. While initial studies documented temporary reductions in UHI intensity and air pollution (Liu *et al.,* 2022; Feng *et al.,* 2023), a comprehensive analysis covering the pre-pandemic, lockdown and post-pandemic periods for a single city is lacking. Feng *et al.* (2023) observed that "the impact of the COVID 19 lockdown on SUHIs only lasted for a month," highlighting the transient nature of these changes. A detailed, three-phase spatiotemporal analysis is needed to decouple the effects of this unique anthropogenic pause from background climate variability and to empirically validate the theoretical link between human activity and urban climate, a link Rizwan *et al.* (2008) described as complex and difficult to quantify.

Another critical gap concerns the mismatch between the physical scale of UHI phenomena and the administrative scale of urban governance. Urban sprawl often extends far beyond official municipal boundaries, creating a disconnect between the geographical extent of the UHI and the jurisdictional limits of the planning authorities responsible for its mitigation (UN HABITAT 2018). As urban expansion "frequently overlaps or spills over between various Local Government Areas (LGAs) or even federal states" (UN HABITAT 2018), it creates a governance challenge. This is compounded by a lack of specific policies; Ramakreshnan *et al.* (2018) noted that in Malaysia, "there are no policies... that specifically address the UHI phenomenon," a situation likely common in many developing nations. Research is needed to understand how to design and implement effective, multi-level policy interventions that can address the transboundary nature of UHIs and GHG emissions in fragmented governance landscapes.

Finally, a persistent gap exists in translating academic research into practical, cost-effective mitigation plans. While the literature is rich with general mitigation strategies such as using high-albedo materials, increasing urban greenery and promoting cool roofs (Salata *et al.,* 2017; Rizwan *et al.,* 2008), there is a shortage of fine-scale, localized studies that evaluate the feasibility and cost-benefit of these strategies in the specific context of a sprawling African city. Ooka (2007) stressed that for mitigation to be effective, "the priorities for various countermeasures should be clearly shown... It is also important to indicate the cost benefit of each countermeasure." Moving from generic recommendations to spatially explicit, prioritized and economically viable action plans tailored to the unique socio-economic and climatic conditions of cities like Abuja is a necessary next step for applied urban climate research.

In conclusion, this study is designed to address the following key research gaps:

1. The lack of integrated, high-resolution spatiotemporal analyses that simultaneously examine UHI intensity, LST patterns and GHG fluxes.
2. The geographical bias in existing literature, which has neglected detailed study of UHI-GHG dynamics in sprawling mid-sized cities of Sub-Saharan Africa, such as Abuja, Nigeria.
3. An incomplete understanding of the UHI-GHG relationship, which can be illuminated by a full temporal analysis (before, during and after) of the unique anthropogenic pause caused by the COVID 19 pandemic.
4. The governance and policy gap concerning the development of effective mitigation strategies for UHI and GHG emissions in politically and administratively fragmented, rapidly sprawling urban regions.
5. The need for applied research that translates general mitigation theory into specific, prioritized and cost-effective implementation plans for defined urban contexts.

By addressing these interconnected gaps, this research will contribute a comprehensive spatiotemporal assessment of UHIs and GHG reductions, providing evidence-based insights with direct implications for urban planning, climate change mitigation and the enhancement of urban resilience in Abuja and similar cities.

CHAPTER THREE

METHODOLOGY

3.1 Study Area Description

The study focuses on Abuja, Nigeria, the Federal Capital Territory (FCT), situated between latitudes 8°25′ and 9°25′N and longitudes 6°45′ and 7°45′E. Abuja's landscape is characterized by undulating topography, comprising granitic outcrops, hills and low-lying plains with elevations ranging from 150 to 760 m above sea level. The climate is typically tropical with two main seasons: a wet season (April–October) and a dry season (November–March), marked by an annual mean temperature of 26–30°C (Folorunsho *et al.,* 2017; Uju *et al.,* 2025). Rapid population growth and urban expansion, accelerated since the 1990s, have transformed the area's natural vegetation into built-up zones, contributing to urban heat accumulation and greenhouse gas (GHG) emissions (Abimbola *et al.,* 2025).

Given Abuja's designation as Nigeria's administrative capital, it presents a suitable case for assessing the spatiotemporal interaction between urban heat island (UHI) dynamics, GHG emissions and urban sprawl across the COVID-19 periods.

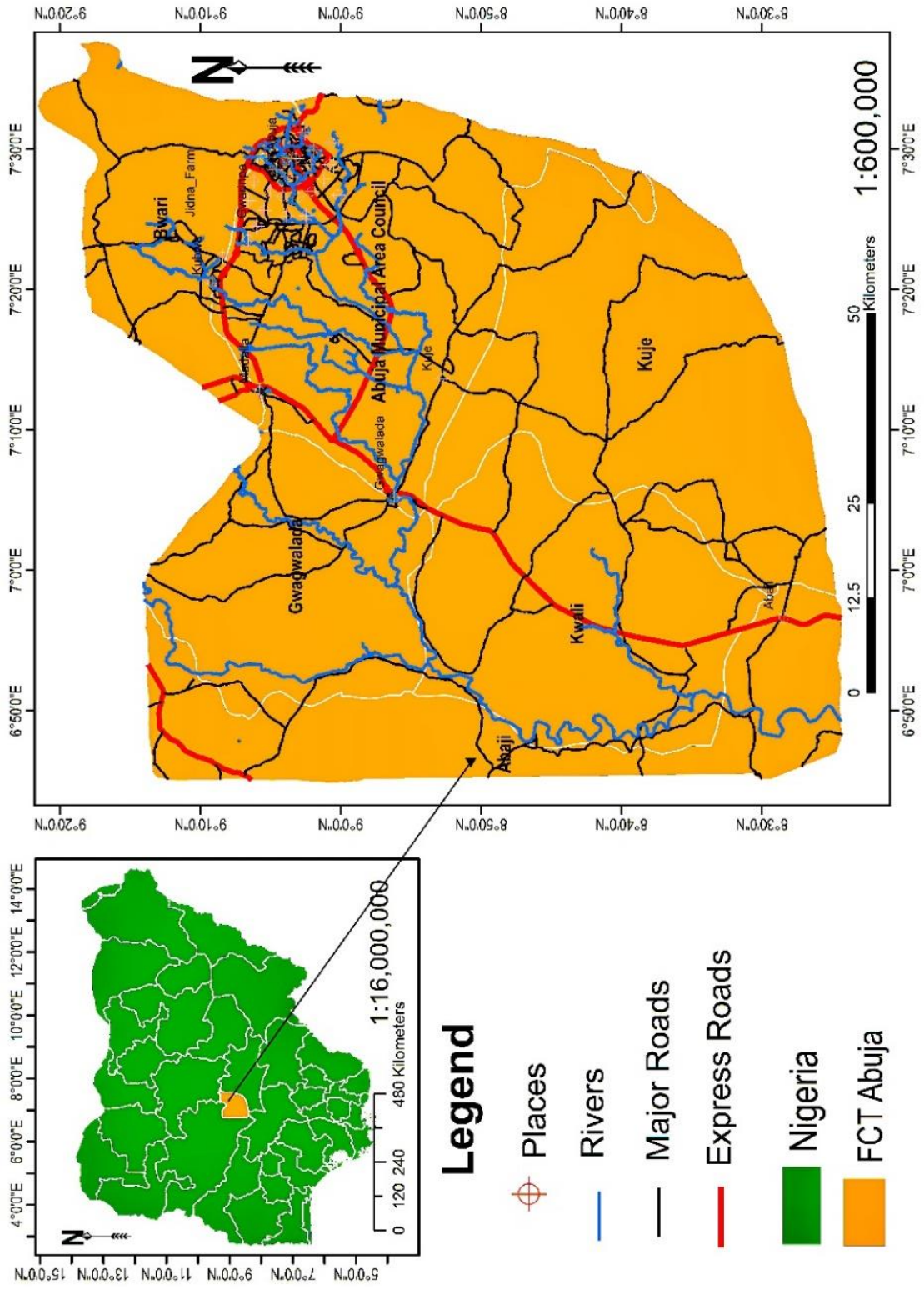

Figure 3.1: Study Area Map Showing Map of Abuja and Map of Nigeria.

3.2 Research Design

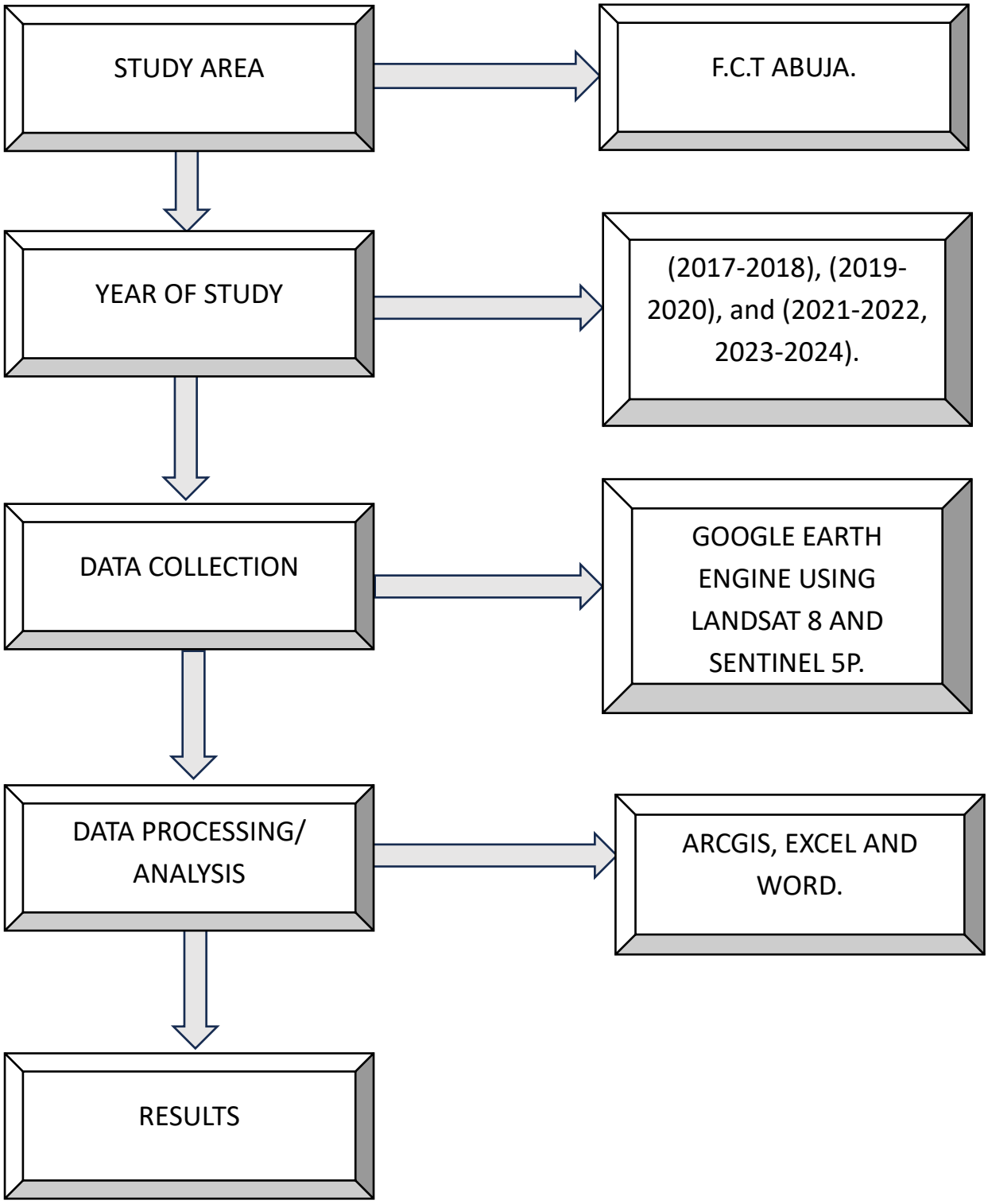

Figure 3.2: Schematic representation of the research design.

3.3 Data Type and Data Source

This study primarily utilized raster data, representing spatially continuous variables stored as grid cells (pixels), where each pixel corresponds to a specific geographic coordinate. The main datasets include:

- Landsat 8 (30 m) – for multispectral and thermal data used in generating Urban Heat Island effect (UHI) and Land Surface Temperature (LST)
- Landsat 7 ETM+ – used for historical comparison and pre-pandemic baselines (Folorunsho *et al.,* 2017).
- Sentinel-5P – for sulphur dioxide (SO_2), Aerosols and Ozone (O_3) concentrations representing GHG variations (Dong *et al.,* 2017).

All satellite imagery was accessed through the Google Earth Engine (GEE) cloud computing platform, which hosts pre-processed surface reflectance and temperature products. The GEE environment ensured efficient processing and reproducibility of results across all study periods (Gorelick *et al.,* 2017; Guo *et al.,* 2022). For this study we would use Google Earth Engine (GEE), with La Landsat 8 to collect data on the UHI and Sentinel 5p for SO_2, Aerosols and O_3.

3.4 Method of Data Collection

Data collection was performed exclusively within the GEE Code Editor using cloud-based scripts. The following steps were followed:

The boundary of Abuja, which served as the Area of Interest (AOI), was delineated using the rectangular tool in Google Earth Engine (GEE) to define the spatial extent (geometry) for image processing. Landsat and Sentinel-5P image collections were then filtered based on specific criteria, including the date range corresponding to the study periods, pre-, during- and post-COVID-19 lockdowns and a cloud cover percentage threshold of less than 10% to ensure clear and high-quality

imagery, after which median composites were generated for each study period to produce cloud-free representative images.

Subsequently, spectral indices relevant to Urban Heat Islands (UHIs) and greenhouse gases (GHGs) were computed within GEE to extract the necessary data for the research. The processed indices and UHI raster layers were then exported as GeoTIFF files for advanced spatial and statistical analyses in ArcGIS. To maintain consistency across datasets, all exported images were reprojected to the World Geodetic System 1984 (WGS 1984), Universal Transverse Mercator (UTM) Zone 32N coordinate system and resampled to a uniform spatial resolution of 30 meters.

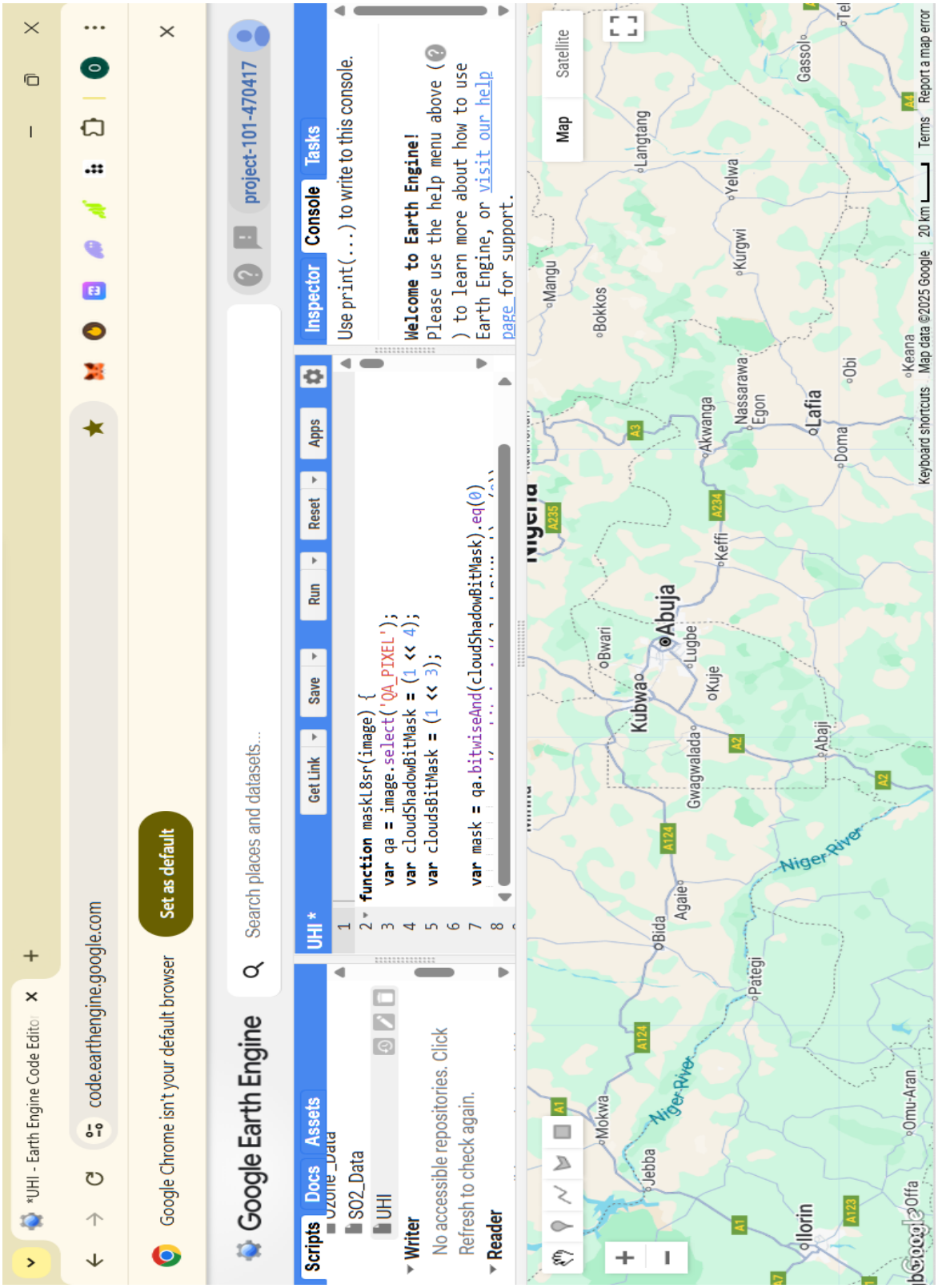

Plate 3.1; Using GEE and Landsat 8 code for UHI

Calculation of Land Surface Temperature (LST) from Satellite Imagery

The derivation of LST from satellite thermal infrared sensors, such as those on Landsat, involves a multi-step process to convert the raw sensor data (Digital Number) into a physically meaningful temperature value.(Uju *et al.,* 2025; Oyeniyi *et al.,* 2025; Chinedu *et al.,* 2024), outline this procedure.

Step 1: Conversion of Digital Number (DN) to Spectral Radiance (Lλ)

The raw data from the satellite's thermal band is first converted to spectral radiance, which is the amount of energy received by the sensor.

$$L_\lambda = M_L \times Q_{cal} + A_L$$

Where:

- L_λ = Top of Atmosphere (TOA) spectral radiance (Watts/(m² * sr * μm))
- M_L = Band-specific multiplicative rescaling factor (from the satellite image's metadata)
- Q_{cal} = Quantized and calibrated standard product pixel value (DN)
- A_L = Band-specific additive rescaling factor (from the metadata)

Step 2: Conversion of Spectral Radiance to At-Satellite Brightness Temperature (TB)

The spectral radiance is then converted to brightness temperature, which is the temperature of a blackbody emitting the same radiance.

$$T_B = \frac{K_2}{\ln(\frac{K_1}{L_\lambda} + 1)}$$

Where:

- T_B = At-satellite brightness temperature (in Kelvin)
- K_1 and K_2 = Band-specific thermal conversion constants (from the metadata)

Step 3: Estimation of Land Surface Emissivity (ε)

Land surfaces are not perfect blackbodies; their ability to emit radiation is quantified by emissivity. A common method to estimate this uses the Normalized Difference Vegetation Index (NDVI) (Oyeniyi *et al.,* 2025; Anyakora *et al.,* 2025).

First, calculate NDVI:

$$NDVI = \frac{(NIR - Red)}{(NIR + Red)}$$

Then, calculate the proportion of vegetation (Pv):

$$P_v = (\frac{NDVI - NDVI_{min}}{NDVI_{max} - NDVI_{min}})^2$$

Finally, land surface emissivity (ε) can be derived:

$$\varepsilon = 0.004 \times P_v + 0.986$$

Where 0.986 is the emissivity of bare soil and 0.004 is a modification value accounting for vegetation presence.

Step 4: Calculation of Land Surface Temperature (LST)

The brightness temperature is corrected for surface emissivity to obtain the true Land Surface

Temperature. This is often done using a form of the radiative transfer equation (Uju *et al.,* 2025; Oyeniyi *et al.,* 2025).

$$LST = \frac{T_B}{1 + (\lambda \times \frac{T_B}{\rho}) \times \ln(\varepsilon)}$$

Where:

- LST = Land Surface Temperature (in Kelvin)
- λ = Wavelength of emitted radiance (e.g., 10.8 μm for Landsat 8 TIRS Band 10)
- $\rho = h \times c/\sigma$ (1.438 × 10^{-2} m K), where σ is the Boltzmann constant, h is Planck's constant and c is the speed of light.

  The final LST is often converted to degrees Celsius: $LST(°C) = LST(K) - 273.15$.

Calculation of Urban Heat Island (UHI) Intensity

UHI intensity quantifies the thermal difference between an urban area and its surrounding rural environs. Two primary methods are prevalent in the literature.

1. Surface Urban Heat Island (SUHI) Intensity

This method uses the LST derived from satellite data to calculate the difference between the average urban temperature and the average rural temperature (Feng *et al.,* 2023; Liu *et al.,* 2022).

$$SUHI = LST_{urban} - LST_{rural}$$

Where:

- $SUHI$ = Surface Urban Heat Island Intensity (°C)
- LST_{urban} = Mean Land Surface Temperature within the urban boundary
- LST_{rural} = Mean Land Surface Temperature within the surrounding rural reference area

2. Standardized UHI Index (for Spatial Analysis)

To map the spatial distribution of UHI effects across a city, the LST is often standardized (Oyeniyi *et al.,* 2025; Anyakora *et al.,* 2025). This method highlights how much hotter or cooler a pixel is compared to the city-wide average.

$$UHI_{index} = \frac{(LST - LST_{mean})}{LST_{STD}}$$

Where:

- UHI_{index} = Standardized UHI intensity for a pixel (unitless)
- LST = Land Surface Temperature of the pixel
- LST_{mean} = Mean Land Surface Temperature of the entire study area
- LST_{STD} = Standard deviation of the LST across the study area

A related index, the **Urban Thermal Field Variance Index (UTFVI)**, is used to assess ecological and thermal comfort impacts (Odunsi and Rienow 2024; Anyakora *et al.,* 2025).

$$UTFVI = \frac{(LST - LST_{mean})}{LST}$$

This index helps classify areas into different UHI intensity and thermal comfort levels, which is crucial for identifying vulnerability hotspots.

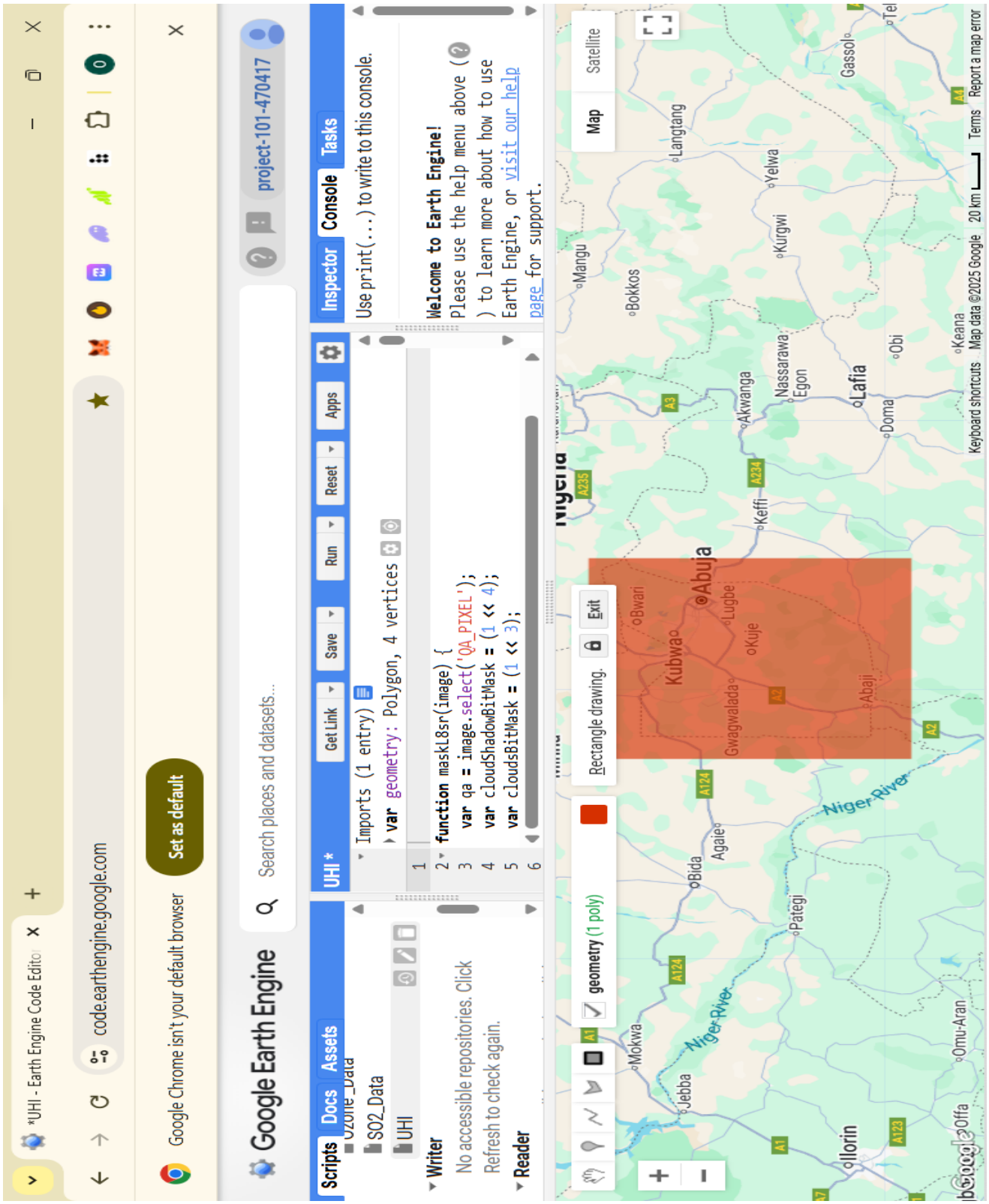

Plate 3.2; Using GEE and Landsat 8 code for UHI to collect data for UHI

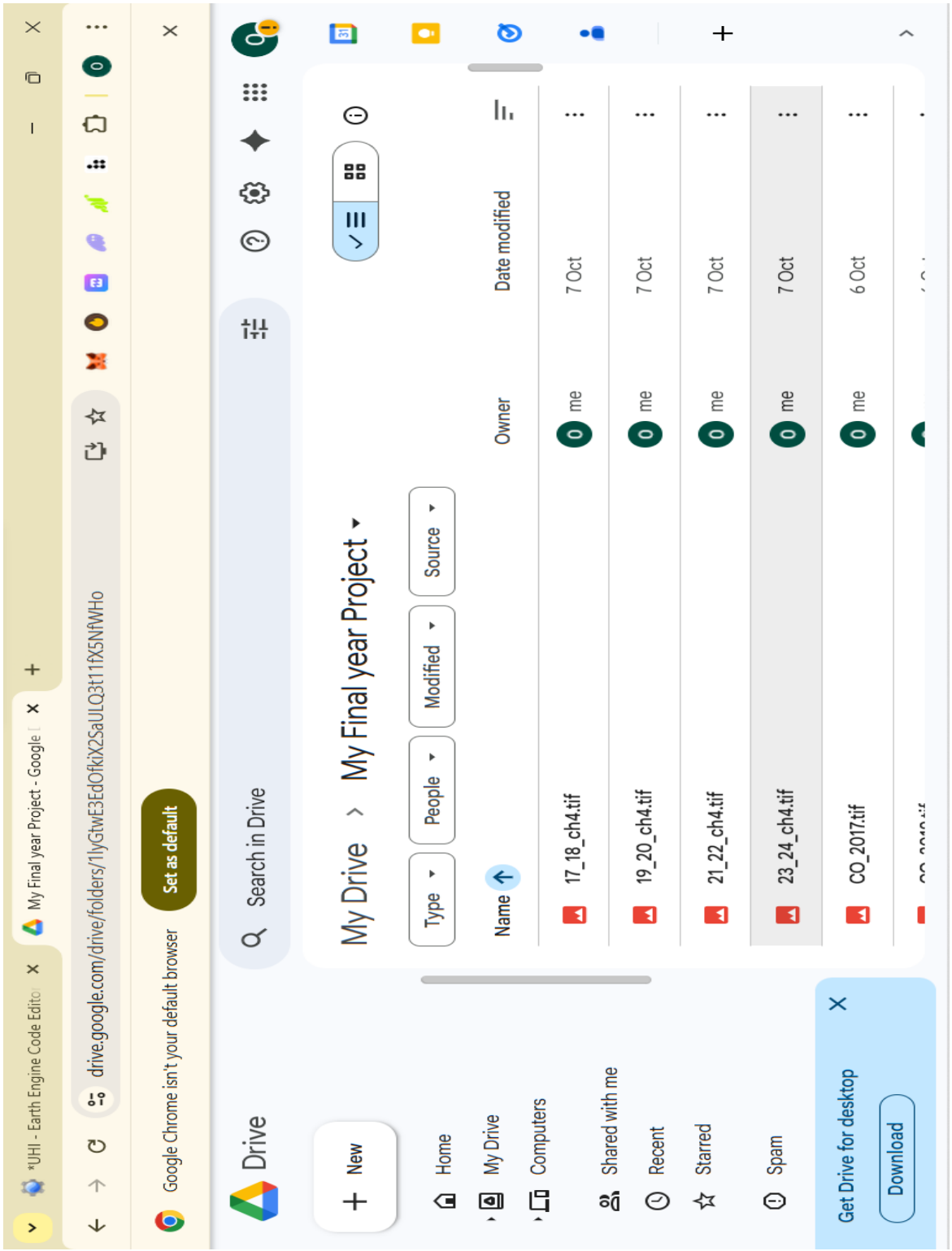

Plate 3.3; Google drive for exporting and downloading data

3.5 Method of Data Analysis

The data analysis combined remote sensing, GIS and statistical procedures for quantitative and spatial interpretation.

Satellite imagery from Landsat 8, accessed and processed through the Google Earth Engine (GEE) platform, was used to analyse and monitor the spatial and temporal variations of Urban Heat Island (UHI) effect within the study area using the mean value over the date range. The processing involved cloud masking, atmospheric correction and the derivation of surface temperature parameters to ensure accuracy. After generating the raster outputs, the datasets were exported in Geographic Tagged Image File Format (GeoTIFF) and subsequently imported into the ArcGIS software environment for spatial analysis and visualization. This integration enabled the identification of spatial patterns, hot and cool zones and the quantification of thermal intensity variations across Abuja.

In addition, Sentinel-5P TROPOMI datasets were utilized to assess the spatial distribution of greenhouse gases, specifically sulphur dioxide (SO_2), Aerosols and Ozone (O_3). The data were processed within GEE to generate cloud-free daily composites, which were then averaged annually to minimize atmospheric distortions and enhance representativeness. The resulting datasets were imported into ArcGIS. This approach provided continuous spatial coverage and improved the reliability of emission mapping.

The derived GHG concentration maps were normalized and compared with UHI datasets to examine spatial correlations between urban heat island effects and emission levels. Overlay analysis in ArcGIS facilitated the identification of areas where elevated gas concentrations coincided with higher surface temperatures and dense urban development. This combined geospatial approach allowed for a comprehensive understanding of how urban expansion, anthropogenic emissions and heat distribution interact within Abuja's urban environment (Dong *et al.,* 2017).

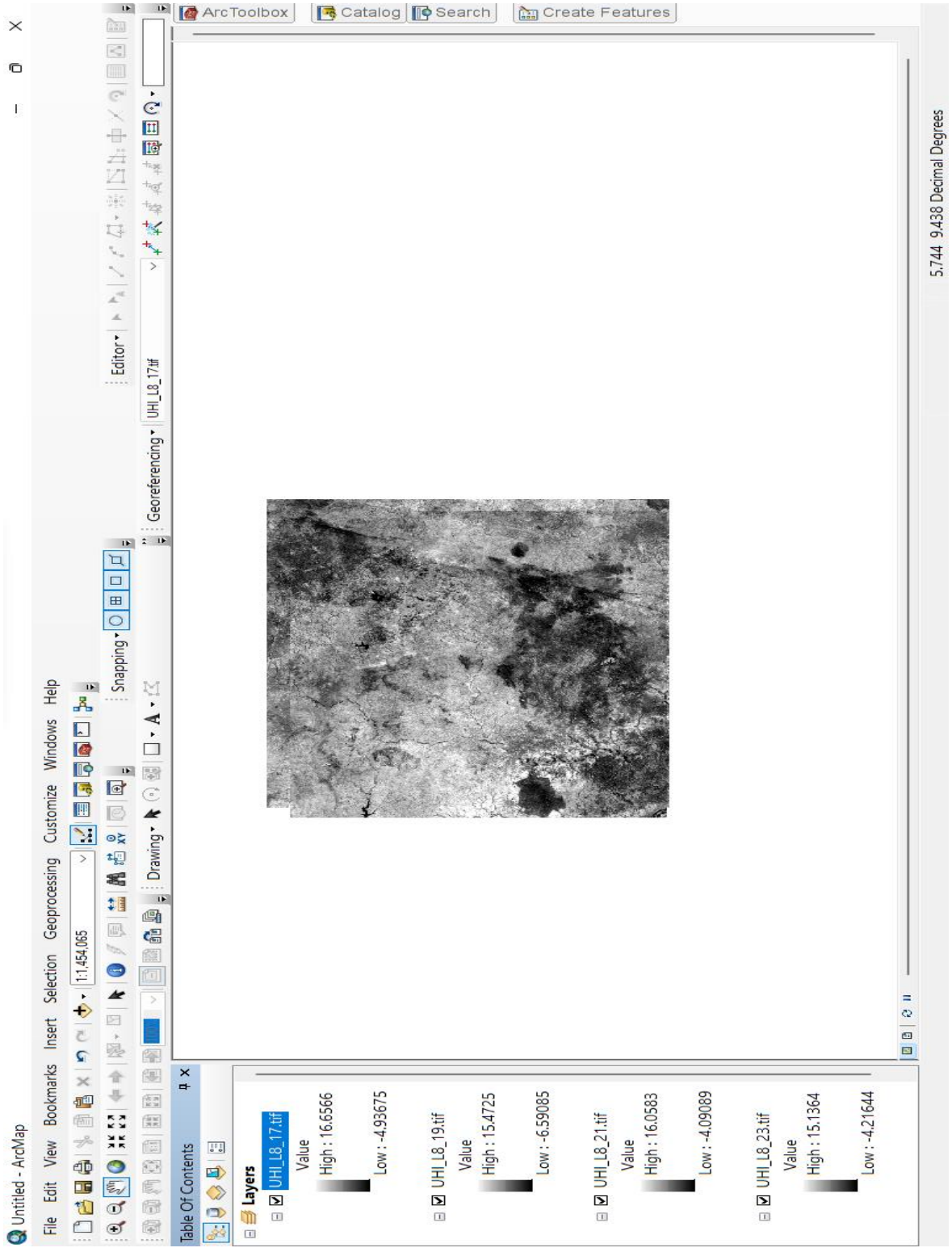

Plate 3.4; Using the downloaded raster image for UHI from Landsat 8 displayed in the ArcMap environment.

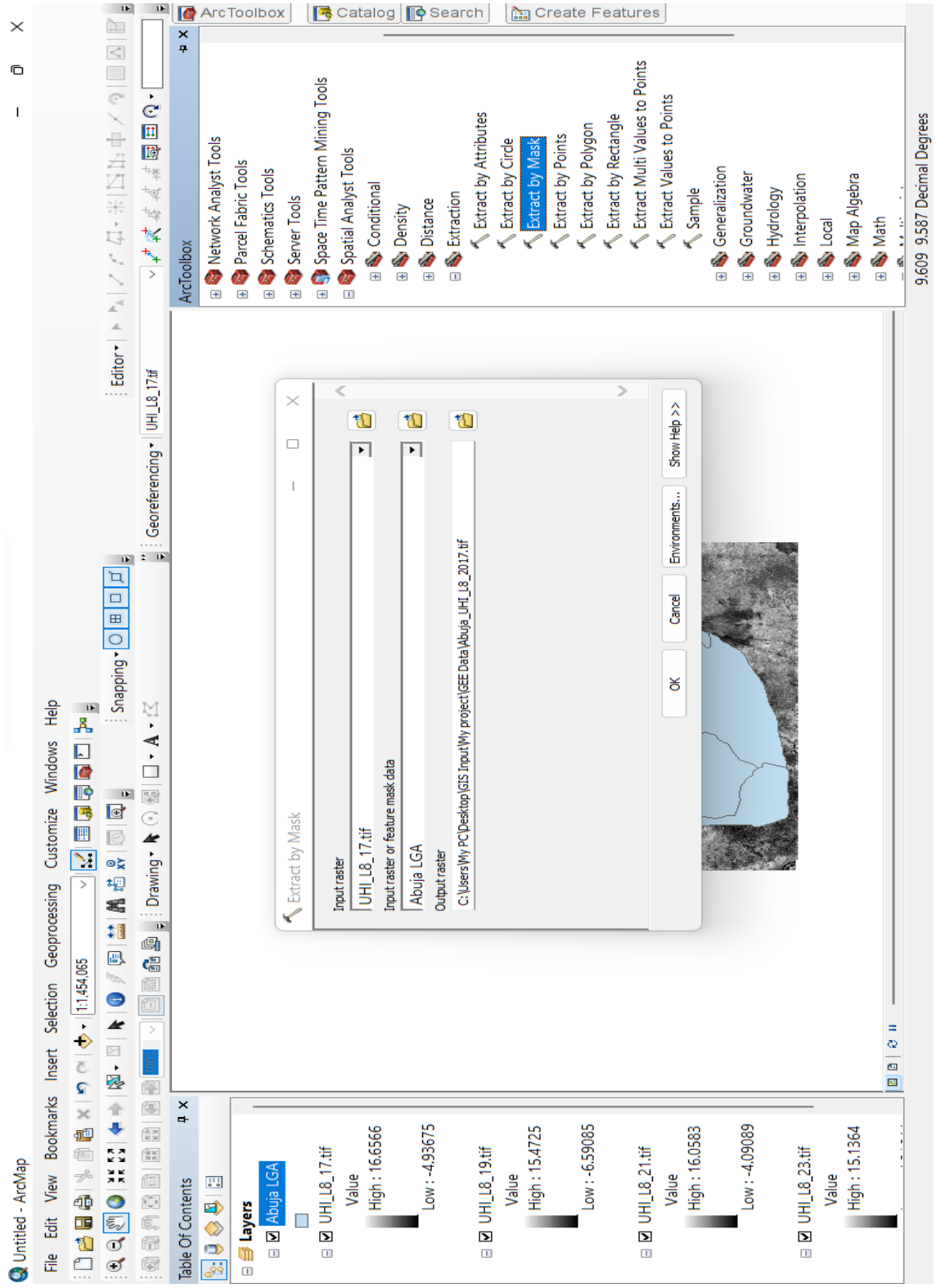

Plate 3.5; Showing the extraction of a raster data through extraction by mask to get the study area of interest.

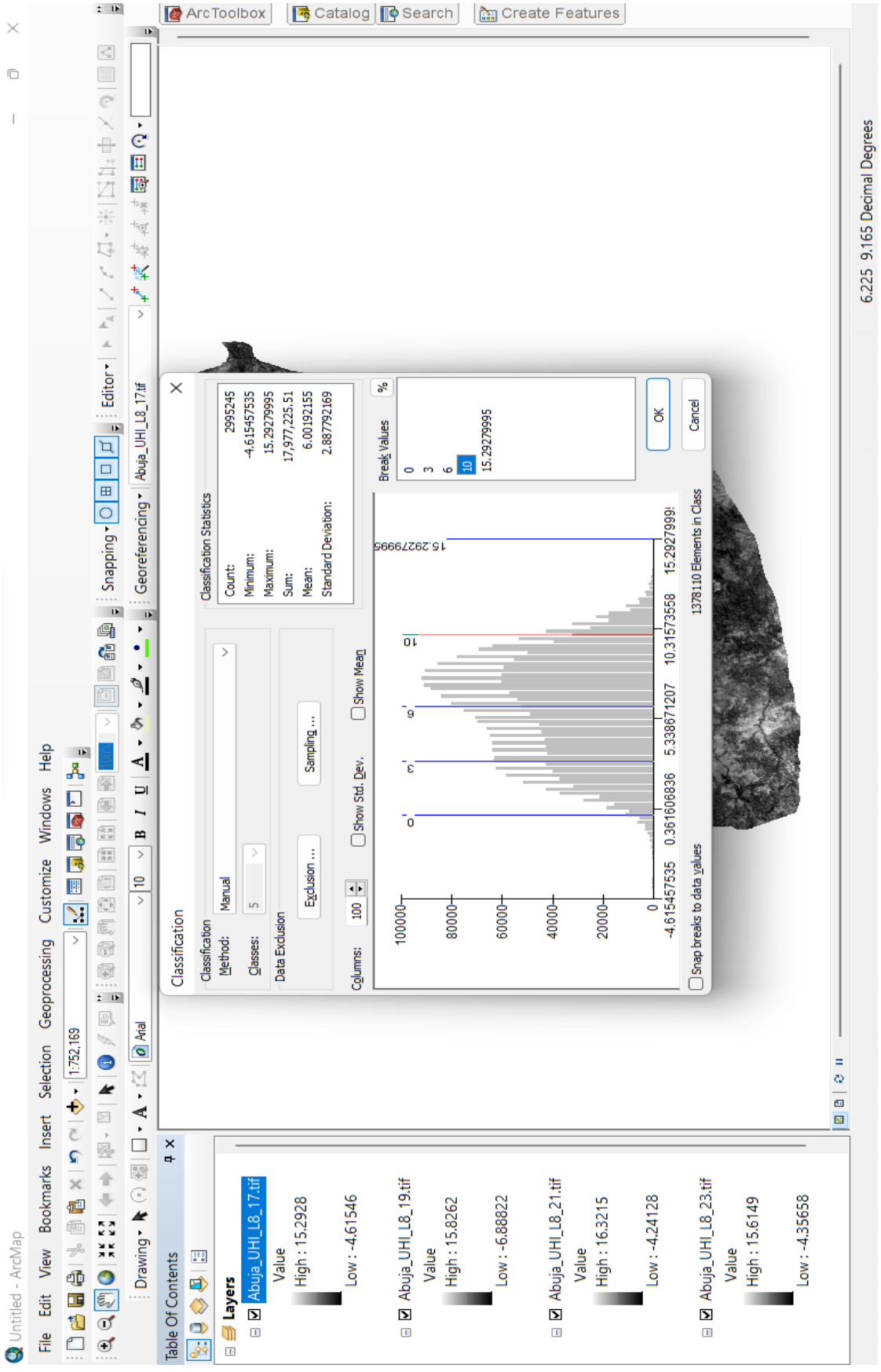

Plate 3.6; Showing Raster data ranges for the data to be classified into 5 classes to represent the data.

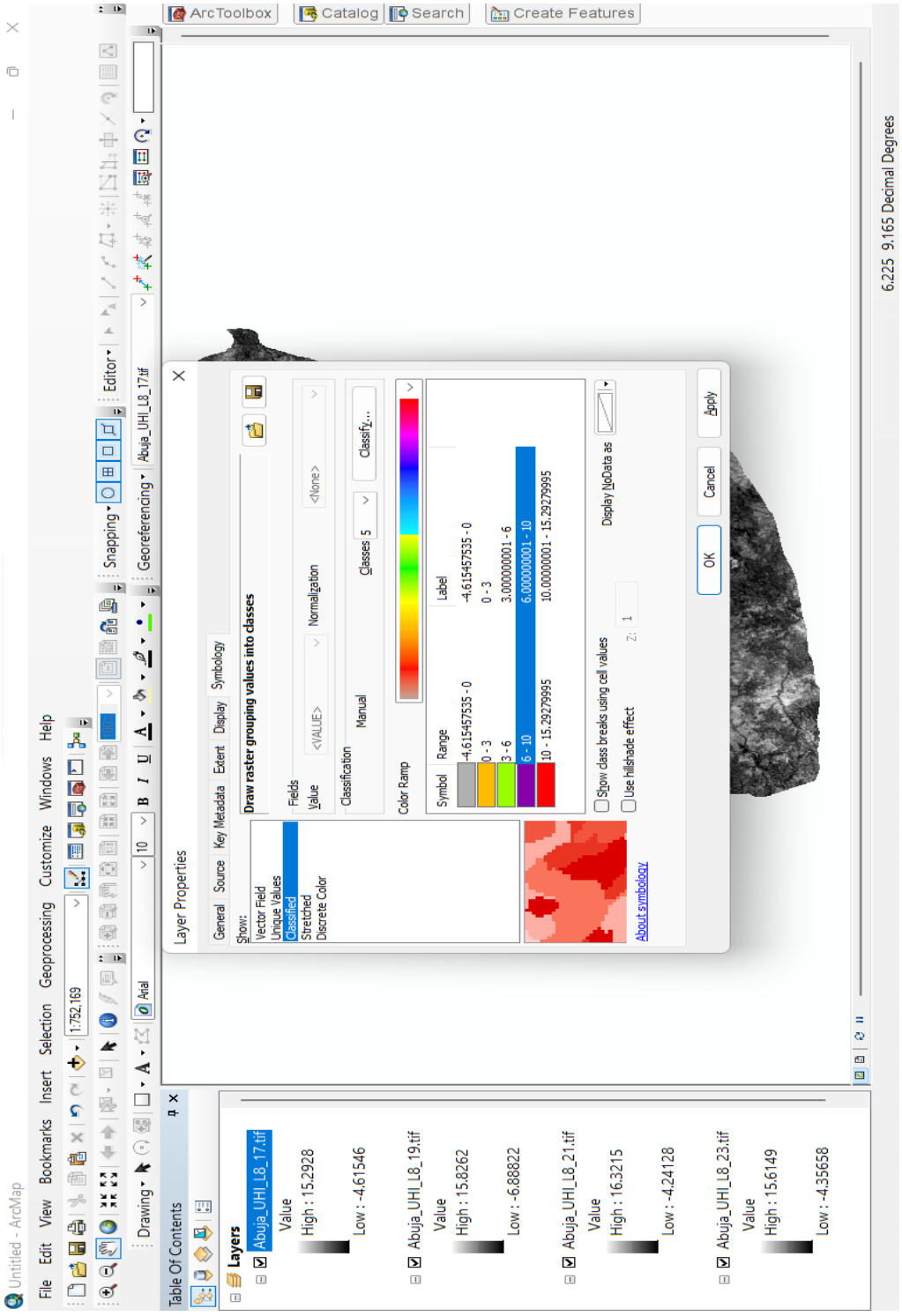

Plate 3.7; Showing colour ramp used to represent the raster data ranges for the data to be classified into 5 classes to represent the data.

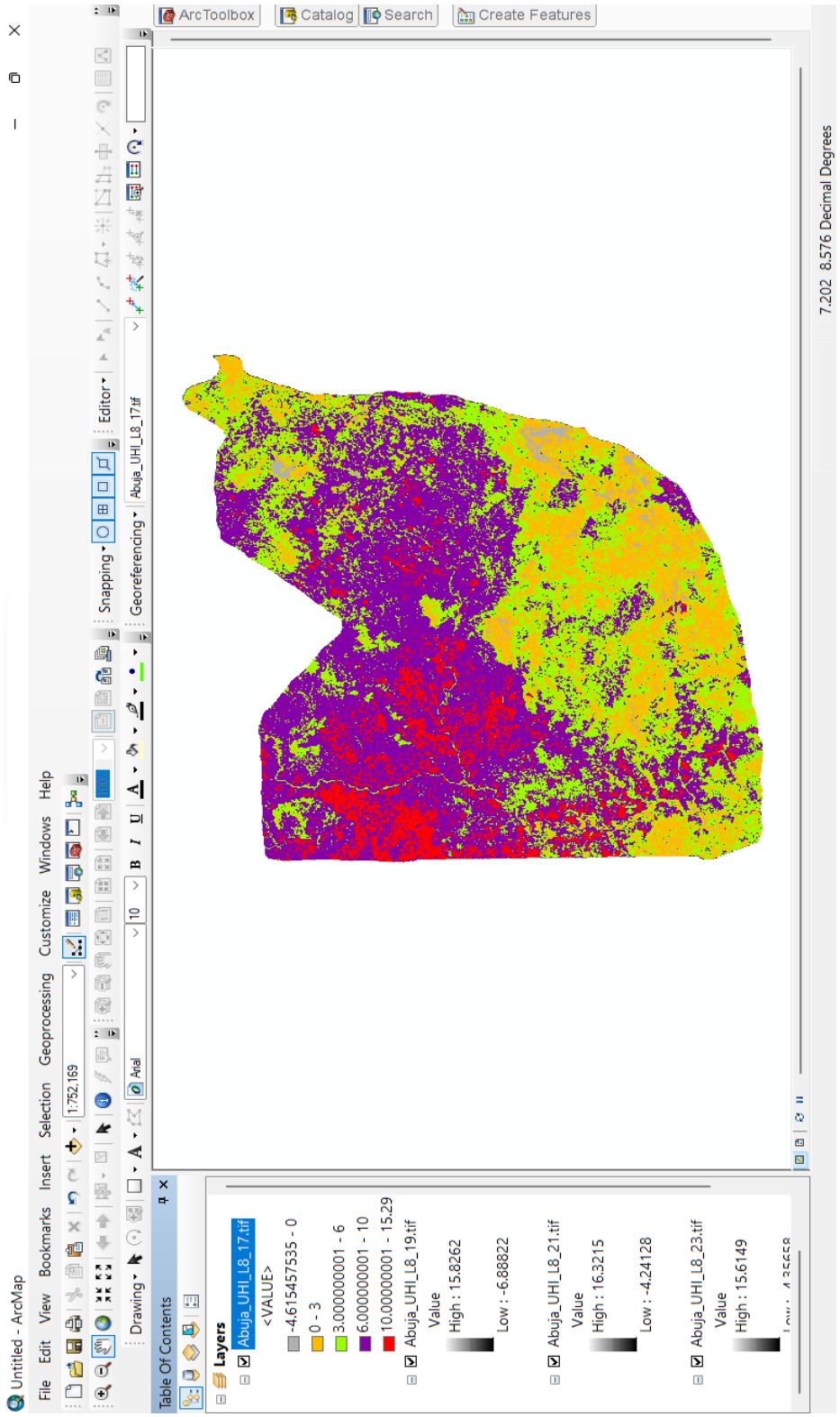

Plate 3.8; Showing Raster data that was extracted by mask and classified into 5 classes to represent the data.

Table 3.1; Classification and Range for UHI Data.

Classification	**Ranges**
Very Low	<0
Low	0 - 3
Moderate	3 - 6
High	6 - 10
Very High	>10

Table 3.2; Classification and Range for SO_2 Data.

Classification	**Ranges**
Very Low	<0
Low	0 – 0.000015
Moderate	0.000015 – 0.00003
High	0.00003 – 0.000045
Very High	>0.000045

Table 3.3; Classification and Range for O_3 Data.

Classification	**Ranges**
Very Low	<0
Low	0.1197 – 0.1199
Moderate	0.1199 – 0.1201
High	0.1201 – 0.1204
Very High	>0.1204

Table 3.4; Classification and Range for Aerosols Data.

Classification	**Ranges**
Very Low	<0
Low	0 – 0.05
Moderate	0.05 – 0.1
High	0.1 – 0.15
Very High	>0.15

Table 3.5; Classification and Range for LSTs Data

Classification	**Ranges**
Very Low	<0
Low	0 - 3
Moderate	3 - 6
High	6 - 10
Very High	>10

CHAPTER FOUR

RESULTS

4.1 MEAN CONCENTRATION OF URBAN HEAT ISLAND (UHI) IN ABUJA FOR YEARS 2017–2018, 2019–2020, 2021–2022 and 2023–2024 (PRE, DURING and POST COVID PANDEMIC LOCKDOWN)

The figures below illustrate the spatial distribution maps of Urban Heat Island (UHI) intensity in Abuja for the four study periods: 2017–2018 (pre-COVID)**,** 2019–2020 (during the COVID lockdown)**,** 2021–2022 (immediate post-COVID) and 2023–2024 (post-COVID phase*)***.** The statistical summaries derived from remote sensing analysis using Google Earth Engine (GEE) and ArcGIS are presented in Table 4.1.1, highlighting the variations in UHI mean concentration and dispersion across these temporal phases.

Urban Heat Island (UHI) Concentration in 2017–2018 (Pre-COVID Pandemic)

During the pre-pandemic period (2017–2018), Abuja exhibited noticeable spatial variations in surface temperature between urban and rural areas. The UHI intensity ranged from a minimum of -4.56°C to a maximum of 15.24°C, with **a** mean value of 6.00°C and *a* standard deviation of 2.87°C**.**

Urban Heat Island (UHI) Concentration in 2019–2020 (COVID-19 Lockdown Period)

The COVID-19 lockdown period (2019–2020) was characterized by a significant reduction in human and industrial activities, resulting in a measurable decrease in surface temperature and heat accumulation. The UHI intensity during this period recorded a minimum of -6.71°C and *a* maximum of 15.74°C*,* with a mean of 4.93°C and a standard deviation of 3.02°C**.**

Urban Heat Island (UHI) Concentration in 2021–2022 (After COVID Lockdown Period)

In the After COVID Lockdown phase (2021–2022), human activities and economic operations resumed fully, leading to renewed thermal buildup within Abuja's metropolitan zones. UHI intensity

ranged between *a* minimum of -4.20°C and *a* maximum of 16.26°C, with *a* mean value of 6.72°C and *a* standard deviation of 2.53°C**.**

Urban Heat Island (UHI) Concentration in 2023–2024 (Post-COVID Pandemic Phase)

By the period 2023–2024, Abuja's UHI intensity stabilized but remained significantly elevated due to sustained urban growth and infrastructural expansion. The UHI intensity values ranged from *a* minimum of -4.23°C to *a* maximum of 15.34°C, with a mean concentration of 6.56°C and a standard deviation of 2.51°C**.**

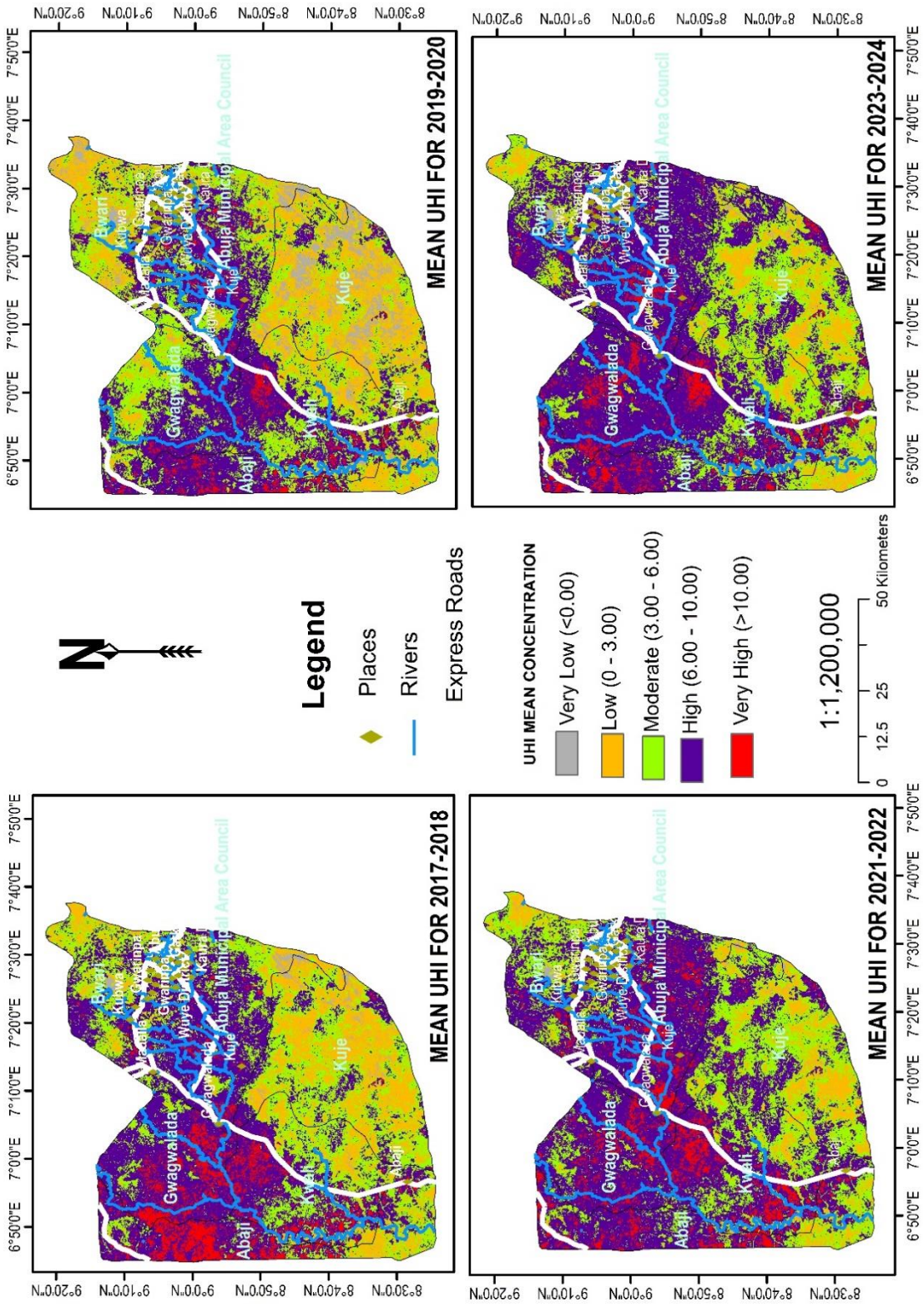

Figure 4.1.1: Map showing Urban Heat Island (UHI) Concentration in Abuja (2017–2024)

Table 4.1.1: Comparative Summary of Urban Heat Island (UHI) Concentration in Abuja (2017–2024)

Study Period	Year Range	Minimum	Maximum	Mean	Standard Deviation
Pre-COVID 19	2017–2018	-4.56315	15.2381	6.00017	2.8704
COVID 19 Lockdown	2019–2020	-6.71382	15.7392	4.9267	3.0162
After-COVID 19 Lockdown	2021–2022	-4.19688	16.2616	6.7167	2.5255
Post-COVID 19	2023–2024	-4.22519	15.3393	6.5552	2.5122

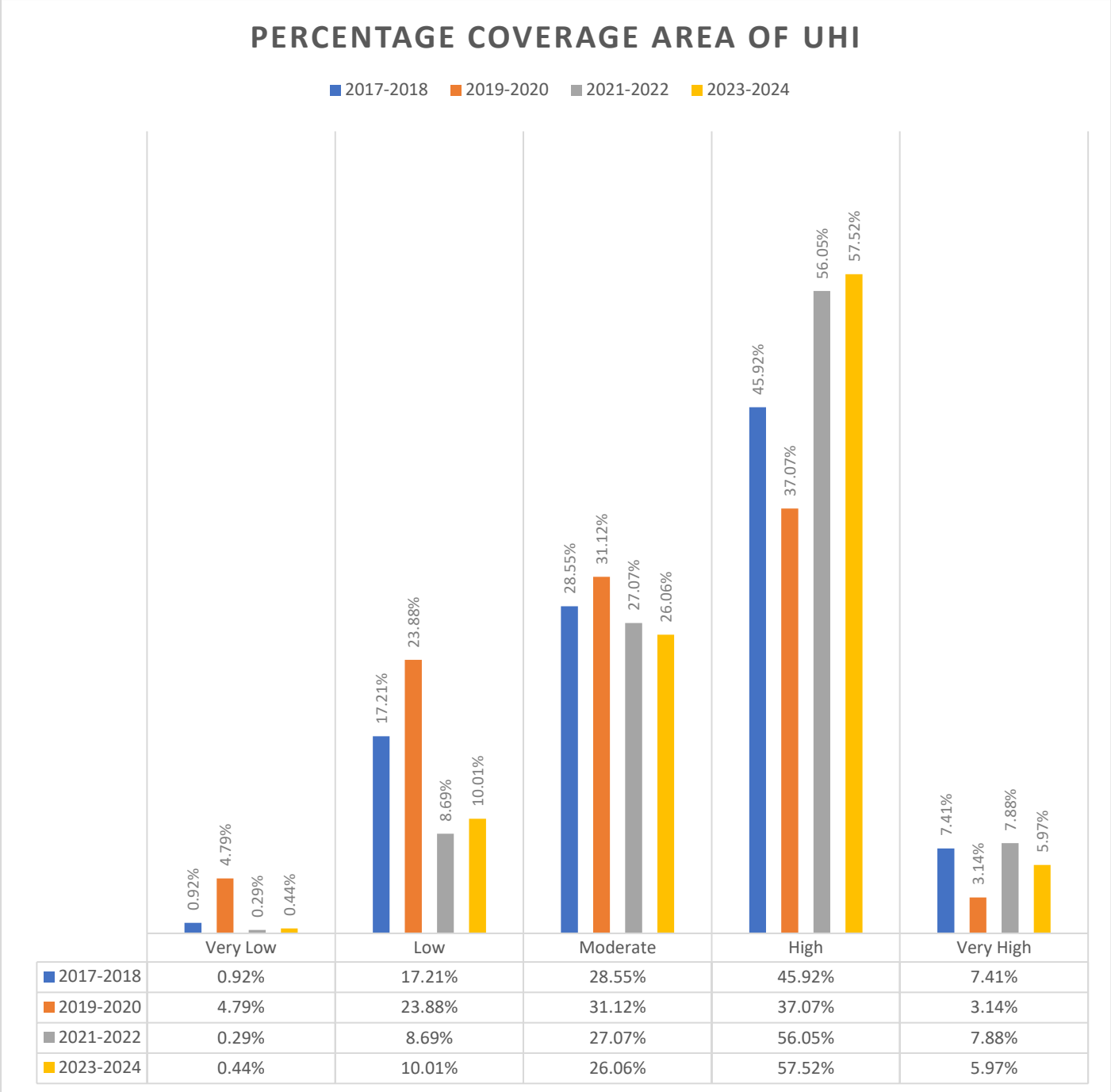

	Very Low	Low	Moderate	High	Very High
2017-2018	0.92%	17.21%	28.55%	45.92%	7.41%
2019-2020	4.79%	23.88%	31.12%	37.07%	3.14%
2021-2022	0.29%	8.69%	27.07%	56.05%	7.88%
2023-2024	0.44%	10.01%	26.06%	57.52%	5.97%

Figure 4.1.2: Bar Charts Showing Percentage Coverage Area of Urban Heat Island (UHI) Concentration in Abuja (2017–2024)

Table 4.1.2: Comparative Summary of Urban Heat Island (UHI) SqKm Area coverage in Abuja based on the concentration (2017–2024)

	Very Low (SqKm)	**Low (SqKm)**	**Moderate (SqKm)**	**High (SqKm)**	**Very High (SqKm)**
2017–2018	67.31	1265.24	2099.38	3376.41	544.86
2019–2020	352.287	1755.65	2287.97	2726.14	231.153
2021–2022	21.76	639.34	1990.9	4121.58	579.62
2023–2024	32.56	736.15	1915.97	4229.35	439.17

Table 4.1.3: Comparative Summary of Urban Heat Island (UHI) Pair Change by Class 2017 to 2019, 2019 to 2021 and 2021 to 2023

Year Range	Very Low (delta SqKm)	Low (delta SqKm)	Moderate (delta SqKm)	High (delta SqKm)	Very High (delta SqKm)
2017>2019	293.6952	482.1039	181.3293	-640.552	-316.577
2019>2021	-342.301	-1108.92	-283.021	1383.217	350.6337
2021>2023	11.0376	94.5225	-76.7592	116.5581	-145.359

Table 4.1.4*;* Showing Percentiles of UHI

Study Period	**Year Range**	**p10**	**p50**	**shannon**	**simpson**
Pre-COVID 19	2017–2018	2.041136	6.289735	1.26122	0.67522
COVID 19 Lockdown	2019–2020	0.815995	5.102192	1.33595	0.707791
After-COVID 19 Lockdown	2021–2022	3.146686	7.061715	1.115209	0.602166
Post-COVID 19	2023–2024	2.916946	6.976345	1.096974	0.590209

Table 4.1.5; Showing Pearson coefficient of UHI

	2017–2018	**2019–2020**	**2021–2022**	**2023–2024**
2017–2018	1	0.876527	0.827245	0.810912
2019–2020	0.876527	1	0.813317	0.786098
2021–2022	0.827245	0.813317	1	0.868634
2023–2024	0.810912	0.786098	0.868634	1

Table 4.1.6; Showing Kappa Values and Pairwise Differences statistics of UHI

Study Period	Year Range	kappa	Mean	Precent positive	Precent negative	Mean absent
Between (Pre-COVID Pandemic and COVID Lockdown)	2017->2019	0.419691	-1.07003	16.37548	54.51603	1.447673
Between (COVID Lockdown and Post-COVID Lockdown)	2019->2021	0.234492	1.785946	60.08611	10.77889	2.040194
Between (COVID Lockdown and Post-COVID)	2021->2023	0.548853	-0.1632	30.05664	40.83114	1.024892

4.2 MEAN CONCENTRATION OF LAND SURFACE TEMPERATURE (LST) IN ABUJA FOR YEAR 2017–2018, 2019–2020, 2021–2022 and 2023–2024 (PRE, DURING and POST COVID PANDEMIC LOCKDOWN)

The figures below show the spatial distribution maps of Land Surface Temperature (LST) across Abuja for the years 2017–2018 (Pre-COVID), 2019–2020 (During COVID Lockdown), 2021–2022 (Immediate Post-COVID) and 2023–2024 (Extended Post-COVID). The tables present the results obtained from the temporal and spatial analysis of satellite-derived data using Google Earth Engine (GEE) and ArcGIS software.

Pre-COVID Period (2017–2018)

During the pre-pandemic period, Abuja experienced moderate surface temperatures across both built-up and semi-urban areas. The Land Surface Temperature (LST) recorded a minimum value of -3.54°C and *a* maximum value of 15.64°C, with a mean temperature of 6.96°C and a standard deviation of 2.83°C, as shown in Table 4.2.1.

During COVID-19 Lockdown (2019–2020)

The COVID-19 lockdown period (2019–2020) marked a significant phase of reduced human mobility and industrial activities, which influenced surface temperature patterns across Abuja. The LST during this period had a minimum value of -6.52°C and *a* maximum of 15.99°C, with a mean value of 5.14°C and a standard deviation of 3.03°C, as indicated in Table 4.2.1.

After COVID Lockdown Period (2021–2022)

In the immediate post-lockdown period (2021–2022), as restrictions were lifted and economic activities resumed, Abuja recorded a gradual increase in surface temperature values. The LST showed a minimum of -3.48°C and a maximum of 15.79°C, with a mean value of 7.03°C and a standard deviation of 2.48°C, as presented in Table 4.2.1.

Post-COVID Pandemic Phase (2023–2024)

During the post-COVID period (2023–2024), the Land Surface Temperature (LST) exhibited a minimum of -3.89°C and a maximum of 14.60°C, with a mean temperature of 6.81°C and a standard deviation of 2.46°C, as shown in Table 4.2.1.

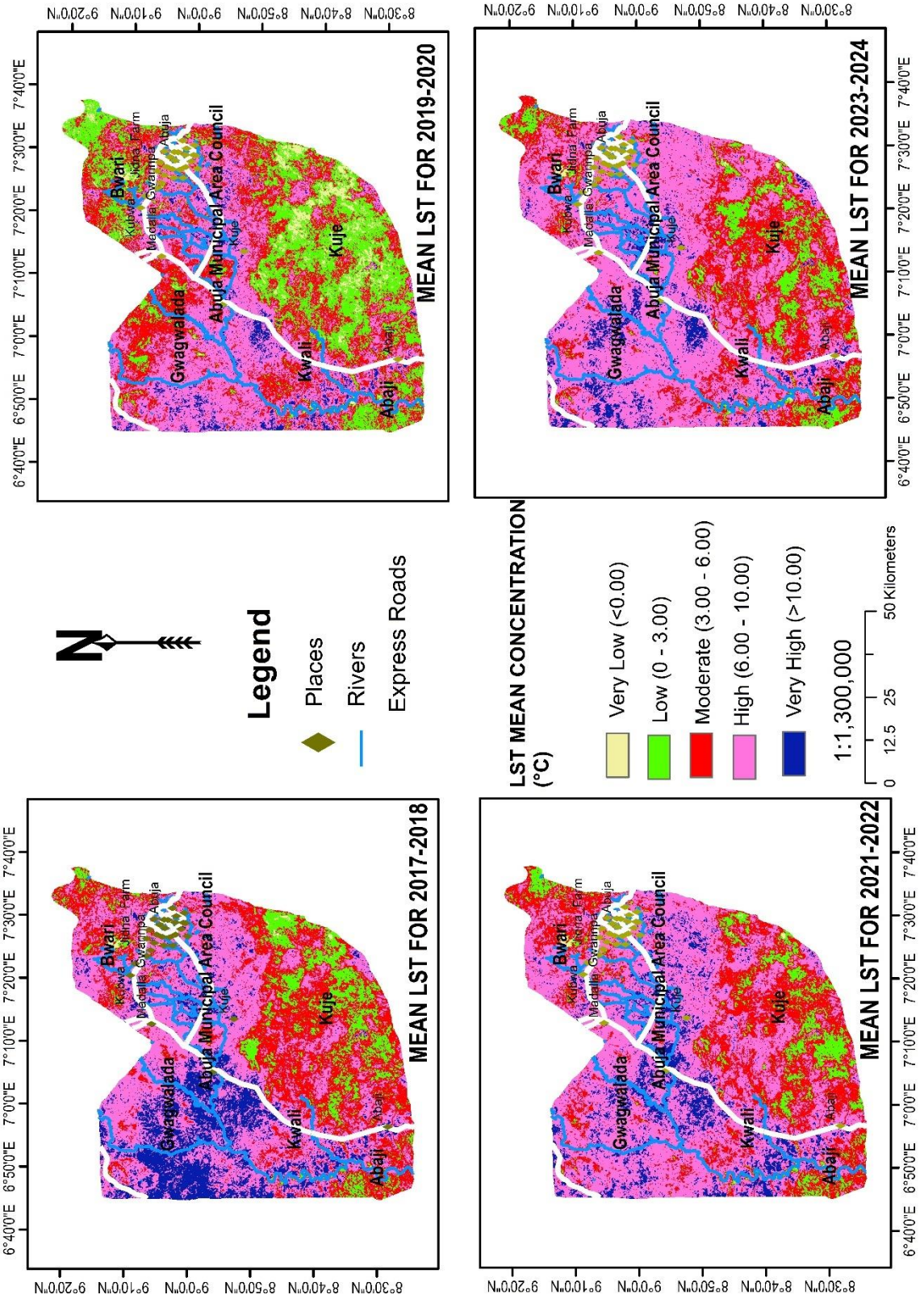

Figure 4.2.1: Map showing Land Surface Temperature (LST) Concentration in Abuja (2017–2024)

Table 4.2.1: Comparative Summary of Land Surface Temperature (LST) Concentration in Abuja (2017–2024)

Study Period	Year Range	Minimum	Maximum	Mean	Standard Deviation
Pre-COVID 19	2017–2018	-3.54222	15.641	6.9634	2.8345
COVID 19 Lockdown	2019–2020	-6.51809	15.9952	5.1357	3.0269
After-COVID 19 Lockdown	2021–2022	-3.47773	15.7928	7.0285	2.4768
Post-COVID 19	2023–2024	-3.88864	14.6009	6.8073	2.4647

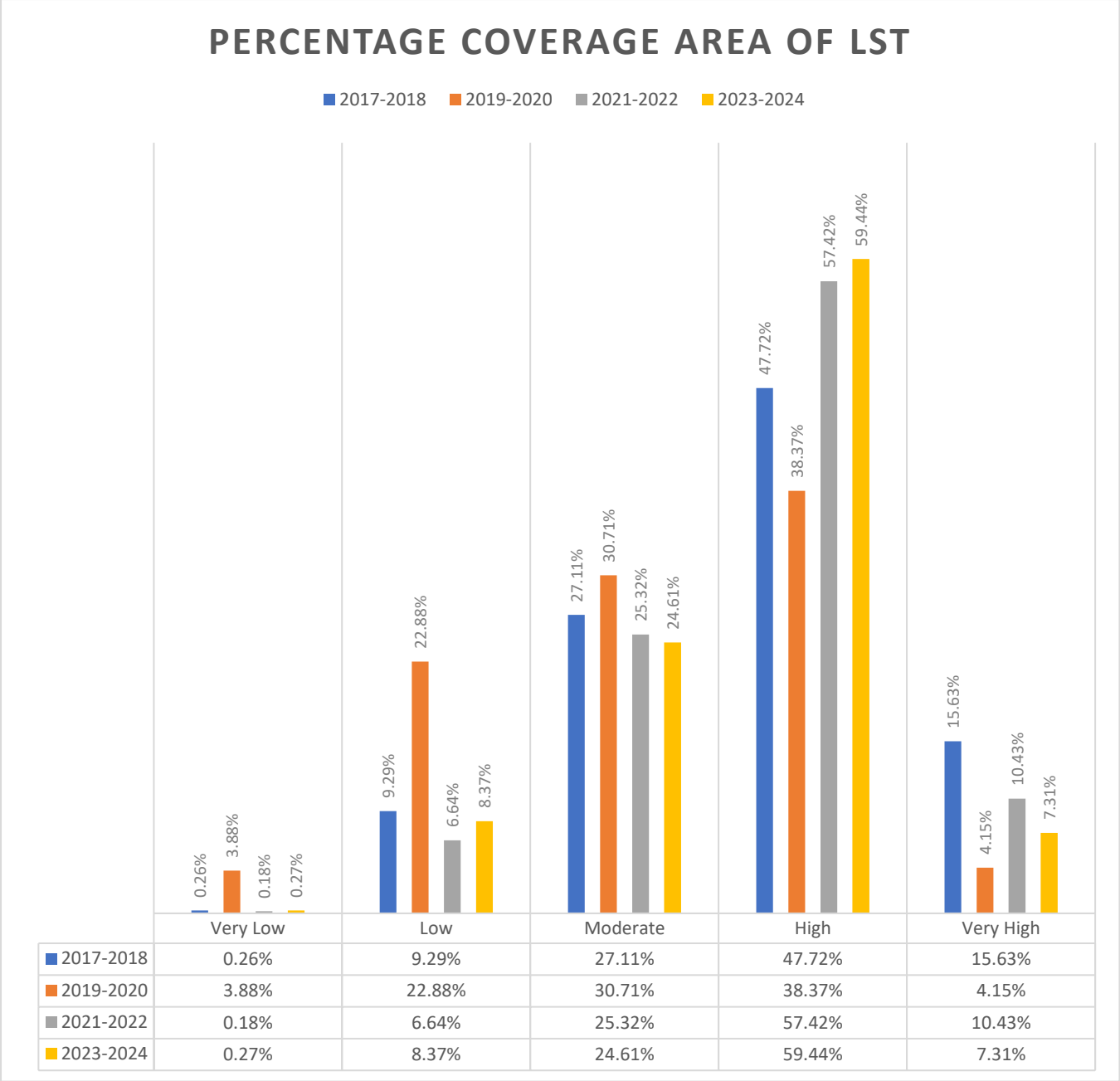

	Very Low	Low	Moderate	High	Very High
2017-2018	0.26%	9.29%	27.11%	47.72%	15.63%
2019-2020	3.88%	22.88%	30.71%	38.37%	4.15%
2021-2022	0.18%	6.64%	25.32%	57.42%	10.43%
2023-2024	0.27%	8.37%	24.61%	59.44%	7.31%

Figure 4.2.2: Bar Charts Showing Percentage Coverage Area of Land Surface Temperature (LST) Concentration in Abuja (2017–2024)

Table 4.2.2: Comparative Summary of Land Surface Temperature (LST) SqKm Area coverage in Abuja based on the concentration (2017–2024)

	Very Low (SqKm)	Low (SqKm)	Moderate (SqKm)	High (SqKm)	Very High (SqKm)
2017–2018	18.86	683.2	1993.33	3508.58	1149.23
2019–2020	285.64	1682.13	2258.25	2821.66	305.52
2021–2022	13.46	488.39	1861.9	4222.35	767.1
2023–2024	19.967	615.25	1809.95	4370.44	537.59

4.3 MEAN CONCENTRATION OF GREENHOUSE GAS (SO_2) IN ABUJA FOR YEARS 2017–2018, 2019–2020, 2021–2022 and 2023–2024 (PRE, DURING and POST COVID PANDEMIC LOCKDOWN)

The figures below show the spatial distribution maps of Sulphur Dioxide (SO_2) concentration over Abuja for the years 2017–2018, 2019–2020, 2021–2022 and 2023–2024, representing the pre, during and post COVID pandemic periods. The tables present the statistical results derived from satellite-based observations and data analysis using Google Earth Engine (GEE) and processed in ArcGIS.

SO_2 Concentration in 2017–2018 (Pre COVID Pandemic Period)

During the pre-pandemic period (2017–2018), Sulphur Dioxide (SO_2) concentration exhibited relatively higher variability across Abuja due to increased anthropogenic emissions from transportation, small-scale industries and open waste burning. The SO_2 concentration recorded a minimum value of -0.0001265 mol/m², a maximum value of 0.000130182 mol/m², a mean value of -0.000007496 mol/m² and a standard deviation of 0.000033998 mol/m², as presented in Table 4.3.1.

SO_2 Concentration in 2019–2020 (COVID Pandemic Lockdown Period)

In the 2019–2020 period, which coincided with the COVID-19 lockdown, the concentration of Sulphur Dioxide (SO_2) showed a noticeable reduction due to the temporary shutdown of major economic and transportation activities. The recorded minimum value was -0.0000714193 mol/m², the maximum value was 0.0000437185 mol/m², with a mean value of -0.00000901 mol/m² and a standard deviation of 0.000014107 mol/m², as shown in Table 4.3.1.

SO_2 Concentration in 2021–2022 (After COVID Lockdown Period)

Following the gradual easing of restrictions and resumption of normal activities, Sulphur Dioxide (SO_2) levels began to rise slightly during the 2021–2022 period. The SO_2 concentration recorded a minimum value of -0.0000546184 mol/m², a maximum value of 0.0000782592 mol/m², a mean value of 0.000006673 mol/m² and a standard deviation of 0.000017454 mol/m², as indicated in Table 4.3.1.

SO_2 Concentration in 2023–2024 (Post-COVID Pandemic Phase)

By the 2023–2024 period, Sulphur Dioxide (SO_2) concentration showed moderate and spatially consistent patterns across the Federal Capital Territory. The SO_2 concentration had a minimum value of -0.0000512865 mol/m², *a* maximum value of 0.0000735454 mol/m², *a* mean value of 0.00000587 mol/m² and a standard deviation of 0.000016936 mol/m², as presented in Table 4.3.1.

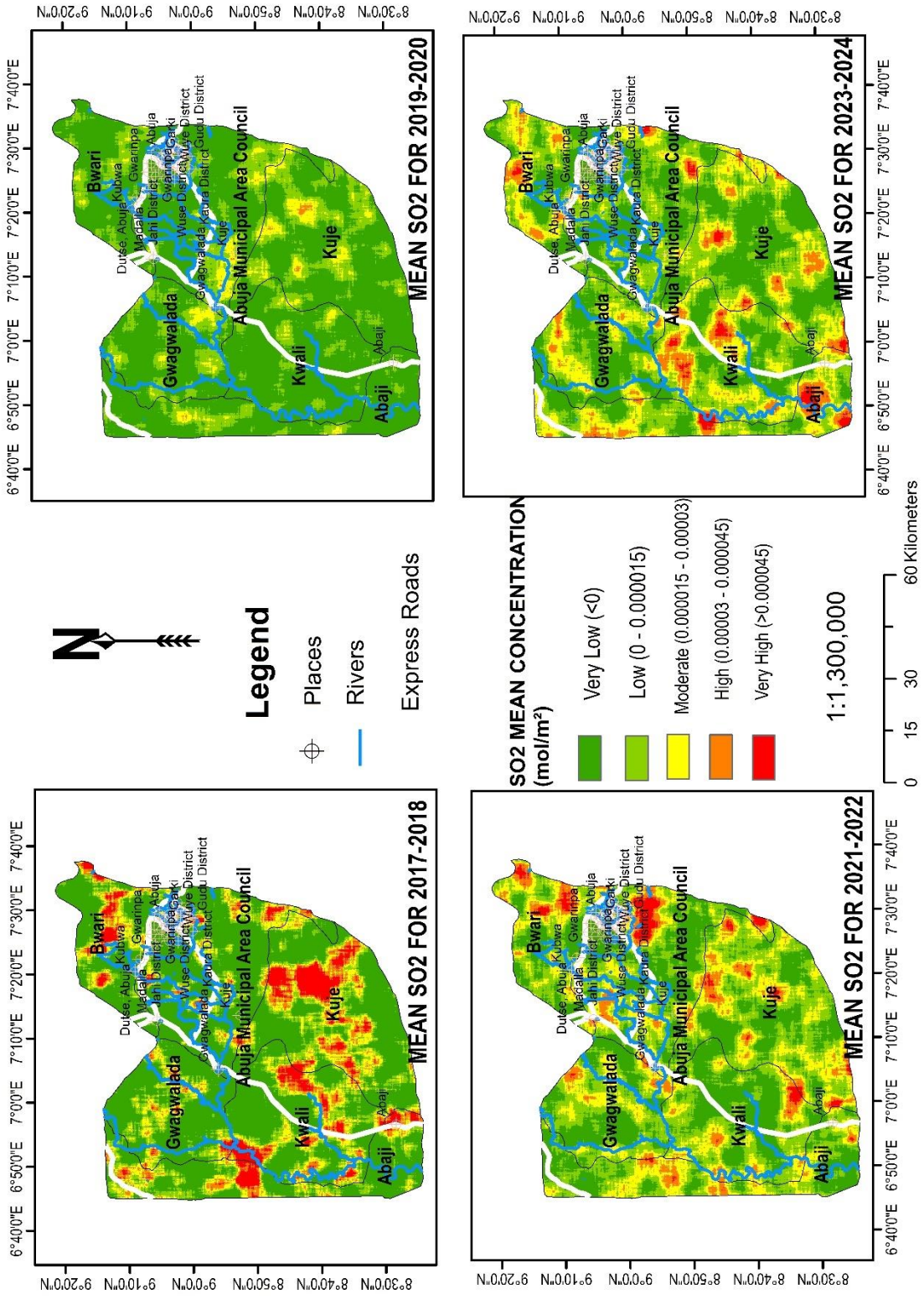

Figure 4.3.1: Map showing Greenhouse Gas (SO_2) Concentration in Abuja (2017–2024)

Table 4.3.1: Comparative Summary of Greenhouse Gas (SO_2) Concentration in Abuja (2017–2024)

Study Period	Year Range	Minimum	Maximum	Mean	Standard Deviation
Pre-COVID 19	2017–2018	-0.0001265	0.000130182	-0.000007496	0.000033998
COVID 19 Lockdown	2019–2020	-0.0000714193	0.0000437185	-0.00000901	0.000014107
After-COVID 19 Lockdown	2021–2022	-0.0000546184	0.0000782592	0.000006673	0.000017454
Post-COVID 19	2023–2024	-0.0000512865	0.0000735454	0.00000587	0.000016936

Table 4.3.2: Comparative Summary Greenhouse Gas (SO_2) SqKm Area coverage in Abuja based on the concentration (2017–2024)

	Very Low (SqKm)	Low (SqKm)	Moderate (SqKm)	High (SqKm)	Very High (SqKm)
2017–2018	4230.01	1145.49	954.83	587.72	435.15
2019–2020	5372.83	1640.25	327.07	13.05	0
2021–2022	2541.52	2579.59	1526.09	554.9	151.1
2023–2024	2720.47	2499.3	1501.64	522.2	109.59

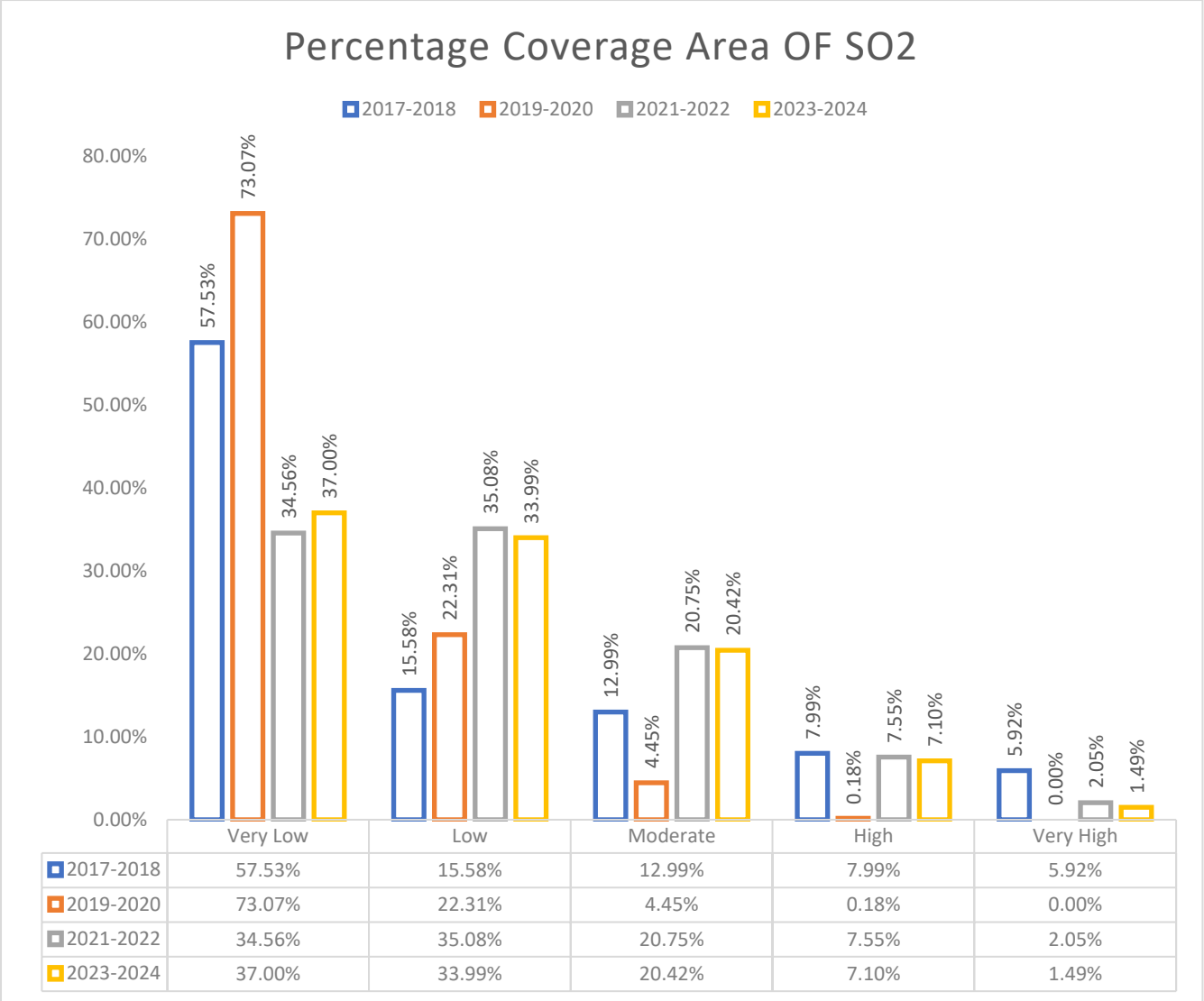

	Very Low	Low	Moderate	High	Very High
2017-2018	57.53%	15.58%	12.99%	7.99%	5.92%
2019-2020	73.07%	22.31%	4.45%	0.18%	0.00%
2021-2022	34.56%	35.08%	20.75%	7.55%	2.05%
2023-2024	37.00%	33.99%	20.42%	7.10%	1.49%

Figure 4.3.2: Bar Charts Showing Percentage Coverage Area of Greenhouse Gas (SO_2) Concentration in Abuja (2017–2024)

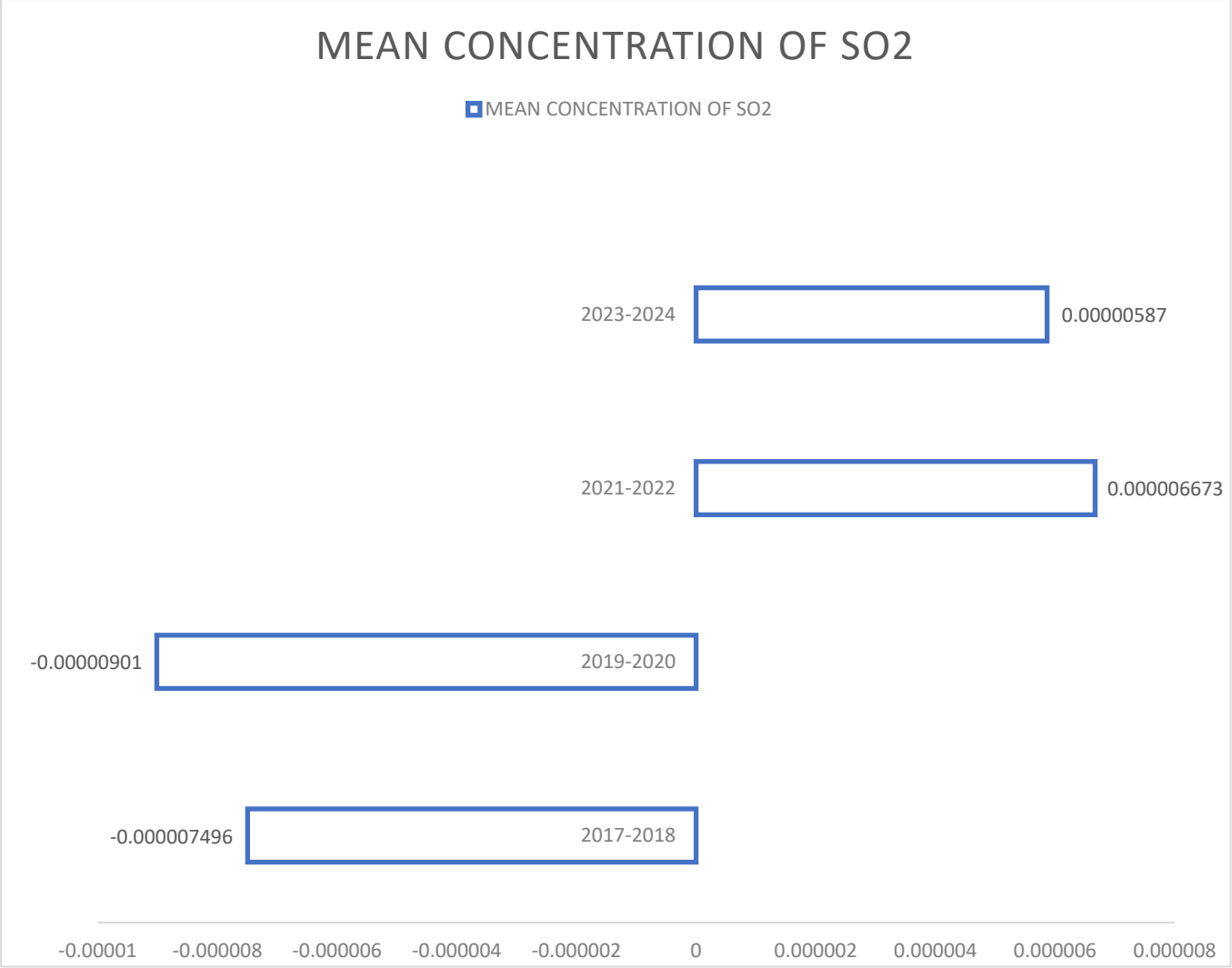

Figure 4.3.3: Bar Charts Showing Mean Concentration of Greenhouse Gas (SO_2) in Abuja (2017–2024)

4.4 MEAN CONCENTRATION OF GREENHOUSE GASES (AEROSOL) IN ABUJA FOR YEAR 2017–2018, 2019–2020, 2021–2022 and 2023–2024 (PRE, DURING and POST COVID PANDEMIC LOCKDOWN)

The figures below show the spatial distribution maps of Aerosol Optical Depth (AOD) concentration over Abuja for the years 2017–2018, 2019–2020, 2021–2022 and 2023–2024, representing the pre, during and post COVID pandemic lockdown periods. The tables present the statistical summaries derived from satellite-based observations and spatio-temporal data analysis conducted using Google Earth Engine (GEE) and processed in the ArcGIS environment.

Aerosol Concentration (2017–2018: Pre COVID Pandemic Period)

During the pre-pandemic period (2017–2018), the Aerosol Optical Depth (AOD) values ranged between -0.760284 and -0.316532*,* with a mean concentration of -0.589920 and a standard deviation of 0.06299208 (Table 4.4.1).

Aerosol Concentration (2019–2020: COVID Pandemic Lockdown Period)

During the COVID-19 lockdown period (2019–2020), the AOD ranged between -0.857201 and -0.541272, with a mean concentration of -0.698495 and a *standard deviation of 0.*06318845 (Table 4.4.1).

Aerosol Concentration (2021–2022: After COVID Lockdown Period)

In the immediate post-lockdown period (2021–2022), the Aerosol Optical Depth (AOD) values increased significantly, ranging between -0.286662 and -0.0924496*,* with a mean concentration of approximately 0.000006673 and a standard deviation of 0.08035217 (Table 4.4.1).

Aerosol Concentration (2023–2024: Post-COVID Pandemic Phase)

For the 2023–2024 period, representing the post-COVID pandemic era, the Aerosol Optical Depth (AOD) values ranged between -0.00963119 and 0.376562, with a mean concentration of 0.18296485 and a standard deviation of 0.07655127 (Table 4.4.1).

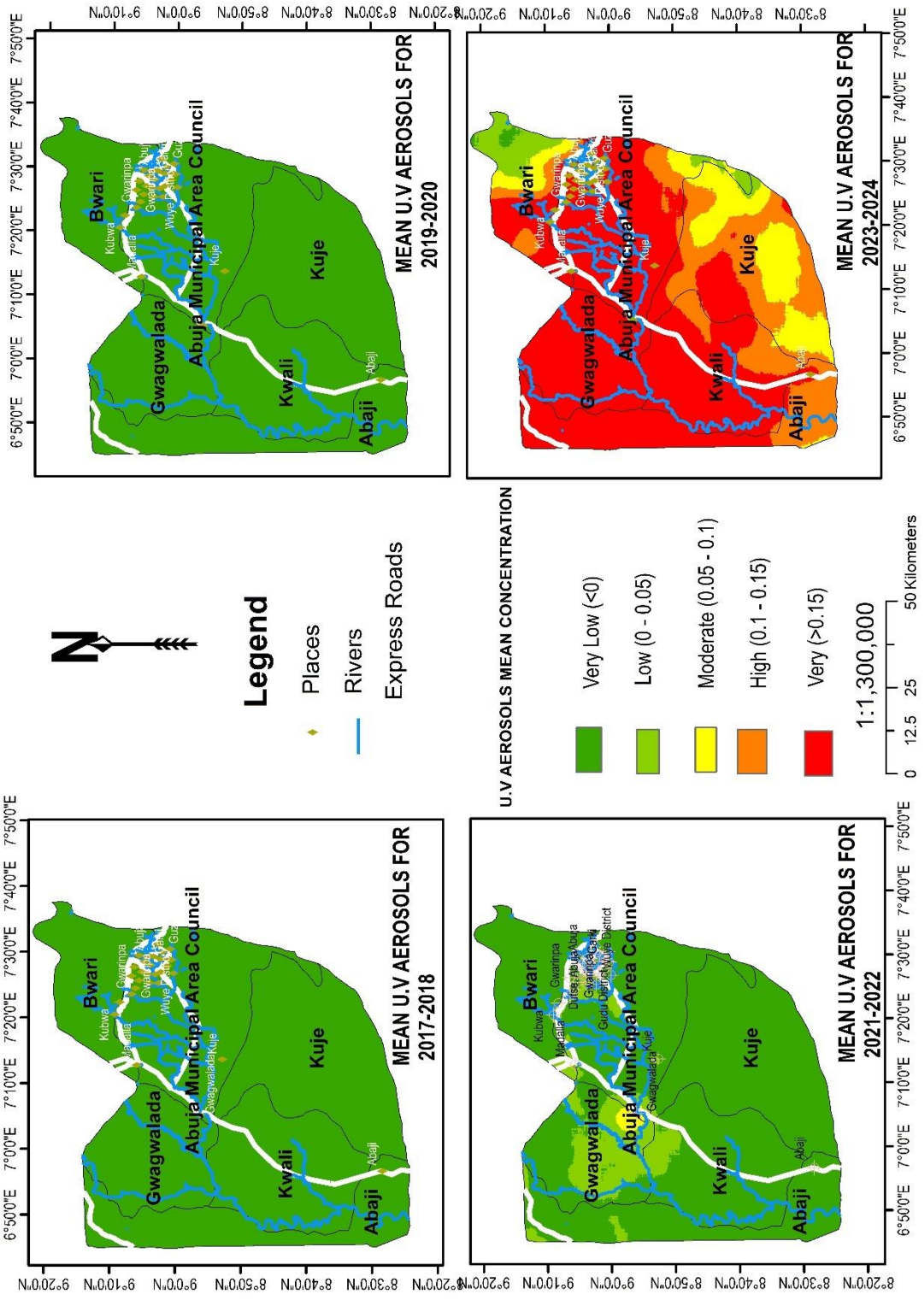

Figure 4.4.1: Map showing Greenhouse Gas (AEROSOL) Concentration in Abuja (2017–2024)

Table 4.4.1: Comparative Summary of Greenhouse Gas (AEROSOL) Concentration in Abuja (2017–2024)

Study Period	Year Range	Minimum	Maximum	Mean	Standard Deviation
Pre-COVID 19	2017–2018	-0.760284	-0.316532	-0.589920	0.06299208
COVID 19 Lockdown	2019–2020	-0.857201	-0.541272	-0.698495	0.06318845
After-COVID 19 Lockdown	2021–2022	-0.286662	0.0831889	-0.0924496	0.08035217
Post-COVID 19	2023–2024	-0.00963119	0.376562	0.18296485	0.07655127

Table 4.4.2: Comparative Summary Greenhouse Gas (AEROSOL) SqKm Area coverage in Abuja based on the concentration (2017–2024)

	Very Low (SqKm)	Low (SqKm)	Moderate (SqKm)	High (SqKm)	Very High (SqKm)
2017–2018	7353.2	0	0	0	0
2019–2020	7353.2	0	0	0	0
2021–2022	6494.5	808.427	50.273	0	0
2023–2024	26.348	273.992	837.03	1488.51	4727.32

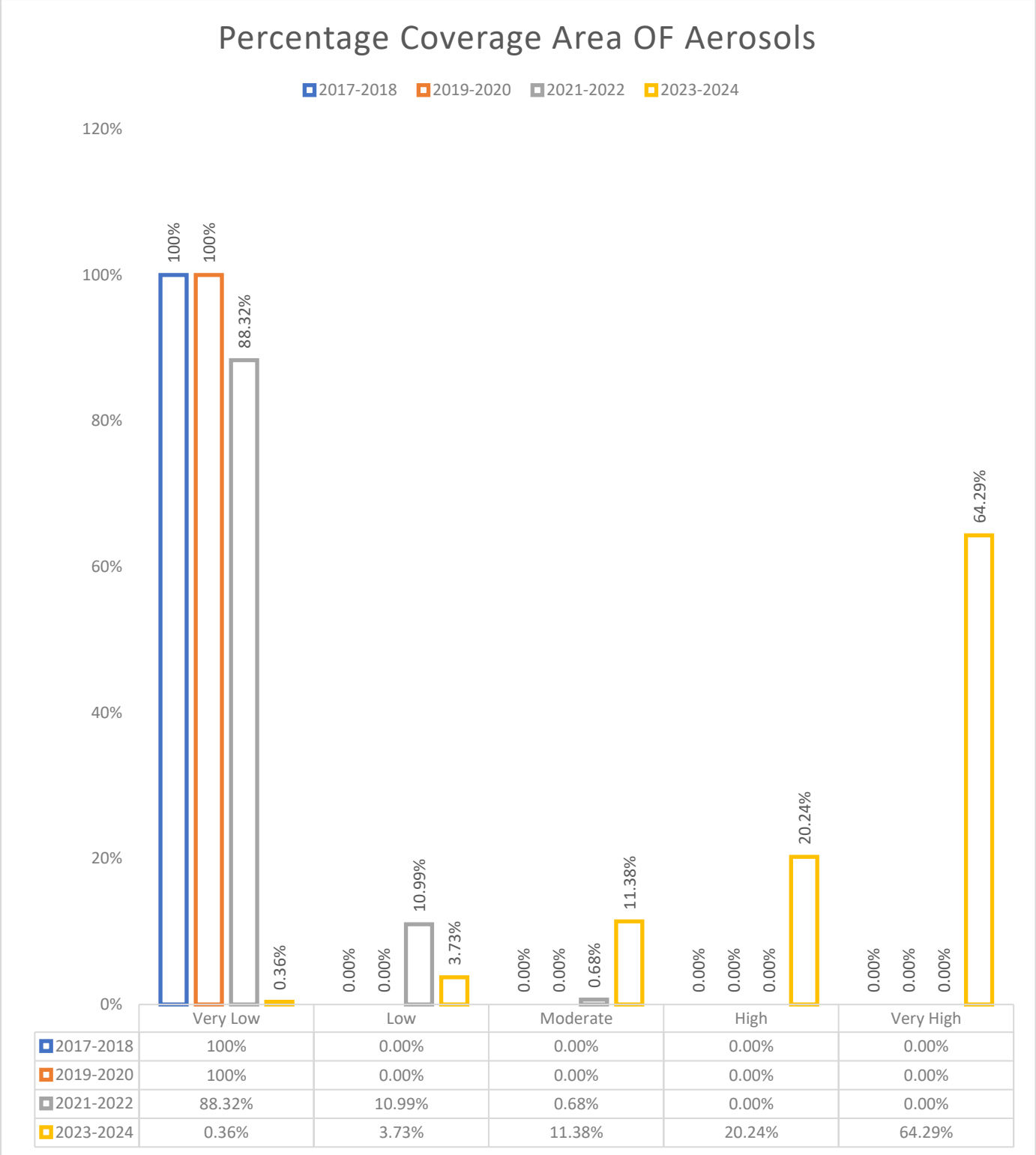

Figure 4.4.2: Bar Charts Showing Percentage Coverage Area of Greenhouse Gas (AEROSOL) Concentration in Abuja (2017–2024)

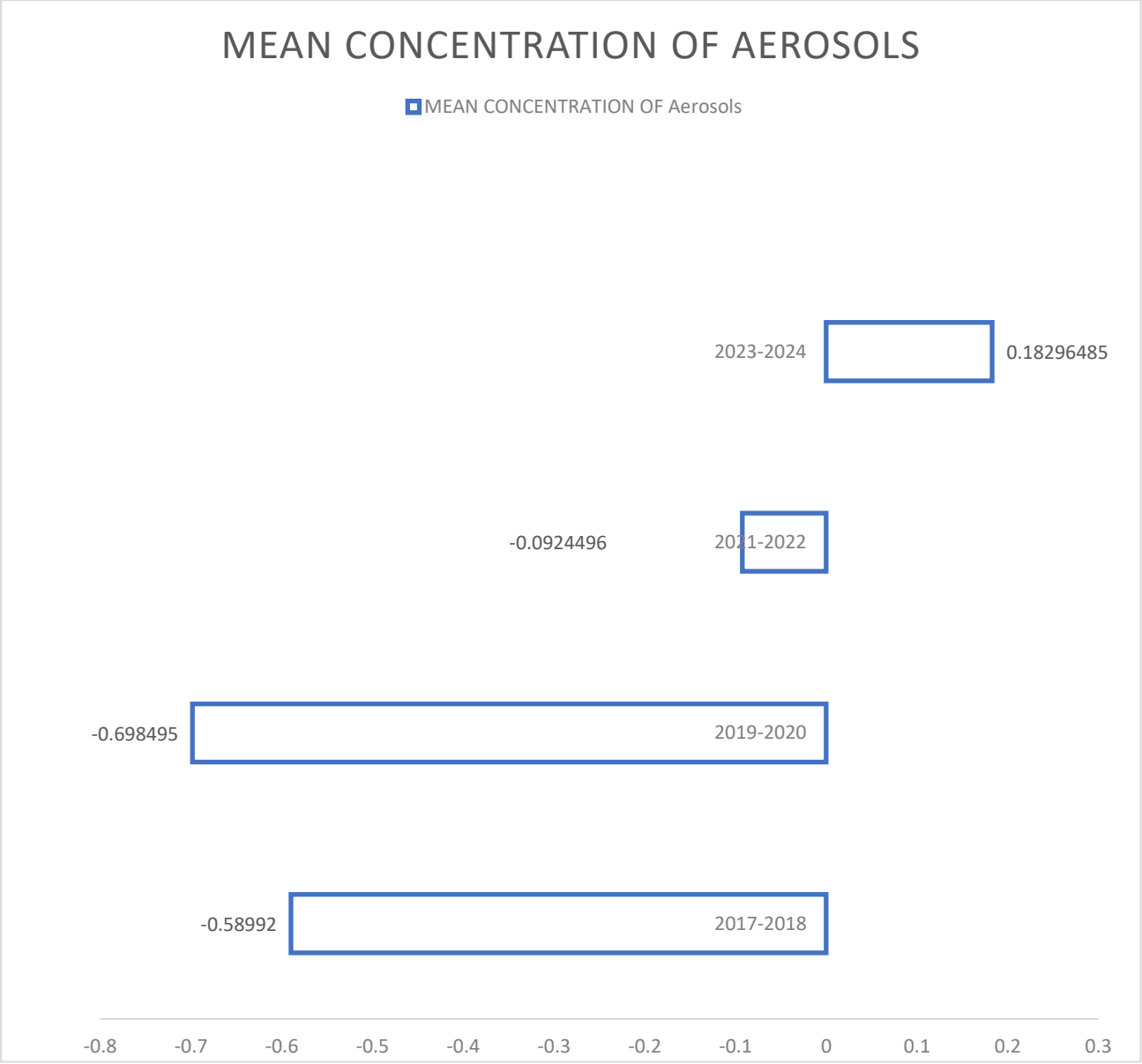

Figure 4.4.3: Bar Charts Showing Mean Concentration of Greenhouse Gas (AEROSOL) in Abuja (2017–2024)

4.5 MEAN CONCENTRATION OF GREENHOUSE GAS (OZONE) IN ABUJA FOR YEAR 2017–2018, 2019–2020, 2021–2022 and 2023–2024 (PRE, DURING and POST COVID PANDEMIC LOCKDOWN)

The figures below illustrate the spatial distribution maps of Ozone (O_3) concentration over Abuja for the periods 2017–2018 (pre-COVID), 2019–2020 (during COVID lockdown), 2021–2022 (post-lockdown phase) and 2023–2024 (post-pandemic period). The accompanying tables present the results derived from the statistical analysis of O_3 data obtained from satellite-based measurements processed through the Google Earth Engine (GEE) platform and analysed in ArcGIS.

Ozone Concentration (2017–2018: Pre-COVID Pandemic Period)

During the pre-COVID period (2017–2018), Ozone (O_3) concentrations ranged between 0.119648 mol/m² and 0.120745 mol/m², with a mean of 0.120326 mol/m² and a standard deviation of 0.00017155 (Table 4.5.1).

Ozone Concentration (2019–2020: COVID Pandemic Lockdown Period)

During the COVID-19 lockdown period (2019–2020), O_3 concentrations slightly decreased, ranging from 0.119552 mol/m² to 0.120368 mol/m², with a mean of 0.120116 mol/m² and a standard deviation of 0.00014610 (Table 4.5.1).

Ozone Concentration (2021–2022: After COVID Lockdown Period)

Following the easing of restrictions in 2021–2022, O_3 concentrations increased marginally, with values between 0.120671 mol/m² and 0.121363 mol/m², a mean of 0.121094 mol/m² and a standard deviation of 0.00011185 (Table 4.5.1).

Ozone Concentration (2023–2024: Post-COVID Pandemic Phase)

In the 2023–2024 post-pandemic period, O_3 concentrations ranged from 0.120186 mol/m² to 0.120892 mol/m², with a mean of 0.120656 mol/m² and a standard deviation of 0.0001184 (Table 4.5.1).

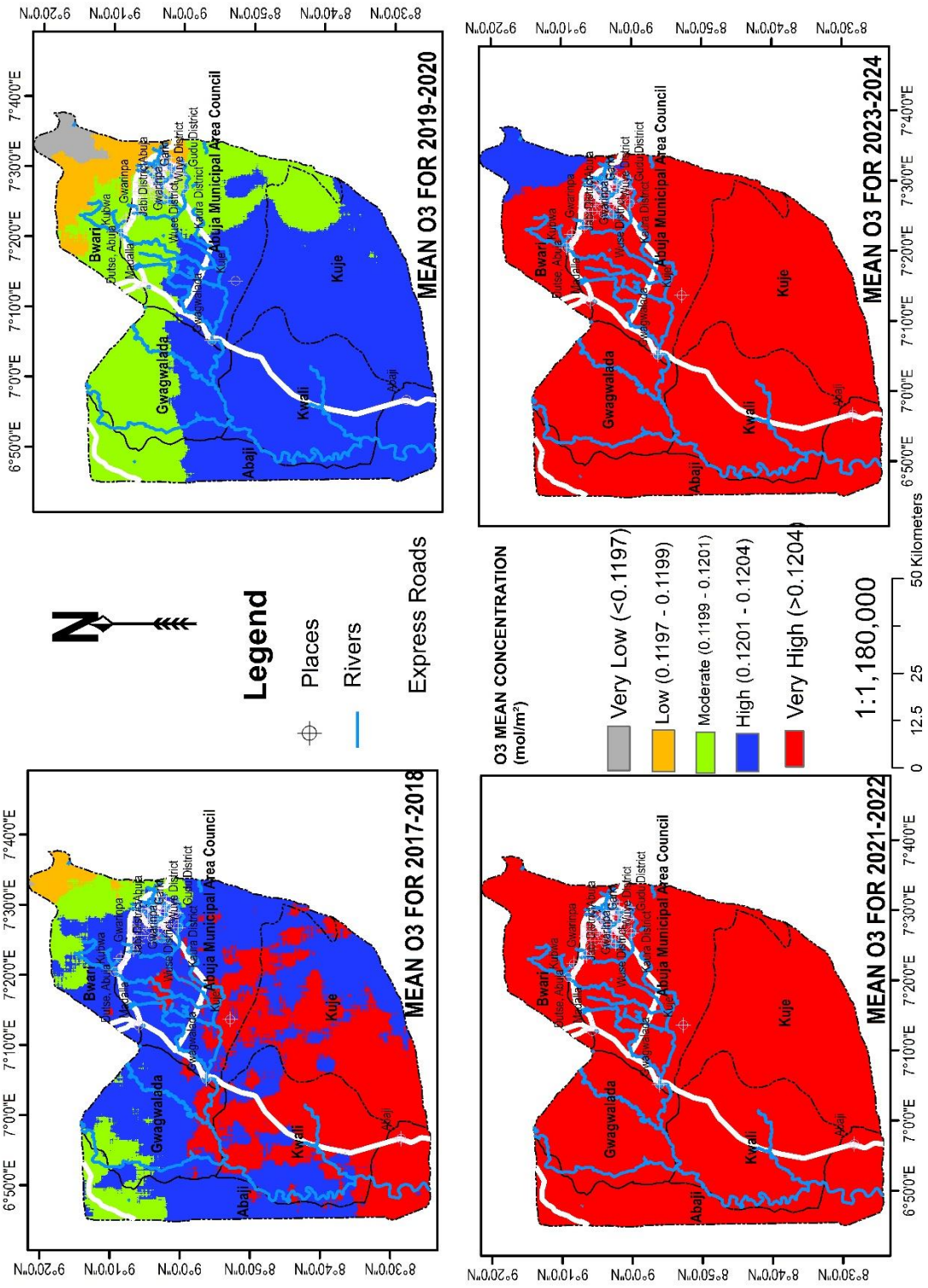

Figure 4.5.1: Map showing Greenhouse Gas (OZONE) Concentration in Abuja (2017–2024)

Table 4.5.1: Comparative Summary of Greenhouse Gas (OZONE) Concentration in Abuja (2017–2024)

Study Period	Year Range	Minimum	Maximum	Mean	Standard Deviation
Pre-COVID 19	2017–2018	0.119648	0.120745	0.120326	0.00017155
COVID 19 Lockdown	2019–2020	0.119552	0.120368	0.120116	0.00014610
After-COVID 19 Lockdown	2021–2022	0.120671	0.121363	0.121094	0.00011185
Post-COVID 19	2023–2024	0.120186	0.120892	0.120656	0.0001184

Table 4.5.2: Comparative Summary Greenhouse Gas (OZONE) SqKm Area coverage in Abuja based on the concentration (2017–2024)

	Very Low (SqKm)	Low (SqKm)	Moderate (SqKm)	High (SqKm)	Very High (SqKm)
2017–2018	2.108143	123.733	702.019	3866.15	2659.19
2019–2020	136.972624	409.377	2345.95	4460.9	0
2021–2022	0	0	0	0	7353.2
2023–2024	0	0	0	265.23	7087.97

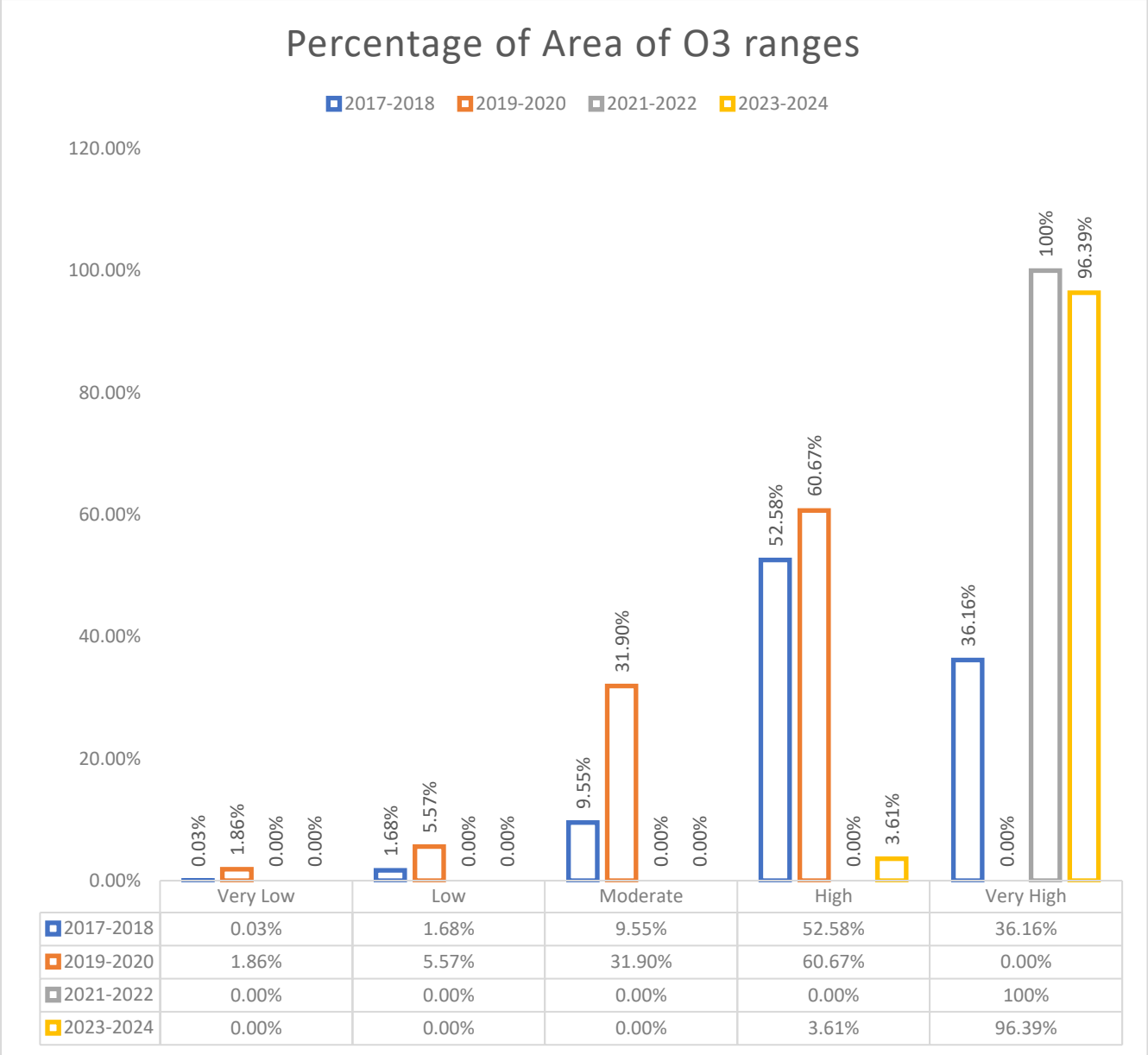

	Very Low	Low	Moderate	High	Very High
2017-2018	0.03%	1.68%	9.55%	52.58%	36.16%
2019-2020	1.86%	5.57%	31.90%	60.67%	0.00%
2021-2022	0.00%	0.00%	0.00%	0.00%	100%
2023-2024	0.00%	0.00%	0.00%	3.61%	96.39%

Figure 4.5.2: Bar Charts Showing Percentage Coverage Area of Greenhouse Gas (OZONE) Concentration in Abuja (2017–2024)

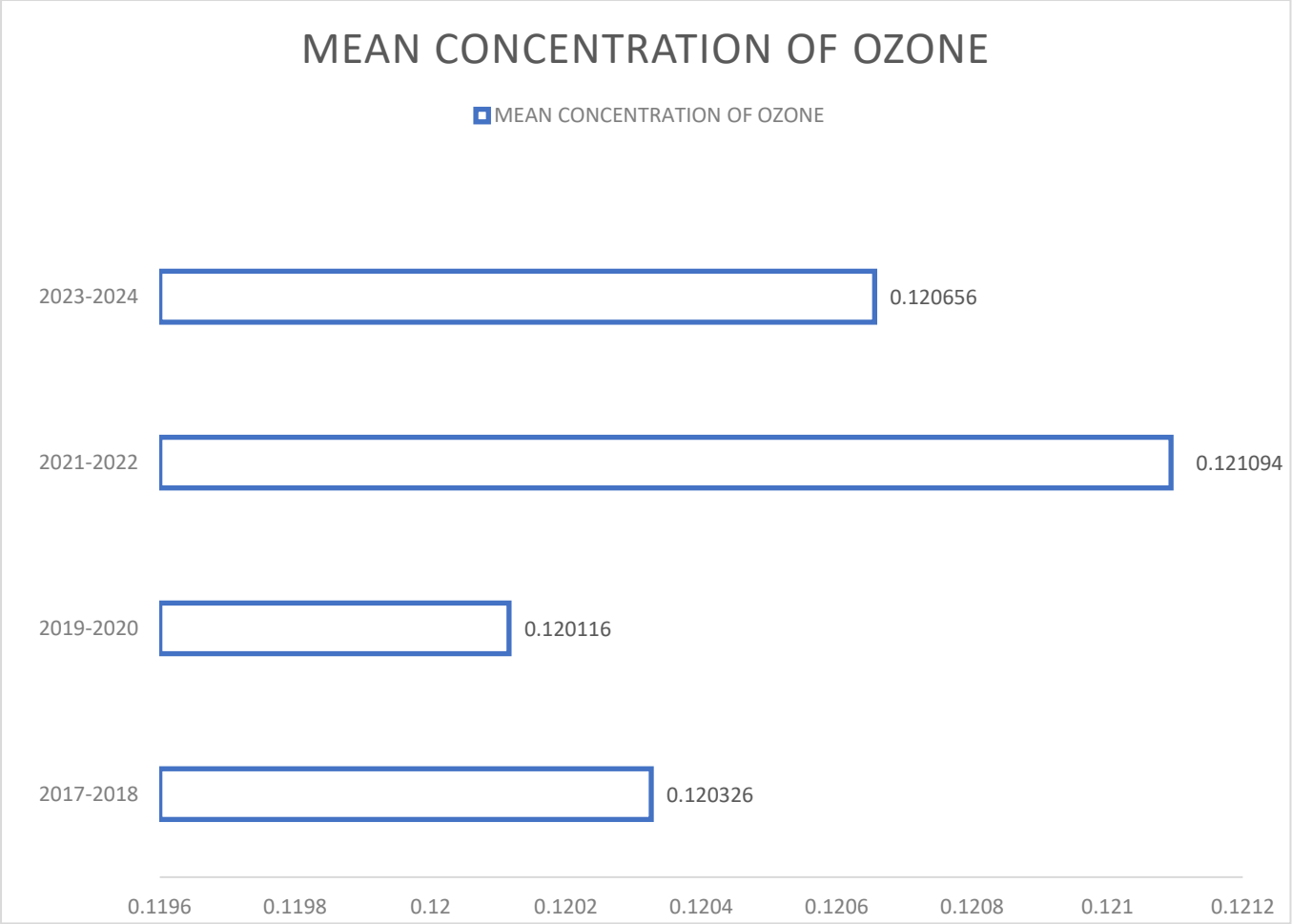

Figure 4.5.3: Bar Charts Showing Mean Concentration of Greenhouse Gas (OZONE) in Abuja (2017–2024)

CHAPTER FIVE

DISCUSSION

This chapter explains the findings from a detailed spatiotemporal analysis to show how Urban Heat Islands (UHIs), Land Surface Temperature (LST) and major greenhouse gases (GHGs) such as ozone (O_3), sulphur dioxide (SO_2) and aerosols interact over Abuja between 2017 and 2024. This period uniquely summarizes the pre-pandemic normal, the drastic reduction in human activity during the COVID-19 lockdown and the subsequent resumption of socio-economic operations. The results provide compelling empirical evidence of the profound influence of anthropogenic forces on the urban climate, effectively validating the theoretical framework established in the literature review (Oke, 1982; Oke *et al.,* 2017).

5.1 The UHI and LST Relationship: Statistical Evidence of Connection

This study confirms a fundamental and tightly coupled relationship between the Urban Heat Island (UHI) effect and Land Surface Temperature (LST) in Abuja, a connection that is central to urban climatology (Voogt and Oke, 2003). The parallel trends observed in their mean concentrations across the four study periods are statistically significant and conceptually aligned with established principles.

The pre-pandemic period (2017–2018) established a baseline, with mean UHI and LST values of 6.00°C and 6.96°C, respectively. The most telling evidence emerged during the COVID-19 lockdown (2019–2020), where both parameters decreased markedly. The mean UHI intensity fell from 6.00°C to 4.93°C, while the mean LST dropped more sharply from 6.96°C to 5.14°C. This coordinated decline underscores that a reduction in the activities that drive the UHI such as transportation and industrial operations which directly translates into a cooler urban surface, reducing the Urban Heat Island (UHI) effect.

The strength of this spatial connection is further validated by the Pearson correlation coefficients, which show a consistently strong positive relationship (r = 0.786 to 0.877) between the UHI and LST rasters across all period pairs. This indicates that where UHI intensity was high, LST was also high and vice-versa, a pattern that held true even as overall conditions shifted.

In this study the percentile analysis adds more details: the 10th percentile (p10) of UHI dropped from 2.04°C in the pre-COVID period to 0.82°C during the lockdown, suggesting that the coolest parts of the city, often associated with green spaces or water bodies (Anyakora *et al.,* 2025), became even cooler. Conversely, the post-lockdown rebound saw both UHI and LST not only recover but exceed pre-pandemic levels (UHI: 6.72°C in 2021–2022; LST: 7.03°C), before stabilizing at a still-elevated level (UHI: 6.56°C; LST: 6.81°C in 2023–2024). This post-recovery overshoot strongly indicates that the resumption of economic activities, potentially intensified, imposed a greater thermal load on the city than before the anthropogenic pause, highlighting a persistent and growing anthropogenic influence.

5.2 Trends and Spatial Patterns of Urban Heat

In this study the spatiotemporal dynamics of urban heat in Abuja extend beyond simple mean values, revealing complex shifts in the city's thermal structure, a common characteristic of rapidly sprawling cities (Oyeniyi *et al.,* 2025). The Shannon Diversity Index, a measure of the distribution and evenness of thermal classes, increased from 1.26 in the pre-COVID period to 1.34 during the lockdown. This indicates a more balanced and diverse spread of temperature zones, likely resulting from the widespread cooling that reduced the dominance of extreme heat classes.

This finding is corroborated by the Pair Change by Class analysis. The transition from the pre-COVID to the lockdown period (2017>2019) shows a substantial expansion of "Very Low" and "Low" UHI zones (increases of 293.70 km² and 482.10 km², respectively) and a concurrent contraction of "High" and "Very High" zones (decreases of 640.55 km² and 316.58 km²). This pattern reversed dramatically

post-lockdown (2019>2021), with "High" and "Very High" UHI areas expanding by 1383.22 km² and 350.63 km², respectively, directly linking the return of human activity to the rapid re-intensification of urban heat.

In this study the Kappa statistic, which measures classification agreement between time periods, quantifies the landscape's instability. The moderate kappa value of 0.42 between the pre-COVID and lockdown periods signifies a discernible but not chaotic shift. However, the low kappa of 0.23 between the lockdown and immediate post-lockdown period signals a strong and rapid transformation of the thermal landscape back towards intense heat. This is detailed in the pairwise difference statistics, which show that 60.09% of the city experienced warming, with a mean temperature increase of 1.79°C during this transition. Collectively, these metrics paint a picture of a temporarily relieved urban heat environment during the lockdown, which was rapidly and overwhelmingly reversed, highlighting the fragility of the urban thermal environment in the face of returning anthropogenic pressure.

5.3 Trends in Greenhouse Gases: SO_2, Aerosols and Ozone

5.3.1 Sulphur Dioxide (SO_2)

The concentration of SO_2, a direct tracer of fossil fuel combustion in industry and power generation (Piracha and Chaudhary, 2022), exhibited a clear response to the lockdown. In this study the mean concentration was negative in both pre-COVID (-0.000007496 mol/m²) and lockdown (-0.00000901 mol/m²) periods, with a notable reduction in standard deviation from 0.000034 to 0.000014. This indicates not only low concentrations but also significantly reduced spatial variability, consistent with a widespread shutdown of emission point sources. Spatially, the area classified as "Very Low" SO_2 concentration expanded from 4230.01 km² to 5372.83 km², showing a more homogeneously clean atmosphere. The post-lockdown period saw mean values turn positive (0.000006673 mol/m^2 in 2021-2022), signaling the resurgence of industrial and energy-related activities. The partial nature of this

rebound, however, with values not returning to pre-pandemic variability, may suggest some lasting efficiency gains or a slower-than-expected recovery in certain sectors.

5.3.2 Aerosols

In this study the aerosol optical depth (AOD) presented the most dramatic shift among the pollutants studied. Pre-COVID and lockdown periods were characterized by strongly negative mean AOD values (-0.59 and -0.70, respectively), indicating a relatively clean atmosphere with minimal particulate matter (Feng *et al.,* 2023). The spatial data was homogenous, with the entire study area classified as "Very Low" concentration (Table 4.4.2). The post-lockdown phase marked a radical departure. The mean AOD rose to -0.09 in 2021-2022 and further to a positive 0.18 by 2023-2024. By this final period, "Very High" aerosol zones dominated the landscape, covering 4,727.32 km² or approximately 64% of the study area. This surge is attributable to the resumption of construction, increased vehicular traffic raising road dust, biomass burning and industrial emissions. The positive AOD values in the post-COVID phase also suggest that aerosols were contributing to atmospheric warming, thereby intensifying the surface warming observed in the LST and UHI data.

5.3.3 Ozone (O_3)

In this study Ground-level ozone dynamics are more complex, as O_3 is a secondary pollutant formed by photochemical reactions involving precursors like nitrogen oxides (NOx) and volatile organic compounds (VOCs). The data shows a slight dip in mean O_3 concentration during the lockdown (0.120116 mol/m^2) compared to pre-COVID (0.120326 mol/m^2), likely due to a temporary reduction in its precursors. However, it rebounded in the immediate post-lockdown period to 0.121094 mol/m^2, the highest value in the study timeline. This post-lockdown peak can be explained by the complex atmospheric chemistry involving NOx titration. Upon the resumption of activity, returning NOx and VOC emissions, combined with abundant sunlight and high temperatures, created ideal conditions for vigorous ozone production (Piracha and Chaudhary, 2022), leading to the observed increase. The

spatial data reinforces this, showing a shift from a mixed classification to the entire city being classified as "Very High" O_3 in the post-lockdown period.

5.4 Interactions Between LST, UHIs and Atmospheric Pollutants

In this study the results demonstrate a synergistic, positive feedback loop between urban heat and atmospheric pollutants, as theorized in the literature (Santamouris, 2015; Rizwan *et al.,* 2008). The expansion of Abuja's built-up area, as documented in the literature review (Uju *et al.,* 2025), replaces cooling vegetation with heat-absorbing materials, directly elevating LST and strengthening the UHI. This increased thermal energy, in turn, exacerbates the chemical formation of secondary pollutants like ozone.

The data clearly show that air pollutants and urban heat patterns are closely connected. After the lockdown, the increase in Aerosol Optical Depth (AOD) occurred alongside a rise in mean Land Surface Temperature (LST), indicating that the buildup of particles in the air contributed to warming by trapping heat near the surface. Sulphur Dioxide (SO_2) levels followed the same pattern as industrial and energy-related activities droppes sharply during the lockdown when many operations stopped, then rising again afterward as activities resumed. The highest Ozone (O_3) levels were recorded during the warmer post-lockdown period, showing that higher temperatures encourage the chemical reactions that form ozone in the lower atmosphere. Overall, the strong positive correlations ($r = 0.786–0.877$) between Urban Heat Islands (UHI) and LST across all study periods confirm that these factors are closely linked and reinforce each other, creating a self-sustaining cycle of urban warming that is largely driven by human activities.

5.5 The Lockdown as a Natural Experiment

The government-mandated lockdowns during the COVID-19 pandemic served as an unprecedented, large-scale natural experiment, effectively isolating the anthropogenic component of urban climate

change (Liu *et al.,* 2022; Dogan *et al.,* 2024). The results provide quantitative, real-world validation of theoretical models.

The pairwise difference statistics are particularly revealing. The transition from the pre-COVID to the lockdown period saw a mean negative change (cooling) of -1.07°C, affecting 54.52% of the city's area. This cooling was a direct consequence of the drastic reduction in anthropogenic heat flux from vehicles, generators and idled industries. Conversely, the transition from the lockdown to the post-lockdown period was characterized by a strong mean positive change (warming) of +1.79°C, impacting an even larger portion of the city (60.09%). The speed and scale of this thermal rebound demonstrate the urban climate system's high sensitivity to human activity. It underscores that the baseline "normal" state of Abuja's climate is heavily conditioned by carbon-intensive energy and transportation systems and that any deviation from this unsustainable path requires deliberate and structural intervention, not just temporary behavioural change.

5.6 Relevance to the Sustainable Development Goals (SDGs)

The findings of this study have direct and urgent implications for achieving the United Nations' Sustainable Development Goals, particularly SDG 11 (Sustainable Cities and Communities) and SDG 13 (Climate Action).

The massive expansion of "High" UHI area by 1383.22 km² after the lockdown is a clear indicator of urban unsustainability, directly contradicting the aims of SDG 11. This trend points to the critical need for integrating urban cooling measures; such as green belts, rooftop gardens, reflective surfaces and improved ventilation corridors into the core of city planning to enhance livability and resilience for Abuja's growing population.

Simultaneously, the lockdown period provided a tangible, though brief, demonstration of the benefits envisioned by SDG 13. The reductions in UHI, LST, SO_2 and aerosols showed the potential environmental benefits of curbing fossil fuel consumption. However, the rapid and forceful rebound of

all these parameters immediately after restrictions were lifted serves as a stark warning. It emphasizes that without a fundamental, long-term transition to clean energy, sustainable transportation and climate-smart construction, the urban contribution to climate change will continue to intensify.

5.7 Recommendations and Mitigation Strategies

In this study based on the empirical evidence of this study, which highlights the profound impact of anthropogenic activities on Abuja's urban climate, the following integrated recommendations and mitigation strategies are proposed. These are designed to disrupt the positive feedback loop between urban heat and greenhouse gas emissions, fostering a more sustainable and resilient city.

1. **Urban Greening and Green Infrastructure Development:** Prioritize the expansion of tree cover, urban forests and parks. The negative correlation between NDVI and LST is well-established (Oyeniyi *et al.,* 2025); thus, strategic greening in high-UHI zones like Abaji, Gwagwalada and Kwali should be the focus of primary mitigation strategy. This should be coupled with the implementation of vegetative (green) roofs and permeable pavements to enhance evapotranspiration, reduce surface runoff and lower ambient temperatures (Vargo *et al.,* 2016).

2. **Sustainable Urban Planning and Climate-Smart Design:** Enforce land use policies that limit unchecked sprawl and impervious surface proliferation. Introduce and implement zoning laws that mandate green corridors, preserve existing green spaces and promote cool roof technologies and high-albedo materials in new construction to minimize solar heat absorption (Salata *et al.,* 2017). Urban design should incorporate natural ventilation and open spaces to improve microclimate regulation.

3. **Promotion of Clean Energy and Sustainable Transportation Systems:** Incentivize the adoption of solar energy for public and private use and phase down the reliance on diesel generators. Invest in and subsidize hybrid or fully electric public transportation systems to

decouple mobility from pollutant emissions (Jamei *et al.,* 2022). Developing public transport powered by renewable energy is critical to reducing emissions of SO_2, aerosols and O_3 precursors.

4. **Industrial Emission Control and Waste Heat Management:** Strengthen the regulatory framework for monitoring and controlling industrial emissions of SO_2, NOx and particulates. Enforce the use of cleaner production technologies and conduct regular emissions audits. Furthermore, introduce policies that encourage industrial and building-level waste heat recovery technologies to reduce the direct thermal pollution of the urban environment.

5. **Integrated Pollution Reduction Policies and Public Awareness:** Implement a robust Air Quality Management Plan that sets clear targets for reducing ambient concentrations of aerosols, SO_2 and ozone precursors. Concurrently, launch public education campaigns on the health and economic impacts of urban heat and air pollution, promoting community-based environmental stewardship, energy conservation practices and behavioural change.

6. **Data-Driven Policy and Continuous Research:** Maintain a continuous, high-resolution monitoring system for UHI, LST and GHG trends using the integrated GIS and remote sensing approaches demonstrated in this study. This data is essential for setting baselines, tracking progress and evaluating the effectiveness of interventions. Support interdisciplinary research to develop locally adapted, cost-effective climate action plans.

5.8 Challenges

Several challenges were encountered during the course of this study, including:

1. Frequent power interruptions, which affected the smooth progress of the research.
2. Poor internet connectivity, making it difficult to extract and download data from Google Earth Engine.

3. Limited access to relevant academic publications related to the research topic, which constrained the literature review process.

5.9 Conclusion

This spatiotemporal assessment demonstrates that human activities are the principal driver of increasing urban heat and associated pollutant levels in Abuja. The COVID-19 lockdown period provided a powerful, real-world validation of this relationship, showing the environment's capacity for rapid recovery when anthropogenic pressures are alleviated. However, the swift and forceful rebound of UHI, LST and GHG concentrations to levels exceeding the pre-pandemic baseline underscores the profound unsustainability of current urban development patterns.

The evidence presented herein strongly advocates for a paradigm shift in urban management. Achieving the goals of SDG 11 (Sustainable Cities and Communities) and SDG 13 (Climate Action) in Abuja necessitates an urgent and integrated commitment to the strategies outlined above, focusing on sustainable urban planning, a decisive transition to renewable energy and the widespread implementation of green infrastructure. The tools of GIS and remote sensing, as demonstrated, are indispensable for monitoring progress and guiding these essential interventions towards the creation of a more livable, resilient and sustainable city.

REFERENCES

Abimbola, O. J., Adewumi, T. and Abubakar, M. (2025). Dynamics of Urban Heat Island in Lafia, Nasarawa State of Nigeria: A remote sensing analysis of land surface temperature, urban development and vegetation change [Unpublished manuscript]. *Department of Physics, Faculty of Science, Federal University of Lafia,* 1-28.

Almeida, C. R., Teodoro, A. C. and Gonçalves, A. (2021). Study of the Urban Heat Island (UHI) using remote sensing data/techniques: A systematic review. *Environments,* **8**(10), 105.

Alves de Almeida, D. R., Broadbent, E. N., Pinheiro Ferreira, M., Meli, P., Almeyda Zambrano, A. M., Bastos Gorgens, E., De Resende, A. F., Torres de Almeida, C., Hummel do Amaral, C., Dalla Corte, A. P., Silva, C. A., Romanelli, J. P., Atticciati Prata, G., de Almeida Papa, D., Stark, S. C., Valbuena, R., Nelson, B. W., Guillemot, J., Feret, J. B., Chazdon, R. and Brancalion, P. H. S. (2021). Monitoring restored tropical forest diversity and structure through UAV-borne hyperspectral and lidar fusion. *Remote Sensing of Environment,* **264**, 112582.

Anyakora, A. O., Mamudu, O. P. and Fabiyi, O. O. (2025). Geospatial analysis of urban blue and green spaces in Abuja Municipal Area Council. *International Journal of Engineering and Computer Science,* **14**(3), 26970–26981.

Arnfield, A. J. (2003). Two decades of urban climate research: A review of turbulence, exchanges of energy and water and the urban heat island. *International Journal of Climatology,* **23**(1), 1–26.

Aruya, E. I., Iguisi, E. O., Abdulhamed, A. I., Yusuf, Y. O. and Ariko, J. D. (2021). Diurnal variation of urban canopy heat island in the dry season in Benin City, Edo State, Nigeria. *Zaria Geographer,* **28**(1), 36–46.

Bhargava, A., Lakmini, S. and Bhargava, S. (2017). Urban Heat Island Effect: It's relevance in urban planning. *Journal of Biodiversity and Endangered Species,* **5**(1).

Carpio, M., González, Á., González, M. and Verichev, K. (2020). Influence of pavements on the urban heat island phenomenon: A scientific evolution analysis. *Energy and Buildings,* **226**, 110379.

Chinedu, O. I., Alegimenlen, H. O., Ezeagba, J. S., Bello, R. A., Aremu, A. G. and Chinonyerem, C. A. (2024). Urban heat island analysis using GIS and remote sensing in Koshofe Lagos State. *Mediterranean Publication and Research International,* **6**(9), 17–32.

Crutzen, P. (2004). New directions: The growing urban heat and pollution "island" effect—Impact on chemistry and climate. *Atmospheric Environment,* **38**(21), 3539–3540.

Dogan, T., Urban, A. and Hanel, M. (2024). Effect of COVID-19 lockdown on urban heat island dynamics in Prague, Czechia. *Remote Sensing,* **16**(7), 1113.

Dong, Y., Varquez, A. C. G. and Kanda, M. (2017). Global anthropogenic heat flux database with high spatial resolution. *Atmospheric Environment,* **150**, 276–294.

Feng, Z., Wang, X., Yuan, J., Zhang, Y. and Yu, M. (2023). Changes in air pollution, land surface temperature and urban heat islands during the COVID-19 lockdown in three Chinese urban agglomerations. *Science of The Total Environment,* **892**, 164496.

Folorunsho, A., Balogun, I., Adediji, A., Olumide, A. and Abdulkareem, S. (2017). Assessment of Urban Heat Island over Ibadan Metropolis Using Landsat and Modis. *Journal of Environmental Science, Toxicology and Food Technology,* **12**(1), 62–87.

Gorelick, N., Hancher, M., Dixon, M., Ilyushchenko, S., Thau, D. and Moore, R. (2017). Google Earth Engine: Planetary-scale geospatial analysis for everyone. *Remote Sensing of Environment,* **202**, 18–27.

Guo, L., Di, L., Zhang, C., Lin, L., Chen, F. and Molla, A. (2022). Evaluating contributions of urbanization and global climate change to urban land surface temperature change: A case study in Lagos, Nigeria. *Scientific Reports,* **12**(1), 14168.

Jamei, E., Jamei, Y., Seyedmahmoudian, M., Horan, B., Mekhilef, S. and Stojcevski, A. (2022). Investigating the impacts of COVID-19 lockdown on air quality, surface Urban Heat Island, air temperature and lighting energy consumption in City of Melbourne. *Energy Strategy Reviews,* **44**, 100963.

Kuddus, M. A., Tynan, E. and McBryde, E. (2020). Urbanization: A problem for the rich and the poor? *Public Health Reviews,* **41**(1), 1.

Le Quéré, C., Jackson, R. B., Jones, M. W., Smith, A. J. P., Abernethy, S. andrew, R. M., De-Gol, A. J., Willis, D. R., Shan, Y., Canadell, J. G., Friedlingstein, P., Creutzig, F. and Peters, G. P. (2020). Temporary reduction in daily global CO2 emissions during the COVID-19 forced confinement. *Nature Climate Change,* **10**(7), 647–653.

Liu, Z., Lai, J., Zhan, W., Bechtel, B., Voogt, J., Quan, J., Hu, L., Fu, P., Huang, F., Li, L., Guo, Z. and Li, J. (2022). Urban heat islands significantly reduced by COVID-19 lockdown. *Geophysical Research Letters,* **49**(4), 1–10.

Manoli, G., Fatichi, S., Bou-Zeid, E. and Katul, G. G. (2020). Seasonal hysteresis of surface urban heat islands. *Proceedings of the National Academy of Sciences of the United States of America,* **117**(13), 7082–7089.

Mika, J., Forgo, P., Lakatos, L., Olah, A. B., Rapi, S. and Utasi, Z. (2018). Impact of 1.5 K global warming on urban air pollution and heat island with outlook on human health effects. *Current Opinion in Environmental Sustainability,* **30**, 151–159.

Mijani, N., Karimi Firozjaei, M., Mijani, M., Khodabakhshi, A., Qureshi, S., Jokar Arsanjani, J. and Alavipanah, S. K. (2023). Exploring the effect of COVID-19 pandemic lockdowns on urban cooling: A tale of three cities. *Advances in Space Research,* **71**(1), 1017–1033.

Mohajerani, A., Bakaric, J. and Jeffrey-Bailey, T. (2017). The urban heat island effect, its causes and mitigation, with reference to the thermal properties of asphalt concrete. *Journal of Environmental Management,* **197**, 522–538.

Mohammad, P. and Goswami, A. (2021). Quantifying diurnal and seasonal variation of surface urban heat island intensity and its associated determinants across different climatic zones over Indian cities. *GIScience and Remote Sensing,* **58**(7), 1–27.

Odunsi, O. M. and Rienow, A. (2024). Estimating surface urban heat island effects of Abeokuta within the context of its economic development cluster in Ogun State Nigeria: A baseline study utilising remote sensing and cloud-based computing technologies. *Climate,* **12**(12), 198.

Oke, T. R. (1982). The energetic basis of the urban heat island. *Quarterly Journal of the Royal Meteorological Society,* **108**(455), 1–24.

Oke, T. R., Mills, G., Christen, A. and Voogt, J. A. (2017). Urban climates. *Cambridge University Press.* https://doi.org/10.1017/9781139016476

Olorunfemi, I. E., Fasimnirin, J. T., Olufayo, A. A. and Komolafe, A. A. (2018). GIS and remote sensing-based analysis of the impacts of land use/land cover change (LULCC) on the environmental sustainability of Ekiti State, southwestern Nigeria. *Environment, Development and Sustainability*, 1–32.

Ooka, R. (2007). Recent development of assessment tools for urban climate and heat-island investigation especially based on experiences in Japan. *International Journal of Climatology,* **27**(13), 1919–1930.

Oyeniyi, M. A., Odunsi, O. M., Rienow, A. and Edler, D. (2025). Spatiotemporal analysis of land use change and urban heat island effects in Akure and Osogbo, Nigeria between 2014 and 2023. *Climate,* **13**(1), 68.

Pantavou, K., Theoharatos, G., Mavrakis, A. and Santamouris, M. (2011). Evaluating thermal comfort conditions and health responses during an extremely hot summer in Athens. *Building and Environment,* **46**(2), 339–344.

Piracha, A. and Chaudhary, M. T. (2022). Urban air pollution, urban heat island and human health: A review of the literature. *Sustainability,* **14**(15), 9234.

Rahaman, S. N., Shehzad, T. and Sultana, M. (2022). Effect of seasonal land surface temperature variation on COVID-19 infection rate: A Google Earth Engine-based remote sensing approach. *Environmental Health Insights,* **16**, 1–4.

Ramakreshnan, L., Aghamohammadi, N., Fong, C. S., Ghaffarianhoseini, A., Ghaffarianhoseini, A., Wong, L. P., Hassan, N. and Sulaiman, N. M. (2018). A critical review of Urban Heat Island phenomenon in the context of Greater Kuala Lumpur, Malaysia. *Sustainable Cities and Society,* **62**, 131–145.

Rizwan, A. M., Dennis, L. Y. C. and Chunho, L. I. U. (2008). A review on the generation, determination and mitigation of Urban Heat Island. *Journal of Environmental Sciences,* **20**(1), 120–128.

Rosenfeld, A. H., Akbari, H., Romm, J. J. and Pomerantz, M. (1998). Cool communities: Strategies for heat island mitigation and smog reduction. *Energy and Buildings,* **28**(1), 51–62.

Salata, F., Golasi, I., Petitti, D., de Lieto Vollaro, E., Coppi, M. and de Lieto Vollaro, A. (2017). Relating microclimate, human thermal comfort and health during heat waves: An analysis of heat island mitigation strategies through a case study in an urban outdoor environment. *Sustainable Cities and Society,* **30**, 79–96.

Santamouris, M. (2015). Analyzing the heat island magnitude and characteristics in one hundred Asian and Australian cities and regions. *Science of the Total Environment,* **512**–**513**, 582–598.

Stewart, I. D. and Oke, T. R. (2012). Local climate zones for urban temperature studies. *Bulletin of the American Meteorological Society,* **93**(12), 1879–1900.

UN-Habitat. (2018). Abeokuta: City context report. Global Future Cities Programme [online], Available internet https://www.globalfuturecities.org/sites/default/files/2020-07/Nigeria_Abeokuta_CCR.pdf Accessed on the 25th September, 2025

Uju, I. O., Sangari, D. U. and Kpalo, S. Y. (2025). Assessment of land surface temperature in Abuja municipal area council between 2002 and 2023. *International Journal of Built Environment and Earth Science,* **7**(4), 146–168.

Vargo, J., Stone, B., Habeeb, D., Liu, P. and Russell, A. (2016). The social and spatial distribution of temperature-related health impacts from urban heat island reduction policies. *Environmental Science and Policy,* **66**, 366–374.

Voogt, J. A. and Oke, T. R. (2003). Thermal remote sensing of urban climates. *Remote Sensing of Environment,* **86**(3), 370–384.

Yaro, A., Abdulrashid, L., John, J. A. and Sani, Y. (2017). Remote sensing and GIS based assessment of urban heat island pattern in Kaduna metropolis. *International Journal For Research in Applied And Natural Science,* **3**(6), 20–31.

Zhou, D., Xiao, J., Bonafoni, S., Berger, C., Deilami, K., Zhou, Y., Frolking, S., Yao, R., Qiao, Z. and Sobrino, J. A. (2019). Satellite remote sensing of surface urban heat islands: Progress, challenges and perspectives. *Remote Sensing,* **11**(1), 48.